

Doctoral Thesis

Impact of Surface Development on Subsurface Environment in an
Arid Climate: Consideration Based on Groundwater Quality and
Isotopic Signals at the New Reclaimed Land, Eastern Nile Delta,
Egypt

(乾燥地域における地表開発が地下環境に与える影響：エジプトナ
イルデルタ東部の開発地域を対象とした地下水質並びに同位体情報
を用いた検討)

Mahmoud Mostafa Abd ElRahim Mohamed Khalil

マハムッド モスタファ アブド エルラヒム モハメッド カリル

ABSTRACT

Groundwater is increasingly recognized as a main factor in arid land development, i.e., desert reclamation, in many arid countries where the surface water resources are limited or scarce. Throughout the rapid urban and agricultural development, changes of groundwater quantity and quality commonly occur by the increase of groundwater abstraction and the introduction of new sources of recharge. Therefore, understanding the contribution and the changes of various recharge sources, natural and anthropogenic, to aquifer systems will provide important knowledge to develop water resources management and environmental conservation plans, and to assess pollution mechanisms. This study highlights these aspects for the Quaternary aquifer system underlying the new reclaimed lands in the eastern fringes of the Nile Delta, Egypt, through the identification of groundwater end-members and their sources.

Using a set of chemical and isotopic ($\delta^2\text{H}$, $\delta^{18}\text{O}$, $\delta^{13}\text{C}$ and ^{14}C) data in tandem with multivariate data analysis, source components in groundwater of the Quaternary aquifer system were estimated. Electric conductivity (EC) and stable isotopic characteristics of water varied widely and were used to group the samples into four clusters by applying hierarchical cluster analysis (HCA). The water groups were then examined through principal component analysis (PCA) together with the information on the groundwater from the Miocene aquifer, the water from the Ismailia canal, the old Nile water, and wastewater. The overlap of clusters 1 and 2, i.e., low EC groundwater, with the old Nile water and the water from the Ismailia canal in PCA space indicated that groundwater in the northern parts of the Quaternary aquifer are hydraulically connected with the water in the Ismailia canal. Depletion of stable isotopes of water of subcluster 1.3 suggested a different source other than the Nile water. Clusters 3 and 4, i.e., high EC groundwater, were grouped with the groundwater of the Miocene aquifer in PCA space to infer the hydraulic connection with the groundwater in the Miocene aquifer, mainly in the southern part of the study area. Cluster 4 samples were stable-isotopically enriched and showed high nitrate

concentrations. Also, the cluster 4 samples were distributed in the agricultural area where treated/untreated wastewater has been supplied for irrigation. The information obtained from the analysis of city water balance and recent geophysical data suggested the possibility of wastewater infiltration, which may explain the characteristics of the cluster 4 samples. Northward increasing trend of ^{14}C and the lowest ^{14}C values reported in the southern portion, i.e., cluster 3, of the Quaternary aquifer confirmed the stated mixing processes. Subcluster 1.3 was interpreted to be the “native” groundwater component of the Quaternary aquifer from their plotted zones in PCA space, $\delta^2\text{H}-\delta^{18}\text{O}$ plots, and $\delta^{18}\text{O}-\text{Cl}^-$ plots. Overall, five different sources were introduced to the Quaternary aquifer in the area. Salinization, overexploitation and contamination from wastewater infiltration are found to be the main negative environmental impacts of land development as estimated from the end-members analysis while some irrigation practices, i.e., freshwater ponds, might have the positive ones.

From a broader point of view, these results confirm that an understanding of the mixing processes in heavily development lands of arid/semi-arid region is vital for the continued groundwater resource management in similar settings.

ACKNOWLEDGEMENTS

Firstly, I thank my God for giving me the strength and endurance to complete this research.

I want to begin this work by expressing my thanks and appreciation for the financial support I received for my PhD study from the Ministry of Higher Education at Egypt. Without their support, my ambition to study abroad can hardly be realized.

I would like to express my deep and sincere thanks, profound gratitude and deep appreciation to my supervisor, Prof. Tomochika Tokunaga, Department of Environment Systems, Graduate School of Frontier Sciences (GSFS), The University of Tokyo, for his superb supervision, guidance, constructive comments and encouragement. He taught me how to think, argue and write critically as a scientist. I am also very much indebted the many insights he has given me that helped in the overall content and direction of this research.

My deepest gratitude goes to Prof. Tomochika Tokunaga (The University of Tokyo), Prof. Jun Shimada (Kumamoto University), Prof. Kenichi Tonokura (The University of Tokyo), Prof. Shigeru Tabeta (The University of Tokyo), Prof. Jun Yoshinaga (The University of Tokyo), and Prof. Masaatsu Aichi (The University of Tokyo) for serving as thesis committee members and their valuable comments on my findings.

Working with my fellow Japanese and foreign students at the Geosphere Environmental Systems laboratory over the last four years has been one aspect of my graduate education that I treasure most. In particular, I would like to thank Yukiko Kusano, Yuki Suzuki, Sambo Lun and all other lab mates for their guidance, to operate instruments and valuable comments in reviewing the findings.

I would like to express my thanks to The University of Tokyo, Kashiwa Campus, for providing an opportunity to work in a learning environment that will always be an inspiration to me. The Department of Environment Systems at the Graduate School of Frontier Sciences (GSFS) was something of a second home for me and special thanks go to all departmental and administrative staff members who facilitated my

research and life in Japan over the last four years.

Special thanks are given to members of hydrology laboratory at the Kumamoto University, Japan, headed by Prof. Jun Shimada, for their guidance and help during the stable isotope measurement. I particularly appreciate the help and guidance of Saki Ito and Masahiro Tanoue during my visit to Kumamoto. Thanks also go to all the staff at the Environmental Science Center at The University of Tokyo, headed by Prof. Teppei Nunoura, for their help during water chemistry analyses.

My thanks and appreciation goes to Prof. Usama Massoud (National Research Institute of Astronomy and Geophysics, Helwan, Cairo), for his collaboration by doing the geophysical survey, data processing, and interpretation to support my PhD study.

I wish to express my gratitude to Prof. Esam El Sayed Ali (Minia University, Egypt), Prof. Ahmed F. Yousef (Desert Research center, Egypt), Prof. El Sayed M. Abu Ella (Assiut university, Egypt), Dr. Moustafa G. Snousy (Petrotrade company, Egypt), and Mr. Mohamed H. Farag (Petroleum Research Institute, Egypt) for their support, help, and their continuous encourage pursuing my goals.

Besides, my sincere thanks go to everybody in the Geology Department at Minia University, Egypt, for supporting this research.

I wish to express my gratitude to all members of my family (my Mum, brother and sisters) who supported me and encouraged me to continue my work. I would like to thank my wife, Dr. Arwa, for her love, patience, care, and support throughout my PhD study.

Finally, I thank the many friendly and helpful landholders of farms in the study area for providing me with access to their private groundwater wells.

Mahmoud Mostafa Khalil

----- **TABLE OF CONTENTS** -----

LIST OF FIGURES	VIII
LIST OF TABLES	XI
CHAPTER 1: INTRODUCTION	1
1.1. ARID REGION ISSUES	1
1.2. BACKGROUND AND PROBLEM STATEMENT	2
1.3. OBJECTIVES OF THE STUDY	4
1.4. STRUCTURE OF THE THESIS	4
1.5. REFERENCES	5
CHAPTER 2: STUDY AREA	14
2.1. LOCATION	14
2.2. CLIMATE	14
2.3. TOPOGRAPHY AND GEOMORPHOLOGIC SETTING	14
2.3.1. Upland area	15
2.3.2. Cairo-Suez foothills	15
2.3.3. Rolling plain (old Deltaic plain)	15
2.3.4. Nile Delta flood plain	15
2.3.5. The drainage basins	16
2.4. GEOLOGY	16
2.4.1. Neogene units	16
2.4.2. Quaternary units	16
2.4.2.1. Pleistocene deposits	16
2.4.2.1.1. Early Pleistocene	17
2.4.2.1.2. Late Pleistocene	17
2.4.2.2. Holocene deposits	17
2.5. GEOLOGICAL STRUCTURESS	17
2.6. LAND USE	18
2.7. HYDROLOGIC SETTING	19
2.7.1. Surface Water System	19
2.7.2. Aquifer System	20
2.7.2.1. Quaternary Aquifer (main)	20
2.7.2.2. Miocene Aquifer (local)	21
2.7.3. Aquifer Vulnerability	22
2.7.4. Hydro-environmental stresses and their sources	22
2.7.4.1. Wastewater disposal	22

2.7.4.2. Water-logging	25
2.7.4.3. The variation of water table levels	25
2.8. REFERENCES	27
CHAPTER 3: METHODOLOGY AND DATA COLLECTION	51
3.1. OFFICE WORK	51
3.1.1. Gathering data	51
3.1.2. Analysis of borehole data	51
3.1.3. Delineation of aquifer units	51
3.2. FIELD WORK	52
3.2.1. Water sampling	52
3.2.2. Field measurements	52
3.3. LABORATORY ANALYSES	53
3.3.1. Hydrochemistry	53
3.3.2. Environmental tracers	54
3.3.2.1. Background	54
3.3.2.2. Analytical techniques	57
3.4. MULTIVARIATE STATISTICAL ANALYSIS	58
3.4.1. Background	58
3.4.2. Checking the data adequacy	61
3.4.3. Statistical treatment of the dataset	62
3.5. REFERENCES	63
CHAPTER 4: RESULTS	80
4.1. CONVENTIONAL HYDROCHEMICAL ANALYSIS	80
4.2. CONVENTIONAL STABLE-ISOTOPIC ANALYSIS	82
4.3. MULTIVARIATE STATISTICAL ANALYSIS	83
4.3.1. Data preparation and analysis	83
4.3.2. Hierarchical cluster analysis (HCA)	85
4.3.3. Principal component analysis (PCA)	86
4.3.4. Re-evaluation of conventional hydrochemical and isotopic analyses	88
4.4. REFERENCES	91
CHAPTER 5: DISCUSSION	126
5.1. DETERMINATION OF END-MEMBERS AND MIXING PROCESSES	126
5.2. EVIDENCES FROM ^{14}C AND $\delta^{13}\text{C}$	128
5.3. POSSIBLE CONTAMINATION OF THE QUATERNARY AQUIFER	129
5.3.1. Indication of wastewater infiltration	129
5.3.2. Upconing of deep groundwater from the Miocene aquifer by pumping	130

5.4. ENVIRONMENTAL CONSIDERATIONS	131
5.5. REFERENCES	134
CHAPTER 6: CONCLUSIONS	142
6.1. RESEARCH OUTPUTS	142
6.2. RESEARCH APPLICATIONS	143
6.3. FUTURE WORK	143
Appendix A: WELL LITHOLOGIC DATA	144

----- LIST OF FIGURES -----

Fig. 1.1 Distribution of arid land. After Stevens (2011).	9
Fig. 1.2 A map showing temporal (1882-2012) expansion of land reclamation in the Nile Delta. Modified after Richards (1981) and Schewe (2012). Note: boundaries are estimations.	12
Fig. 1.3 A satellite map showing new reclaimed lands for urbanized and agriculture activities at the eastern fringe of the Nile Delta.	13
Fig. 2.1 Location map of the study area indicating the main land use divisions.	33
Fig. 2.2 A general SW-NE geologic cross section of the east Nile Delta. Modified after El-Shazly et al. (1975) (see Fig. 2.4 for the location).	34
Fig. 2.3 Geologic map of the east Nile Delta, simplified and modified from CONOCO (1987) and Research Institute of Groundwater (1992).	35
Fig. 2.4 Schematic correlation of rock units between the flood plain and the study area (modified after Geirnaert and Laeven, 1992).	36
Fig. 2.5 Temporal changes of the Landsat images of the study area for the dates 1978, 1990, 2000, and 2014.	37
Fig. 2.6 Field photographs of the freshwater ponds located northwest of the Tenth of Ramadan city.	38
Fig. 2.7 Distribution of the confinement conditions in the Quaternary aquifer of the east Nile Delta, modified after Sallouma (1983).	39
Fig. 2.8 Hydrogeological cross sections across the Ismailia Canal, modified after Sallouma (1983). See Figs. 2.4 and 2.5 for legend.	40
Fig. 2.9 Water table map of the Quaternary aquifer, south of the Ismailia Canal at year 2009. Modified after Misheloff (2010).	41
Fig. 2.10 Vulnerability map of the Quaternary groundwater aquifer in the east Nile delta, modified after Attia and Fadlelmawla (2005).	43
Fig. 2.11 Field photographs of (A) wastewater pond No. 1, (B) wastewater pond No. 2, and (C) wastewater pond No. 3.	44
Fig. 2.12 Estimated water inflow and outflow for the Tenth of Ramadan city.	46
Fig. 2.13 A field photograph of the water-logging (raised soil-water levels) problem at the center of the Tenth of Ramadan city.	47
Fig. 2.14 Water table map of the Quaternary aquifer with the progress of land use in the study area at 1991, modified after Research Institute of groundwater (1992).	49
Fig. 2.15 Water table map of the Quaternary aquifer with the progress of land use in the study area at 2008, modified after Saleh (2009).	50
Fig. 3.1 Location map of the available boreholes with lithologic data in the study area.	74

Fig. 3.2 Schematic drawings of the subsurface hydrogeological conditions of the study area.	75
Fig. 3.3 Location map of the sampling points.	76
Fig. 3.4 Flowchart of field and office measurements after each sampling day.	77
Fig. 3.5 Various processes which shift the $\delta^{18}\text{O}$ and $\delta^2\text{H}$ values from the meteoric water line (MWL). Modified after Yurtsever (1994) and Geyh (2000).	78
Fig. 3.6 Stable isotope composition ($\delta^{18}\text{O}$ or $\delta^2\text{H}$) versus salinity for the identification of different salinization processes: mixing of fresh water and seawater, dissolution of salt and leaching, and evaporation. Modified after Yurtsever (1994) and Geyh (2000).	79
Fig. 4.1 Representation of temporal change in the concentration of major ions for 14 groundwater samples from the Quaternary aquifer	95
Fig. 4.2 Piper diagram for the different water groups in the study area.	101
Fig. 4.3 Spatial EC distribution of the Quaternary aquifer in the area of study.	102
Fig. 4.4 $\delta^2\text{H}-\delta^{18}\text{O}$ diagram of groundwater from the Quaternary and the Miocene aquifers, surface water and waste water from the ponds.	103
Fig. 4.5 Spatial $\delta^{18}\text{O}$ distribution of the Quaternary aquifer in the area of study.	104
Fig. 4.6 Scatterplot matrix of nine variables for different water groups, i.e., Quaternary and Miocene aquifers, water from the Ismailia canal, old Nile water, and wastewater.	105
Fig. 4.7 Q-Q plot of the nine variables used for PCA	106
Fig. 4.8 Dendrogram for the groundwater samples from the Quaternary aquifer classified into four clusters. The horizontal broken line (<i>phenon line</i>) is an arbitrary line that defines clusters.	111
Fig. 4.9 Spatial distribution of four clusters in the groundwater of the Quaternary aquifer.	112
Fig. 4.10 Correlation circle of the nine variables and each of the PCs.	115
Fig. 4.11 Plot of principal component scores for the first two components for all water groups with groundwater samples from the Quaternary aquifer coded according to the HCA groupings.	116
Fig. 4.12 Piper diagram of the analyzed water samples with groundwater samples from the Quaternary aquifer coded according to the HCA groupings.	119
Fig. 4.13 Stiff diagrams of some selected samples in different water groups of the study area (see Fig. 4.6 for the legend sampling points).	120
Fig. 4.14 Spatial distribution of nitrogen components (as NO_3^- and NH_4^+) in groundwater from the Quaternary (coded according to HCA groupings) and the Miocene aquifers, surface water and wastewater from the ponds (see Fig. 4.6 for the legend sampling points).	121
Fig. 4.15 Cross plot of stable isotope data with groundwater samples from the Quaternary aquifer coded according to the HCA groupings.	122
Fig. 5.1 Cross plot of $\delta^{18}\text{O}-\text{Cl}^-$	137
Fig. 5.2 $\delta^{13}\text{C}$ as a function of (a) HCO_3^- concentration and (b) ^{14}C activities	138
Fig. 5.3 Geoelectric cross section of the area underlying the wastewater ponds, modified after	139

Massoud et al., in press.

Fig. 5.4 Conceptual groundwater flow model of the study area

140

----- **LIST OF TABLES** -----

Table 1.1 Population changes and predications in some developing countries since the beginning of the twentieth century (population in millions).	10
Table 1.2 Annual water use in some arid countries in million cubic meters (MCM) (from FAO AQUASTAT, 2000 and 2005)	11
Table 2.1 Factors affecting the groundwater vulnerability in the Nile Delta (after Khater, 2002)	42
Table 2.2 The characteristics of raw, primary and secondary treated combined domestic and industrial wastewater, taken from El Monayeri et al. (2011).	45
Table 2.3 Reclaimed area till 1990 in the eastern Nile Delta (Research Institute of groundwater/IWACO, 1991).	49
Table 4.1 Chemical and isotopic data of 14 groundwater samples collected from the Quaternary aquifer over two campaigns (2013 and 2014).	93
Table 4.2 Field-measured parameters, hydrochemical and isotopic characteristics of water samples.	96
Table 4.3 Descriptive statistics for the 82 samples from the Quaternary and Miocene aquifers, Water from the Ismailia canal, the old Nile water, and wastewater.	107
Table 4.4 Shapiro-Wilk test for normality for nine variables of the dataset.	108
Table 4.5 Spearman's correlation coefficients of the variables measured for 82 samples from the Quaternary and Miocene aquifers, Water from the Ismailia canal, the old Nile water, and wastewater.	109
Table 4.6 P-values of the calculated Spearman's correlation coefficients	110
Table 4.7 The calculated eigenvalues and their contribution to the total variance	113
Table 4.8 Component loadings, eigenvalues, explained variance, and cumulative percentages of variance for the two principal components (PC1 and PC2) after varimax normalized rotation.	114
Table 4.9 Average, median, and range values of the hydrochemical and stable isotopic composition of the four clusters in the Quaternary aquifer determined from HCA.	117
Table 4.10 Measured $\delta^{13}\text{C}$ (‰) and ^{14}C (pMC) in three groundwater clusters of the Quaternary aquifer.	123
Table 4.11 A summary table for EC (electric conductivity), hydrochemical and isotopic characteristics, and spatial location for different clusters defined in the groundwater of the Quaternary aquifer and water from other groups in the study area, i.e., the old Nile water, water from the Ismailia Canal, groundwater from the Miocene aquifer, and wastewater.	124
Table 5.1 Summary of end-members and possible mixing processes for four clusters defined for the groundwater in the Quaternary aquifer.	141

----- CHAPTER 1: INTRODUCTION -----

1.1. ARID REGION ISSUES

Arid region occupies about one third of the terrestrial Earth (Fig. 1.1) (Simmers, 2003; Şen, 2008; Stevens, 2011). Due to the extreme climate, most part of this arid area is barren desert and left for human challenge to reclaim it for their habitat (Wushiki, 2002). Many developing countries in arid regions have seen their population growth by more than fivefold. For example, Egypt, Iran, and Turkey, all had populations of between 9 and 14 million in 1900, yet by the mid-1900s, these figures had risen to more than 60 million and is predicted to be around 100 million by 2025 (Beaumont, 2001) (Table 1.1). The challenges caused by increases in population are compounded by current and future increases in water stress and limitation of water resources (WHO, 1997; Arnell, 1999). Particularly, the water resources in the Middle East and The Arabian Gulf are anticipated to decline in the next century due to a decrease of rainfall in the range between 10-25 %, and increases of evaporation between 5-20 %, which is being associated with a surge in the demand of water consumption (IPCC, 2008). Generally, the majority of countries located in arid zone depend either on groundwater (from both shallow and deep aquifers) (Table 1.2) or on desalinization for their water supply, both of which enable them to use water in amounts far exceeding the estimated renewable freshwater in the country (IPCC, 1997). Increased food production by agricultural expansion in addition to building new communities over the past several decades has been achieved in many arid areas through groundwater pumping. A demonstration of this is seen in desert reclamation projects in Egypt, Ministry of Jihad-e-Keshavarzi project in combating desertification in Iran, irrigation projects in southern Tunisia, Saudi Arabia, Syria, and Israel (Farshad et al., 2002; Elhadj, 2004; Nativ, 2004; Haddad et al., 2008). This increased demand creates associated problems. In some places, rising groundwater levels have induced water logging or salinization, but many aquifers throughout the world are being depleted at pumping rates in excess of natural recharge (Simmers, 2003). For example, in Egypt, Libya, and Saudi Arabia, groundwater abstraction exceeds the total availability of annual

renewable groundwater resources by between 300 and 900 % (Giordano, 2009). Aquifers have also been increasingly suffered from water quality impairment, but remedial procedures are expensive and slow to take their effect (Lerner et al., 1990; Merrick, 2000). Despite or because of these problems, the optimum course of action for sustainable water resources management in arid areas will in most cases be a ‘combination of surface- and groundwater use, with a range of storage options’ (Cosgrove and Rijsberman, 2000). However, for effective and sustainable management in arid regions, there is a need for proper understanding, continued monitoring, and a structured scientific assessment of the effects of human activities on land and water resources (Simmers, 2003).

1.2. BACKGROUND AND PROBLEM STATEMENT

As groundwater withdrawals increase, the need also increases for more precise hydrologic data to help refine management or protection decisions on water use (Plummer and Sprinkle, 2001). For the arid regions, data related to these issues are quite difficult to obtain because hydrogeological information and long-term series of observation data are usually missing (Fontes and Edmunds, 1989; Simmers, 2003). Other constraint is related to the groundwater recharge that can occur over a wider area under unconfined aquifer conditions and has a high sensitivity to small environmental changes; this, in turn, will make the recharge sources and mechanisms complex. These challenges are even more relevant for groundwater aquifers in areas that were historically called “deserts” and represent nowadays some of the most cultivated lands with high economic significance in arid environments, i.e., Tunisia, Egypt, Saudi Arabia, and Israel.

An imbalance between available land in the Nile Valley and Delta and a growing population has become and will be one of the most critical problems facing Egypt (Springborg, 1979). To address this issue, the Government of Egypt has created policies to reclaim areas which were originally deserts (Meyer, 1978; Wolff, 1993). The national strategy of Egypt for the expansion of agricultural land until 2017 aims at adding about 4.4 million acres in different regions, depending on land suitability and water

resources (Ismail et al., 2010). About 61% of the priority reclaimable land is located on the fringes of the Nile Delta region where water conveyors fed from the Nile, promising groundwater aquifers, wide plains with sandy soil, and relatively good accessibility are available (Biswas, 1993; El-Sayed et al., 2012).

In the Eastern Nile Delta region, the land reclamation projects in desert fringes and coastal zones started in the early 1950s but have rapidly increased since 1980 (Fig. 1.2) (Richards, 1981; Schew, 2012). As a result, desert fringe of the East Nile Delta, south of the Ismailia canal, is now home to many agricultural projects, i.e., El Adlia, El Mullak, Ramsis, El Shabab, El Shabab extension, and Orabi farms, in addition to new urbanized and industrial settlements, i.e., the Tenth of Ramadan city, El Obour city, Badr city, etc. (Fig. 1.3). These surface activities have expanded over the highly vulnerable Quaternary aquifer, the second water resource after the Nile River in Egypt, without proper protection and management plans (El Arabi, 1997). Salinization, contamination, upconing of deep saline water, and dramatic water level changes are the aspects of mismanagement of the Quaternary aquifer that may increase with continuous development and expansion of the area (Khalil et al., 2015). The problem becomes massive in the south, i.e., the Tenth of Ramadan city, due to water-logging and downward seepage from unlined wastewater ponds (Abd El-Samie et al., 2002; Khalil et al., 2015). Regionally, the future challenge to the sustainability of groundwater resources in these new lands will be likely the shortage of surface water supplies by the year 2017 to cope with the increasing demand (Ministry of Water Resources and Irrigation, 2005). This in turn will place significant pressure on groundwater aquifers and will result in more water quality and quantity degradation problems that have started to be a major concern globally (Foster and Chilton, 2003; Wada et al., 2010; Aeschbach-Hertig and Gleeson, 2012). Given the aforementioned complex set of environmental and anthropogenic issues pertaining to groundwater management, information on the mixing between source components in groundwater system is required for the scoping and implementation of management and protection initiatives to guarantee the sustainability of these new lands.

1.3. OBJECTIVES OF THE STUDY

The objectives of this research include developing a more comprehensive understanding of the groundwater recharge sources and their mixing processes in response to the progress of land development and subsequent human-induced activities in an arid to hyperarid environment. Hopefully, by doing so, more informed water resources management and environmental conservation plans could be decided to protect and sustain the new developed lands in arid settings.

1.4. STRUCTURE OF THE THESIS

This thesis contains six chapters. Chapter 1 provides an introduction to arid region issues, the research topic, and research objectives. Chapter 2 gives a summary of the basic geology, hydrogeology and hydro-environmental stresses of the study area. Methodology and data collection is presented in Chapter 3. Chapter 4 shows the results from hydrochemistry, environmental tracers and multivariate analysis. Discussion on the results and the environmental implications are presented in Chapter 5. Chapter 6 presents the main conclusions obtained from this thesis.

1.5. REFERENCES

- Abd El-Samie, S.G., Sadek, M.A., Mahmoud, N.S., 2002. Assessment of groundwater pollution from the oxidation ponds in Tenth of Ramadan city, using isotopic techniques and hydrogeological modeling. *Arab J. Nucl. Sci. appl.*, 35, 35-47.
- Aeschbach-Hertig, W., Gleeson, T. 2012. Regional strategies for the accelerating global problem of groundwater depletion. *Nature Geosciences*, 5(12), 853–861.
- Arnell, N. W., 1999. Climate change and global water resources. *Global Environ. Change*, 9, S31–S49.
- Beaumont, P., 2001. Water management issues in drylands in the twenty-first century. In *Water and Development. UNESCO – Encyclopaedia of Life Support Systems*.
- Biswas, A.K., 1993. Land resources for sustainable agricultural development in Egypt. *Ambio*, 22, 556–560.
- Clarke, J. I., Fisher, W. B. 1972. *Populations of the Middle East and north Africa. Africana*. New York.
- Cosgrove, W.J. and Rijsberman, F.R. 2000. *Making Water Everybody's Business. World Water Vision/World Water Council, Earthscan Publications Ltd, London, 108 pp.*
- El Arabi, N. E., 1997. Environmental impact of new settlements in Egypt. In: Chilton, J. et al. (Eds.), *Groundwater in the Urban Environment. Proc. of the 27th IAH Congress on Groundwater in the Urban Environment, Nottingham, UK, 21-27 September 1997, Rotterdam: A. A. Balkema, 1, 285-290.*
- Elhadj, E. 2004. *Camels Don't Fly, Deserts Don't Bloom: an Assessment of Saudi Arabia's Experiment in Desert Agriculture. School of Oriental and African Studies (SOAS)/King's College London, Univ. of London, Occasional Paper No 48: 1-38.*
- El-Sayed, M.H., El-Aassar, A.M., Abo El-Fadl, M.M., Abd El-Gawad, A.M., 2012. Hydrogeochemistry and pollution problems in 10th of Ramadan city, East El-Delta, Egypt. *J. Appl. Sci. Res.* 8, 1959–1972.

FAO , 2000 and 2005. AQUASTAT Main Database, Food and Agriculture Organization of the United Nations (FAO).

<http://www.fao.org/nr/water/aquastat/data/query/index.html;jsessionid=0D1CCA9760E0D5A22A90B4805F9FF9DF> accessed on December 3rd, 2015

Farshad, A., W. F. Erian, S. H. Zarei Abarghuei and D. P. Shrestha, 2002. Towards sustainable use of deserts. In: Proceedings 17th WCSS, 14-21 August 2002, Bangkok, Thailand, 683-1: 683-9.

Fontes, J.Ch. and Edmunds, W. M. 1989. The use of environmental isotopes in arid zone hydrology – a critical review. IHP-III. PROJECT 5.2. UNESCO, Paris, 75p.

Foster, S. S. D., Chilton, P. J. 2003. Groundwater: the processes and global significance of aquifer degradation. Philos Trans R Soc Lond B Biol Sci. Dec 29; 358 (1440),1957–1972.

Giordano, M. 2009. Global Groundwater? Issues and Solutions. Annual Review of Environment and Resources 34 (1) (November), 153–178.

Haddad, G., Szeles, I., Zsarnoczai, J.S. 2008. Water management development and agriculture in Syria. Bull. of the Szent István Univ., Gödöllő, 183-194.

IPCC (Intergovernmental Panel on Climate Change), 1997. An introduction to simple climate models used in the IPCC Second Assessment Report. In Houghton JT, Filho LGM, Griggs DJ, Maskell K, IPCC Working Group I. Available online at <http://www.ipcc.ch>.

IPCC (Intergovernmental Panel on Climate Change), 2008. Fourth assessment Report: climate change in the Middle East and North Africa," The World Bank.

Ismail, M., Nasr, Y.A., Kotb, Y. 2010. Assessment of Soils of Wadi El-Natron Area , Egypt Using Remote Sensing and GIS Techniques. Journal of American Science, 6(10), 195- 206.

Khalil, M. M., Tokunaga, T., Yousef, A. F. 2015. Insights from stable isotopes and hydrochemistry to the Quaternary groundwater system, south of the Ismailia canal, Egypt. J. Hydrol., 527, 555-564.

- Lerner, D.N., Issar, A.S. and Simmers, I. 1990. Groundwater Recharge. A Guide to Understanding and Estimating Natural Recharge. IAH-ICH 8, Verlag Heinz Heise, Hannover, 345 pp.
- Merrick, N.P. 2000. Optimization Techniques for Groundwater Management. unpublished Doctoral thesis, University of Technology, Sydney, NSW, Australia, 439 pp.
- Meyer, G., 1978. Erschliessung und entwicklung der agyptischen neulandsgebiete. Erdkunde 32, 212–227.
- Ministry of Water Resources and Irrigation (MWRI) 2005. National Water Resources Plan for Egypt – 2017, Ministry of Water Resources and Irrigation, Egypt. 268 p. Available online: <https://jkbharris.files.wordpress.com/2010/09/egypt-national-water-resources-plan-2017.pdf> Accessed on April 15th, 2015.
- Nativ, R. 2004. Can the desert bloom? Lessons learned from the Israeli case. Groundwater, 42, 651-657.
- Plummer, L.N., and Sprinkle. C.L. 2001. Radiocarbon dating of dissolved inorganic carbon in groundwater from confined parts of the Upper Floridan aquifer, Florida, USA. Hydrogeology Journal, 9, 127–150.
- Population Reference Bureau. 1995. World population data sheet. Washington, DC: Population Reference Bureau
- Richards, A. 1981. Egypt's Agricultural Development, 1800–1980. Technical and Social Change. Boulder, Colo., Westview Press, 296 p.
- Schewe, E. 2012. District Map of the Presidential Election in Lower Egypt: An Environmental History. Retrieved from <https://ericSchewe.wordpress.com/2012/07/07/district-map-of-the-presidential-election-in-lower-egypt-an-environmental-history/> accessed on October 5th, 2015.
- Şen, Z. 2008. Wadi Hydrology, CRC Press, New York, 347 p.
- Simmers, I., 2003. Understanding Water in a Dry Environment: Hydrological processes in Arid And

- Semi-Arid Zones. Intern. Assoc. Hydrogeologists/ A.A. Balkema Publ., Lisse, the Netherland, 341p.
- Springborg, R., 1979. Patrimonialism and policy making in Egypt: Nasser and Sadat and the tenure policy for reclaimed lands. *Middle Eastern Studies*, 15 (1), 49–69.
- Stevens, A. N. P. 2011. Factors affecting global climate. *Nature education knowledge* 3 (10):18. Available online at <http://www.nature.com/scitable/knowledge/library/factors-affecting-global-climate-17079163> accessed on October 11th, 2015.
- Wada, Y., van Beek, L. P. H., van Kempen, C. M., Reckman, J. W. T. M. Vasak, S. and Bierkens, M. F. P. 2010. Global Depletion of Groundwater Resources. *Geophysical Research Letters*, 37 (20). L20402, 5pp.
- WHO (World Health Organization), 1997. *Comprehensive Assessment of the Freshwater Resources of the World*. WHO, Geneva, 34 pp.
- Wolff, P., 1993. Land reclamation in Egypt. *Tropenlandwirt* 94, 103–117.
- Wushiki, H. 2002. Water in Arid Lands, in: Yoshida, N. (Ed.), *Hydrogen and Oxygen Isotopes in Hydrology*, UNESCO, 153-179.

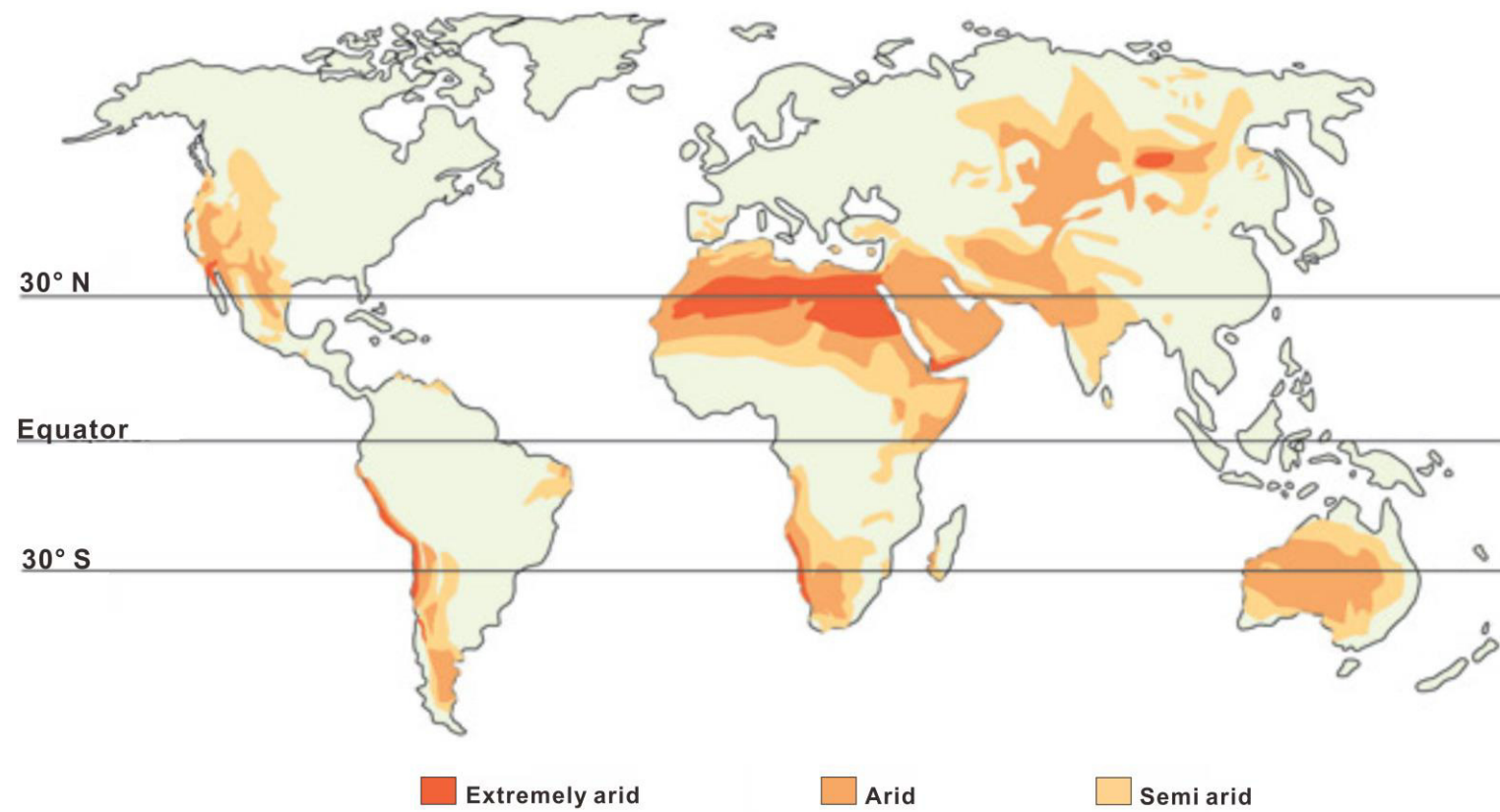


Fig. 1.1 Distribution of arid land. After Stevens (2011).

Table 1.1 Population changes and predictions in some developing countries since the beginning of the twentieth century (population in millions)

Country	1900s	Late 1930s	1960s	1985	1995	2010	2025
Turkey	13.9	17.8	31.4	50.7	61.4	79.2	95.6
Iran	9.9	14.6	25.1	49.7	61.3	83.7	106.1
Egypt	9.7	15.9	30.9	46.6	61.9	80.7	97.9

Source: Population Reference Bureau's 1995 World Population Data Sheet (<http://www.ucar.edu/communications/gcip/m9popgrowth/m9pdfc7.pdf>), Clarke and Fisher (1972), and Beaumont (2001).

Table 1.2 Annual water use in some arid countries in million cubic meters (MCM) (from FAO AQUASTAT, 2000 and 2005)

Source	Yemen	Tunisia	Saudi Arabia	Egypt
Surface water (MCM)	1,000	916	1,100	56,000
Groundwater (MCM)	2,400	1,900	21,400	9,252
Source	Oman	Iran	Morocco	Libya
Surface water (MCM)	0	40,000	9,430	170
Groundwater (MCM)	1,180	53,000	3,170	3,650

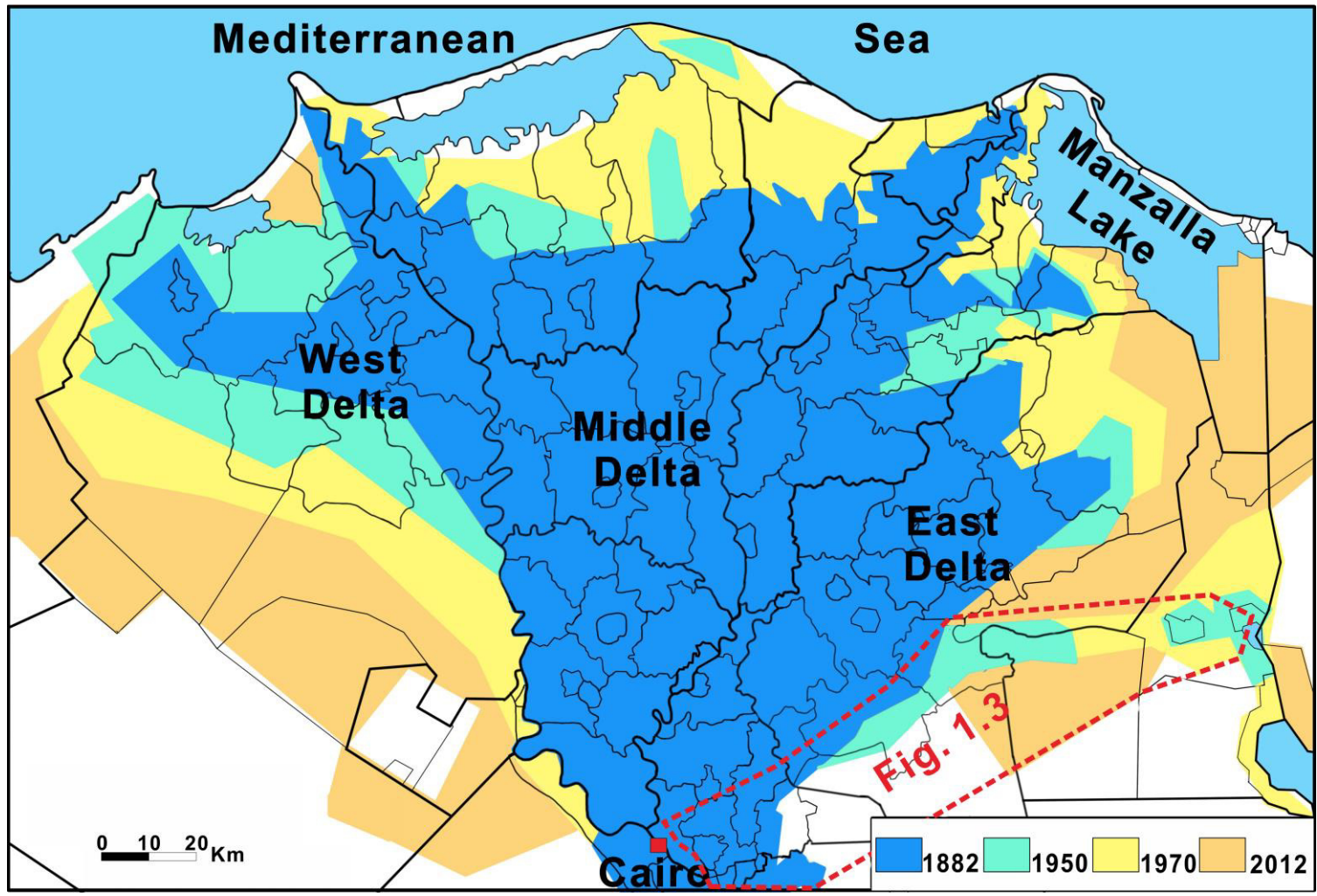


Fig. 1.2 A map showing temporal (1882-2012) expansion of land reclamation in the Nile Delta. Modified after Richards (1981) and Schewe (2012).

Note: boundaries are estimations.

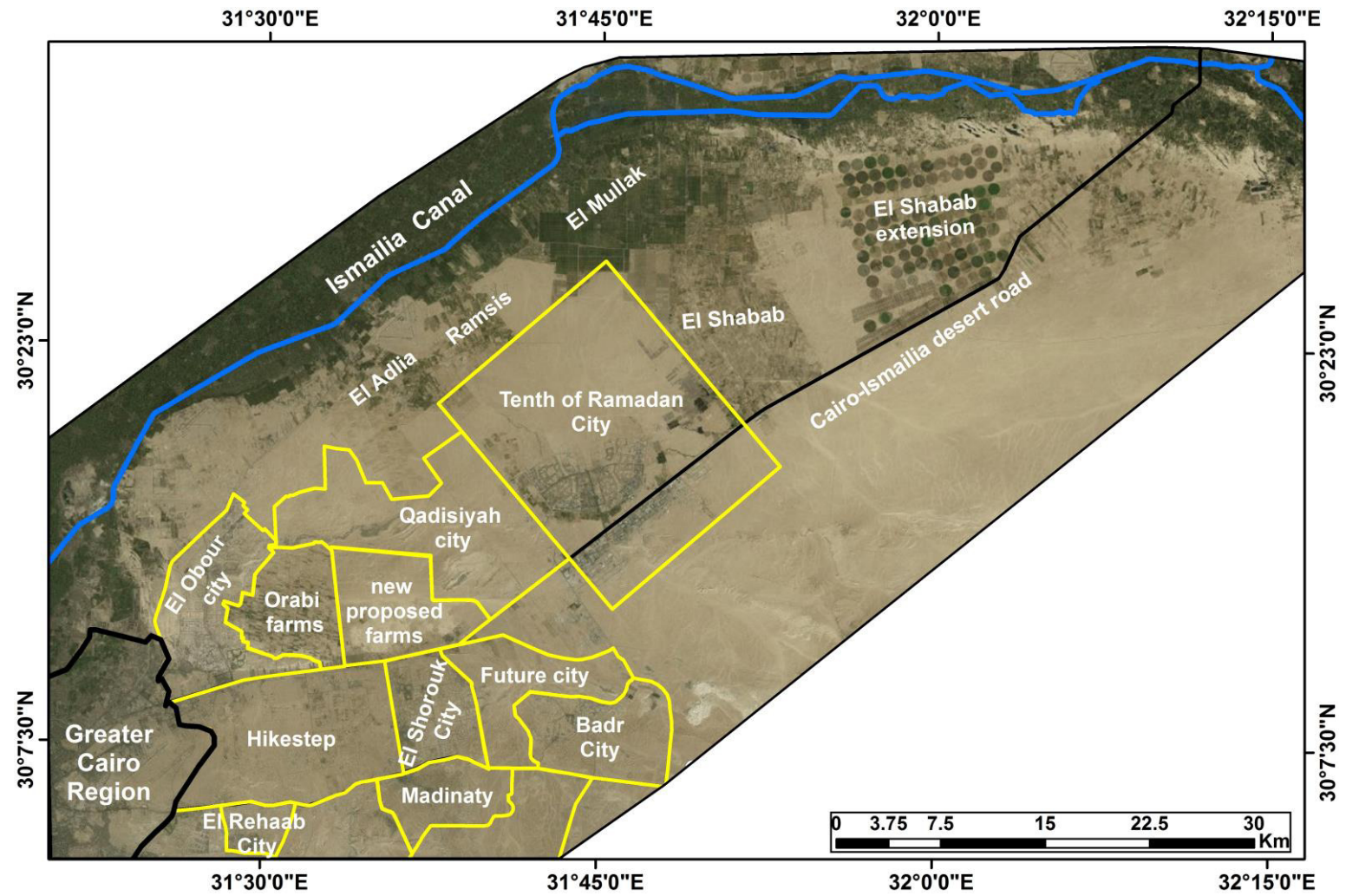


Fig. 1.3 A satellite map showing new reclaimed lands for urbanized and agriculture activities at the eastern fringe of the Nile Delta. See Fig. 1.2 for location

----- CHAPTER 2: STUDY AREA -----

2.1. LOCATION

The study area is located on the desert fringe of the East Nile Delta, Egypt. It covers an area of about 600 square kilometers and is enclosed between longitudes 31°34' and 31°56', and latitudes 30°15' and 30°27'. It is bordered to the north by the Ismailia Canal, to the west by Al Asher-Belbeis road, to the east by El Mullak and Shabab agricultural areas, and to the south by the Cairo-Ismailia desert road (Fig. 2.1).

2.2. CLIMATE

The area of study occupies a portion of the desert belt of Egypt. So, the climate of this area is a typical of arid desert which is characterized by hot, dry and rainless in summer (May–October), and cold, moist with some showers in winter (November–April). The average annual temperature, based on 10 years from 1990 to 2000, varies from 14°C (in January) to 29°C (through July and August) (El-Ghani et al., 2012). Mean daily evaporation based on climatological data (1990-2000) ranges between 9.1 mm/day in August to 5.2 mm/day in December (El-Ghani et al., 2012). All the precipitation falls during months from October to February with very low intensities. The mean precipitation is 13.2 mm/year (El-Ghani et al., 2012).

2.3. TOPOGRAPHY AND GEOMORPHOLOGIC SETTING

The area of study is considered as the transitional zone between the Eastern Desert to the south (high relief) and the Nile Delta (low relief) to the north (Gad, 1995). Elevation varies from less than 30 m above mean sea level near the Ismailia Canal to more than 180 m above mean sea level in the south and south-west (Fig. 2.1). Geomorphologically, the study area occupies a portion of the rolling plain of the old delta (El-Shazly et al., 1975). It is bounded by the Nile flood plain to the north and to the south by upland series and the foothills area. According to the previous studies (Shatta and El-Fayoumi, 1970; El Shazly et al. 1975), the area and its surroundings are discriminated into five major geomorphologic units (Fig. 2.2);

each has its own characteristics as indicated in the following brief description.

2.3.1. Upland area

It constitutes a series of disconnected elevated plateau that oriented in an east-west direction for a distance of about 135 km (Salluma, 1983). Their altitudes range from 150 m to 870 m (El Shazly et al., 1975). It is terminated northward by a steep scarps arranged in an echelon pattern and is dissected by relatively short and steep drainage lines (El-Fayoumi, 1968).

2.3.2. Cairo-Suez foothills

This unit forms the outer margins of the old Nile Delta. It occupies the foot slope of the southern uplands and is separated from upland area by a sharp fault escarpment. It stretches over 50 km distance in the N-S direction between latitude $30^{\circ} 00'$ and $30^{\circ} 15'$. It is represented by a series of elongated sub-parallel structural ridges of low relief, mostly oriented in WNW-ESE and E-W direction (El-Fayoumy, 1968; El-Shazly et al., 1975). On the northern limit, the ridges pass into the rolling plains of the old Delta through fault scarps of low relief. The average altitudes of these ridges range from 150 m to 200 m, and their lengths range from 20 to 50 km (El-Shazly et al., 1975).

2.3.3. Rolling Plain (Old Deltaic Plain)

This unit consists of the flat fluvial areas lying east of the present flood plain and extends from Cairo-Suez foothills in the south to the Ismailia Canal in the north (El-Fayoumy, 1968). The altitudes decrease gradually from 180 m to 40 m within a distance of 15 to 20 km with a roughly 7 m/km slope gradient (El-Shazly et al., 1975). Nowadays, vast areas of this plain have been progressively reclaimed for agriculture and new settlements.

2.3.4. Nile Delta flood plain

It represents the traditionally cultivated land area occupying the majority of the eastern Nile Delta region. The plain has a flat surface and very gentle northward slope (0.1m/km) (El-Fayoumy, 1968).

2.3.5. The drainage basins

In the study area, the surface of the rolling plain is incised by the downstream portions of two dry drainage channels, i.e., Wadi El Gafra and Wadi El Watan (Fig. 2.3).

2.4. GEOLOGY

As shown from the schematic lithostratigraphic correlation (Fig. 2.4) of the Nile flood plain and the eastern desert fringe (the study area), rock units that range in age from Eocene to Quaternary constitute the main lithostratigraphic units in the area of study (Said, 1990; Geirnaert and Laeven, 1992). The surface geological map (Fig. 2.3) shows the Quaternary (Pleistocene and Holocene) deposits extensively cover about 85% of the area, particularly to the north and east. Further to the south and southwest, Neogene rocks constitute piedmont slopes of foothills and cover about 15% of the total area (Said, 1981; Eleraki et al., 2010). The followings are the general description of the stratigraphic succession of formations in the studied area from old to young.

2.4.1. Neogene units

The Miocene deposits have a wide spatial distribution in the Neogene sequence. It is mainly represented by sandy limestones and sandy marls of shallow marine origin with variable intercalations of clays, sands and sandstones (El-Shazly et al., 1975). These deposits dominate major portion of the surface exposures in the southern high slopes overlying the Oligocene sands and gravels or basalt flows (Hefny et al., 1980). Sediments older than Miocene are not of interest to the purpose of this study.

2.4.2. Quaternary units

The Quaternary sediments have a great extension over the land surface and unconformably overlie the Neogene units. It can be classified into the following units.

2.4.2.1. Pleistocene deposits

These deposits are dominated by unconsolidated sands and gravels, with clay intercalations. According to their mode of formation, the Pleistocene sediments can be subdivided into two units (Fig.

2.2); Early and Late Pleistocene sediments (El-Fayoumy, 1968; El-Shazly et al., 1975).

2.4.2.1.1. Early Pleistocene

These deposits are thick gravelly sand and sandy gravel beds that are composed of coarse quartz sand, cherty and flinty pebbles, and igneous fragments together with few and occasional fossil wood remains (El-Fayoumy, 1968; El-Shazly et al., 1975). It wedges out on the northern rim of the southern structural ridges and increases the thickness in the northward direction (up to 500 m thickness) to form the bulk of the rolling plains region (El-Shazly et al., 1975). Gradual vertical and horizontal changes in grain size have been reported and the unit generally increases the grain size with depth and towards the east (El Fayoumi, 1968). Such deposits may be transported to the study area by the Nile River and by the local wadis (Sandford and Arkell, 1939; El-Fayoumy, 1968).

2.4.2.1.2. Late Pleistocene

It is composed of fluvial deposits which are dominated by fine to medium quartz sands with thin beds of silt and clay intercalations. These deposits constitute low terraces (30 to 40 m high) in the environs of wadi El Tumilat, north of the study area (El-Shazly et al., 1975).

2.4.2.2. Holocene deposits

The young deltaic (Nile silt, fine sands and clays) and wadi deposits (calcareous and ferruginous loamy sands, mixed with pebbles and rock fragments) are the forms of these deposits. Young deltaic deposits are distributed northward along the course of the Ismailia canal while wadi deposits occur in the course of large wadis (e.g., Wadi El Gafra). Generally, the thickness of these deposits is less than 5 m in the study area (El-Fayoumy, 1968).

2.5. GEOLOGICAL STRUCTURES

From the structural geological point of view, the east Nile Delta region is classified into two distinct tectonic zones, up-thrown south delta block and down-thrown north delta embayment separated by number of step faults (Said, 1981). Regionally, the study area is located within the up-thrown south

delta block (Fig. 2.2). The study area and its environ represent a wide northward sloping plain (El Shamy and Mohammed, 1999). Two fault sets, ENE-WSW (Syrian Arc Trend) and NW-SE (Suez Canal Trend), are dominated. They are mostly normal faults with vertical displacement ranging between 1 m and 100 m (El-Fayoumy, 1968; El Dairy, 1980). The ENE-WSW faults, most pronounced fault sets, configure a series of alternating uplifted and down-dropped blocks giving rise to the unique structural pattern and escarpments of the southern highland. Such faults are evident from the study of the Miocene and Eocene surface exposures (El-Fayoumy, 1968; El Dairy, 1980). The NW-SE faults represent the northern extension of the Gulf of Suez rift and probably configure the eastern low lands of the rolling plain and the flood plain (El Fayoumi, 1968; El Dairy, 1980; Geriesh, 1994). Unlike the southern highland, these faults are likely to exist in the subsurface underneath the Quaternary deposits of the rolling plain (El-Fayoumy, 1968; El-Shazly et al., 1975; Geriesh, 1994) (Fig. 2.2).

2.6. LAND USE

Unbalanced ratio between land resources and population has become and will be one of the most critical problems in Egypt. This imbalance and the continuous loss of land resources in the Nile Valley and Delta due to overpopulation justify the Government of Egypt to reclaim new lands through horizontal expansion policy (Meyer, 1978; Wolff, 1993). Priorities of land reclamation are given both to the west and east Nile Delta desert fringes (Fig. 2.1) due to the presence of good quality aquifers, wide plains with sandy soil, and relatively good accessibility (El Sayed et al., 2012). Land reclamation of the study area has been started 35 years ago and is still in progress as shown by multi-temporal Landsat images for the dates 1973, 1990, 2000 and 2014 (Fig. 2.5). The continuous reclamation activities in the study area have resulted in an agricultural zone in the north and a new settlement, the Tenth of Ramadan city, in the south (Fig. 2.1). Agriculture zone includes four agricultural projects, i.e., Adlia, Ramsis, El Mullak, and El Shabab, mostly in the lowlands nearby the Ismailia canal (Fig. 2.1). The Tenth of Ramadan city consists of three main parts; an urban zone together with two small industrial zones for

small-scale industries (north of the Cairo-Ismailia road), and a large industrial zone for all types of industries south of the road (Fig. 2.1) (El Arabi, 1997).

2.7. HYDROLOGIC SETTING

With the increase of the reclaimed lands, more and more water will be required for different uses. Furthermore, desert fringes of the eastern Nile Delta are a good example for water scarcity region where rapid population growth and many development projects are competing under the condition of limited water resources (Saleh, 2009). Here, the water resources can be divided into two systems; the surface water system and the aquifer system.

2.7.1. Surface Water System

Land reclamation projects along the fringes of the eastern Nile Delta depend mainly on the Ismailia Canal for their water needs. The Canal was constructed in 1862 for the Nile water supply in the area between Cairo and Ismailia. It is 128 kilometer long, and for much of its length, it was constructed through sandy strata. Particularly in the sandy areas, there is a significant amount of seepage from the Canal and this has contributed to the relatively high water table in the adjoining land. The original Canal depth is reported to have been 2-4 m and its width about 18 m (Abu-Zeid, 1983). Canal widening was completed in two stages to increase the capacity of the Canal so as to provide the expansion of water supplies to the irrigated area. The enlargement of the Canal has caused the cut-off of the low permeable layers deposited along the sides and the beds of the Canal. This has caused the total seepage rate to increase from 17.0 to 22.4 m³/sec after the completion of the second stage (Abu-Zeid, 1983). Recently, in order to satisfy the increased irrigation requirements in the study area, a number of lined canals branched out from the Ismailia Canal are constructed, i.e., El Shabab, and El Mullak canals (Fig. 2.1). Also, a group of freshwater ponds were placed west of the city (Fig. 2.6) to dispose of excess water during overproduction from the water purification stations.

2.7.2. Aquifer System

2.7.2.1. Quaternary Aquifer (main)

The Quaternary deposits constitute the main water-bearing formation in the study area. The aquifer is considered as an extension and part of the huge Nile Delta reservoir (Hefny et al., 1980). This extension lies between the Ismailia Canal in the north and the east-west faulted zone in the south (Fig. 2.2). Quaternary deposits, in the Delta and its adjacent desert fringes, show variable proportions of gravel, sands and clay in lateral and/or vertical directions (FAO, 1966; El Fayoumy, 1968; Hefny et al., 1980) that result in variations of hydraulic properties throughout the aquifer. The Quaternary aquifer has been classified into three hydrogeologic units, i.e., A (aquitard to aquiclude), B (aquifer) and C (main aquifer) units (El Fayoumi, 1968). The aquifer system in the study area consists of two hydraulically connected water-bearing layers, B and C units (Fig. 2.2). The lower layer (unit C) is composed of highly permeable Pleistocene graded sand and gravel of fluvial origin while the upper layer (unit B) is composed of fine to medium sands with clay intercalations (El Fayoumi, 1968; El-Shazly et al., 1975; Geriessh 1994; Ghodeif et al., 2013). The total saturated thickness of the Quaternary aquifer increases from south to north and northwest and becomes about 250 m near the Ismailia canal (El-Shazly et al., 1975; Hefny et al., 1980). The aquifer is unconfined due to the absence of unit A (El Fayoumi, 1968; El-Shazly et al., 1975; Hefny et al., 1980) and changes to the east, i.e., toward the Suez Canal, into variable confinement conditions (Fig. 2.7). In the vicinity of the Ismailia Canal (which runs through unit B), the aquifer is directly connected with the Canal, and the wells located nearby the Ismailia Canal show a depth to water to be less than 7 m (El Haddad, 1996; AlShahat et al., 2014). This is attributed to the presence of coarse sand in the banks and the bottom of the Ismailia Canal and the coarser facies of unit B (Abdulaziz, 2007). In the south of the Ismailia Canal, the change in the depth to water increases dramatically, i.e., 73 m and 67.5 m at the east and north of the Tenth of Ramadan city, respectively (AlShahat et al., 2014) that might be explained by the increase in ground elevation southward (180 m above mean sea level) due to the

presence of fault systems dominating the area. The aquifer is recharged mainly by the seepage from the Ismailia Canal, unlined irrigation canals and percolation of excess irrigation water (Hefny et al., 1980; Geirnaert and Laeven, 1992; Gad, 1995). Fig. 2.8 shows the interaction and connection between the Ismailia Canal and the groundwater system where the bottom of the Canal cuts through the sand and gravel of the Quaternary deposits allowing the free seepage of surface water down to groundwater. The regional flow of groundwater, before the reclamation, was directed to east and northeast (El Arabi, 1997). From the water table map (Fig. 2.9), the course of the Ismailia Canal constitutes a water divide with groundwater flow mainly from west to east in the study area. Based on the tracer technique using radioactive ^{131}I , the net seepage from the Ismailia canal was estimated to be $326 \times 10^6 \text{ m}^3/\text{year}$ which is equivalent to 8 % of the total flow (Hamza et al., 1988). Groundwater discharge takes place either naturally through natural outflow to the Suez Canal or artificially through pumping wells (Hefny et al., 1980). Groundwater abstraction from 24 wells at the well field situated at the northwest of the Tenth of Ramadan city (Fig. 2.1) is at around $60,000 \text{ m}^3/\text{day}$ (Shedid, 2005). Porosities of the Quaternary aquifer in the study area and its surroundings are reported to be 25% to 30%, horizontal and vertical hydraulic conductivities to be $8.7 \times 10^{-4} \text{ m/sec}$ and $2.9 \times 10^{-4} \text{ m/sec}$, respectively (Research Institute of Groundwater, 1994).

2.7.2.2. Miocene Aquifer (local)

The basal portion of the Pleistocene sediments rests unconformably on the Miocene aquifer. The latter attains extensive areal distribution to the south and to the west of the Tenth of Ramadan city. This aquifer is not fully understood due to the lack of detailed exploratory hydrogeological work. The Miocene aquifer is either unconfined or semi-confined depending on the occurrence of clay intercalations (Gomaa et al., 2003). The aquifer thickness is not accurately determined due to partial penetration of the wells. The depth to water varies from 160 m to 240 m along the Cairo-Ismailia desert road. The recharge of the Miocene aquifer is thought to be from precipitation in the past wet periods and to less extent from

irrigation water (El-Shazly et al., 1975; Gomaa et al., 2003). Groundwater in this aquifer flows from southeast to north and northwest (Abou Heleika and Atwia, 2014). Higher total dissolved ions (TDI), with large variability, were reported by Abou Heleika and Atwia (2014), and due to its low quality, abstraction from this aquifer is limited to irrigation after mixing the abstracted water with surface water.

2.7.3. Aquifer Vulnerability

Vulnerability of an aquifer is defined as the sensitivity of groundwater quality to an imposed contaminant load, which is determined by the intrinsic characteristics of the aquifer (Lobo-Ferreira, 1999). The thickness and hydraulic properties of the geologic formations above the aquifer, the unsaturated zone, and confining layers above the aquifer, are the key factors determining the vulnerability of an aquifer system (Harter and Walker, 2001). Within the Nile Delta region, the groundwater vulnerability to pollution is determined by the thickness of the clay layer, depth to groundwater, rate of recharge and direction of natural vertical groundwater flow (Table 2.1) (Khater, 2002). According to these parameters, the vulnerability increases from low in the northern part of the Nile Delta to moderate in the southern part and to high along the desert fringes of the Nile Delta (Fig. 2.10) (Khater, 2002).

2.7.4. Hydro-environmental stresses and their sources

2.7.4.1. Wastewater disposal

All types of wastewater from the Tenth of Ramadan city are discharged to the sewer network that finally leads to three unlined oxidation ponds (Fig. 2.1), and some of the wastewater were used directly for irrigation in between the early to late 1980s (El Arabi, 1997). The oxidation ponds (Fig. 2.11) were established at the eastern boundaries of the city with a design capacity of 60,000 m³/day, including anaerobic, facultative and maturation basins (El Monayeri et al., 2011). The location of the ponds is characterized by low altitude compared with the nearby residential area, and this allows the discharge to the ponds by gravity. During the last decades, the Tenth of Ramadan city has witnessed an explosive growing of Egyptian industry (more than 1130 industries). These large industrial compounds have

discharged a large amount of toxic persistent components either organic ones or heavy metals. El Monayeri et al. (2011) reported two sources of industrial wastewater. The first source includes industrial waste only (treated and untreated) with a flow rate of about 130,000 m³/day coming from heavy industrial zone (including food processing, dye and textile industry, glass factories, and oil industry) at the south of the city (Fig. 2.1). This sewerage system is directed to the pond No.3. The second source involves the industrial waste (including painting factories, food factories, textile, and chemical industry) coming from light industries within the residential zone of the city and is combined with domestic sewage. Despite the presence of independent networks for every area, the industrial and sanitary wastewaters are combined in the main common lines to go through gravity and pumping stations to the first and second stabilization ponds. The flow rate of the combined industrial and sanitary wastewater is estimated to be approximately 90,000 m³/day, 70 % - 80 % of which represents industrial wastewater (El Monayeri et al., 2011). Most of the factories violate the law (Decree 22, 2000) and do not apply any wastewater treatment for their liquid effluents (El Karamany, 2010), leading to the deterioration in the sewage pipe network and the increase of the environmental risk of wastewater seepage to subsurface. Currently, the efficiency of these three ponds is deteriorated due to hydraulic overloads and the lack of purification and maintenance ever since they have been established (El Monayeri et al., 2011). Moreover, some ponds have been being turned into forests full of trees, grass and ditch reed which affect the efficiency of treatment in these ponds. The effluent concentrations as displayed in Table 2.2 don't comply with the allowable standards (El Monayeri et al., 2011).

As an integrated part of the treatment system, the final effluent was planned to be used for irrigation of new reclamation schemes around the city (El Arabi, 1997; Misheloff, 2010). However, there are about 465 hectares close to the three ponds that are in use for storage and evaporation of wastewater instead of irrigation as planned (El Karamany, 2010). Consequently, flooding and overflow of wastewater to adjacent agricultural area happened as seen by the existence of the lands inundated by wastewater (Fig.

2.1).

To highlight the environmental impact of oxidation ponds, an overview of the water budget is estimated and presented for the Tenth of Ramadan city (Fig. 2.12). As the comprehensive information on the water volumes is not available, this overview is computed using 2007 census data (GOPP and JICA, 2008) and other reference data which are indicated in Fig. 2.12. Water supply was mainly secured from the Ismailia Canal, providing the city with roughly 184.4 million cubic metres per year (MCM/y) (GOPP and JICA, 2008). About 67% of this input is directed to residential and industrial purposes where about 20% is estimated to be consumed (GOPP and JICA, 2008). The total output of wastewater is about 99.2 MCM/y, in which about 21% is efficiently treated considering the pond's capacity and wastewater retention time within the pond system (28 days). About 59% of raw wastewater is over the capacity of the treatment system, and hence, it is either discharged directly to vast desert or inefficiently treated by accelerating the treatment process. Water losses from water mains and sewers are considered to be in the range 20% of the delivered water, however, high losses (40-50%) are reported to occur due to poor maintenance and rehabilitation (Attia, 1999; GOPP and JICA, 2008). The evaporation loss is estimated to be 2.1 MCM/y (10% of water delivered to ponds), based on the isotopic difference between inflow and outflow of ponds' water (Abd El-Samie et al., 2002).

Misheloff, (2010) detected various metals, including nickel, lead, and arsenic at low concentrations; and mercury and chromium at concentrations exceeding limits in groundwater at several localities surrounding the ponds, and it was considered to be due to poor disposal of industrial effluent or due to irrigation with poorly treated and/or raw wastewater.

In view of above, pollution risks to soil and groundwater are expected to become high due to high groundwater vulnerability to pollution within pond's vicinity, poor construction of ponds, the overflow of wastewater during peak water consumption and/or direct discharge, and utilization of wastewater prior to treatment (El Arabi, 1997; Margane, 2003; Misheloff, 2010). The problem of how to

accommodate large and growing water requirements (supply and disposal) will be further complicated with the continued rapid growth in population and industry.

2.7.4.2. Water-logging

Water-logging and flooding have occurred since 1998 near the center of the Tenth of Ramadan city (Fig. 2.13). From the local monitoring wells, depth to the subsoil water table was found to range from 1.2 to 3.2 m (Eleraki et al., 2010; Abou El-Magd, 2011). This water accumulates above the shallow (about 2 m depth) impervious layer (hydraulic conductivity is $< 1.2 \times 10^{-6}$ m/s) which prevents vertical infiltration, and water moves laterally to appear at the surface in low topographic locations as the hydraulic conductivity of the upper layers is high, ranging from 1.2×10^{-5} to 4.1×10^{-5} m/s (Eleraki et al., 2010; Abou El-Magd, 2011). The sources of soil water are attributed to the leaked water from water mains and sewers, flood irrigation of cultivated areas within the city and possibly the horizontal flow from the wastewater ponds in the east of the city (Research Institute of Groundwater, 2005; Eleraki et al., 2010).

2.7.4.3. The variation of water table levels

The first regional plan for the development of groundwater was drafted in 1980 for reclamation and cultivation of large desert areas along the fringes of the eastern Nile Delta (Farid and Tuinhof, 1991). Table 2.3 gives the average area of the cultivated land irrigated by groundwater for each project until 1990. These large-scale agricultural projects have changed groundwater quality by fertilizer and pesticide applications but have also changed groundwater quantity as shown by the drawdown of the water tables in the El Mullak and Ramsis areas (Fig. 2.14). Plans for further reclamation of about half a million feddans (210,000 hectares) are formulated by Research Institute of Groundwater/IWACO (1988). Accordingly, the Ministry of Water Resources and Irrigation (MWRI) plans to supply surface water to the areas in the eastern Nile Delta fringes by constructing branches from the Ismailia Canal to cope with the increase of water demand. As a result of long-term irrigation with surface water without proper drainage water system in the new reclaimed lands (e.g. Ramsis and El Mullak), groundwater table has been

elevated (Fig. 2.15), and soil salinization and water-logging have started to occur (Abou El Magd, 2011).

2.8. REFERENCES

- Abdulaziz, A. M., 2007. Applications of remote sensing, GIS, and groundwater flow modeling in evaluating groundwater resources: Two case studies; East Nile Delta, Egypt and Gold Valley, California. USA. PhD Thesis, University of Texas at El Paso, 402 p.
- Abd El-Ghani, M., Shehata, M. N., Mobarak, A., Bakr, R. 2012. Factors affecting the diversity and distribution of synanthropic vegetation in urban habitats of the Nile Delta, Egypt. *Rend. Fis. Acc. Lincei.*, 23, 327-337.
- Abd El-Samie, S.G., Sadek, M.A., Mahmoud, N.S., 2002. Assessment of groundwater pollution from the oxidation ponds in Tenth of Ramadan city, using isotopic techniques and hydrogeological modeling. *Arab J. Nucl. Sci. appl.*, 35, 35-47.
- Abou El-Magd, M. H., 2011. The Environmental Impact Assessment of Urbanization in the Eastern Nile Delta Fringes on Groundwater System (Case Study Tenth of Ramadan Region). Unpublished PhD Thesis, Fac. Eng., Menoufia Univ., Shebin El-Kom, Egypt, 234 p.
- Abou Heleika, M. M., Atwia, M. G. 2014. Integrated electrical resistivity and hydrogeological studies for delineating the Miocene aquifer at Eastern side of Nile Delta, Egypt. *Arab J. Geosci.*, 1-11.
- Abu-Zeid, M., 1983. The River Nile: Main water transfer projects in Egypt and impacts on Egyptian agriculture. In: Biswas, A. K., Dakang, Z., Nickum, J. E., Changming, L. (Eds.), *Long-Distance Water Transfer: A Chinese Case Study and International Experiences*, Dublin: Tycooly International, Ireland, pp. 15-34.
- Alshahat, F.M., Sadek, M.A., Mostafa, W.M., and Hagagg, K. 2014. Hydrogeochemical indicators for radioactive waste disposal site survey to the east of Nile Delta, Egypt. *Int. J. of current Engineering and Technology*, 4(2), 549-556.
- Attia, F. A. 1999. Water and development in Greater Cairo (Egypt). *Afers Internacionals*, 45-46, 81-102.
- Center for Arab Development Studies And Consultancy (CADSAC), 1994. Green belt development study

- at the Tenth of Ramadan city – final report (in Arabic). An internal report, 123 p.
- CONOCO, 1987. Geological Map of Egypt, 1: 500 000, sheet NH 36 NW Cairo.
- El Arabi, N. E., 1997. Environmental impact of new settlements in Egypt. In: Chilton, J. et al. (Eds.), Groundwater in the Urban Environment. Proc. of the 27th IAH Congress on Groundwater in the Urban Environment, Nottingham, UK, 21-27 September 1997, Rotterdam: A. A. Balkema, 1, 285-290.
- El Dairy, M.D. 1980. Hydrogeological studies on the eastern part of Nile Delta using isotope techniques. Unpublished M.Sc. Thesis, Fac. Sci., El-Azhar Univ., Egypt, 220 p.
- Eleraki, M., Gadallah, M., Gemal, K., Attwa, M. 2010. Application of resistivity method in environmental study of the appearance of soil water in the central part of Tenth of Ramadan City, Egypt. q. J. Eng. Geol. Hydrogeol., 43,171–184.
- El-Fayoumi, I. F. 1968. Geology of the groundwater supplies in the eastern region of the Nile delta and its extension in the north Sinai. Unpublished PhD Thesis, Fac. Sci., Cairo Univ., Egypt. 207 p.
- El-Haddad , I. M., 1996. Groundwater Sources and Soil Evaluation for the Tenth of Ramadan City Area and its Surroundings, Egypt. Unpublished M.Sc. Thesis, Fac. Sci., Mansoura Univ., Mansoura, Egypt, 199 p.
- El Karamany, H. 2010. Study for industrial wastewater treatment using some coagulants. Proceedings of the 14th International Water Technology Conference (IWTC), Cairo, Egypt, 283-291.
- El Monayeri, D. S., El Monayeri, O. D., EL Gohary, E. H., Aboul-fotoh, A. M. , 2011. Industrial wastewater treatment systems in Egypt: Difficulties and proposed solutions, in: Aysel, T. A., Subhas, K.S. (Eds.), Security of Industrial Water Supply and Management. Springer, pp. 209-230.
- El-Sayed, M.H., El-Aassar, A.M., Abo El-Fadl, M.M., Abd El-Gawad, A.M., 2012. Hydrogeochemistry and pollution problems in 10th of Ramadan city, East El-Delta, Egypt. J. Appl. Sci. Res., 8 , 1959-1972.

- El Shamy, I. Z. and Mohammed, S. M. 1999. Hydrogeochemical investigations for the groundwater at Cairo-Belbies district. 4th Intern. Conf. on Geochemistry, Alex. Univ., Egypt, 335-351.
- El-Shazly, E.M., Abdel Hady, M.A., El-Shazly, M.M., El-Ghawaby, M.A., El-Kassas, I. A., Salman, A.B., Morsi, M.A., 1975. Geological and Groundwater Potential Studies of El-Ismailia Master Plan Study Area. Rem. Sens. Res. Project, Acad. Sci. Res. and Techn., Cairo, Egypt, 24 p.
- FAO (Food and Agriculture Organization of the United Nations), 1966. High Dam soil survey project. Food and Agriculture Organization of the United Nations (FAO), Ministry of Agric., Egypt, 3, 1-348.
- Farid, M. S., Tuinhof, A. 1991. Groundwater development planning in the desert fringes of the Nile Delta. Water Science, special issue, 43-52.
- Gad, M. I., 1995. Hydrogeological studies for groundwater reservoirs, east of Tenth of Ramadan City and vicinities, Unpublished M.Sc. Thesis, Fac. Sci., Ain Shams Univ., Egypt, 187 p.
- Geirnaert, W., and Laeven, M. P. 1992. Composition and history of ground water in the western Nile Delta. J. Hydrol., 138 (1), 169-189.
- Gerisesh, M. H., 1994. Hydrogeological and hydrogeochemical evaluation of groundwater resources in the Suez Canal region, Unpublished PhD Thesis, Fac. Sci., Suez Canal Univ., Egypt,
- Ghodeif, K. O., Arnous, M. O., Geriesh, M. H. 2013. Define a protected buffer zone for Ismailia Canal, Egypt using Geographic Information Systems. Arab J Geosci., 6, 43-53.
- General Organization for Physical Planning (GOPP) and Japan International Cooperation Agency (JICA), 2008. The strategic urban development master plan study of the Greater Cairo region in the Arab Republic of Egypt-Final Report (in Arabic), 2, pp. 182-221.
- Gomaa, M.A., Sadek, M.A., Ezz El Din, H. 2003. Delineation of paleowater-recent water interface, using isotopic and hydrochemical techniques at Heliopolis basin and its surroundings, east Delta, Egypt. Isotope and Radiation research, 35 (3), 465-488.
- Greish, M. H. 1994. Hydrogeological and hydrogeochemical evaluation for the groundwater resources in

- the Suez Canal region, Egypt. Unpublished PhD Thesis, Fac. Sci., Suez Canal Univ., Egypt, 100 p.
- Hamza, M. S., Aly, A. I. M., Nada, A. A., Awad, M. A. & Swailem, F. M. 1988. Estimation of seepage from Ismailia Canal using Iodine-131. *Isotopenpraxis Isotopes in Environmental and Health Studies*, 24 (3), 110-114.
- Harter, T., Walker, L. G. 2001. Assessing vulnerability of groundwater. U.S. Nat. resources Conservation Service, Washington DC.
- Hefny, K., Farid, M.S., Morsi, A., Khater, A.R., El-Ridi, M.R, Khalil, Z.B., Atwa, A. Attia, D., 1980. Groundwater Studies for the Tenth of Ramadan City. Unpublished internal rept., Research Institute for Groundwater, Ministry of Public works and Water Researches, El Kanater, Cairo, Egypt, 54 p.
- Khater, AR, 2002. Evaluation of the current practice of groundwater monitoring and protection in Egypt. Submitted to the Arab Centre for the Study of Arid Zones and Dry Lands (ACSAD). ACSAD-BGR Technical Cooperation Project, vol. 5, Annex C-2
- Lobo-Ferreira JP 1999. The European Union experience on groundwater vulnerability assessment and mapping. – COASTIN A Coastal Policy Research Newsletter 1: 8–10.
- Margane A. 2003. Guideline for Groundwater Vulnerability Mapping and Risk Assessment for the Susceptibility of Groundwater Resources to Contamination. – Unpublished report prepared by ACSAD & BGR, Technical Cooperation Project 'Management Protection and Sustainable Use of Groundwater and Soil Resources in the Arab Region, 177 p, Damascus.
- Meyer, G., 1978. Erschliessung und entwicklung der agyptischen neulandsgebiete. *Erdkunde* 32, 212–227.
- Misheloff, R. 2010. Integrated water resource management II feasibility of wastewater reuse. United States Agency for International Development (USAID). Report No. 14. 809 pp.
- Research Institute of Groundwater /IWACO, 1988. Groundwater development in the eastern Nile Delta. Identification of policy options, TN 70.120-88-06. Research Institute for Groundwater, El-Khanatar,

Cairo, Egypt.

Research Institute of Groundwater /IWACO, 1991. Development and management of groundwater resources in the Nile Valley and Delta. TN 77.01300-91-11. Research Institute for Groundwater, El-Khanatar, Cairo, Egypt.

Research Institute for Groundwater, 1992. Hydrogeological map of Nile Delta, Scale 1:500.000, 1st Ed., Research Institute for Groundwater, El-Khanatar, Cairo, Egypt.

Research Institute of Groundwater, 1994. Extraction of groundwater east Nile Delta, Unpublished Internal Report, Research Institute for Groundwater, Ministry of Public works and Water Researches, El-Khanatar, Cairo, Egypt.

Research Institute of Groundwater, 2005. Study of Groundwater Rising Problem in Tenth of Ramadan City. Unpublished internal report, Development. Soc. of Tenth of Ramadan City, Egypt.

Said, R., 1981. The Geological Evolution of the River Nile. Springer, New York, 151p.

Said, R., 1990. The Geology of Egypt. A. A. Balkema, Rotterdam, 734 p.

Saleh, W. S. M. A. 2009. Environmental management of groundwater resources in the Nile Delta region. Unpublished PhD Thesis, Fac. Eng., Cairo Univ., Egypt. 266 p.

Sallouma, M. K. 1983. Hydrogeological and hydrogeochemical studies east of the Nile Delta. Unpublished PhD Thesis, Fac. Sci., Ain Shams Univ., Cairo, Egypt.

Sandford, K. S., Arkell, J. W. 1939. Palaeolithic man and the Nile Valley in Lower Egypt with some notes upon a part of the Red Sea littoral, Oriental Inst., Chicago, Publ. 46.

Shata, A., El-Fayoumi, I. 1970. Remarks on the regional geological structure of the Nile Delta. In Hydrology of Deltas, IASH/UNESCO Bucharest Symposium. Paris: UNESCO, I, 189–197.

Shatta, A. A., Abdel Salam, A. A., Harga A. A. and others 1979. Soil map of the Eastern Delta Region, El Tumilat-Suez, 4th Report. Academy of Scientific Research Technology, Cairo – Egypt. Internal Report, 89-105.

- Shedid, A.G., 2005. Impacts of oxidation ponds on groundwater chemistry in the Tenth of Ramadan City, Egypt. Proc. of the 4th International Conference on the Geology of Africa, Geol. Dept., Fac. Sci., Assiut Univ., Assiut, Egypt, 2, 145-164.
- Wolff, P., 1993. Land reclamation in Egypt. Tropenlandwirt 94, 103–117.

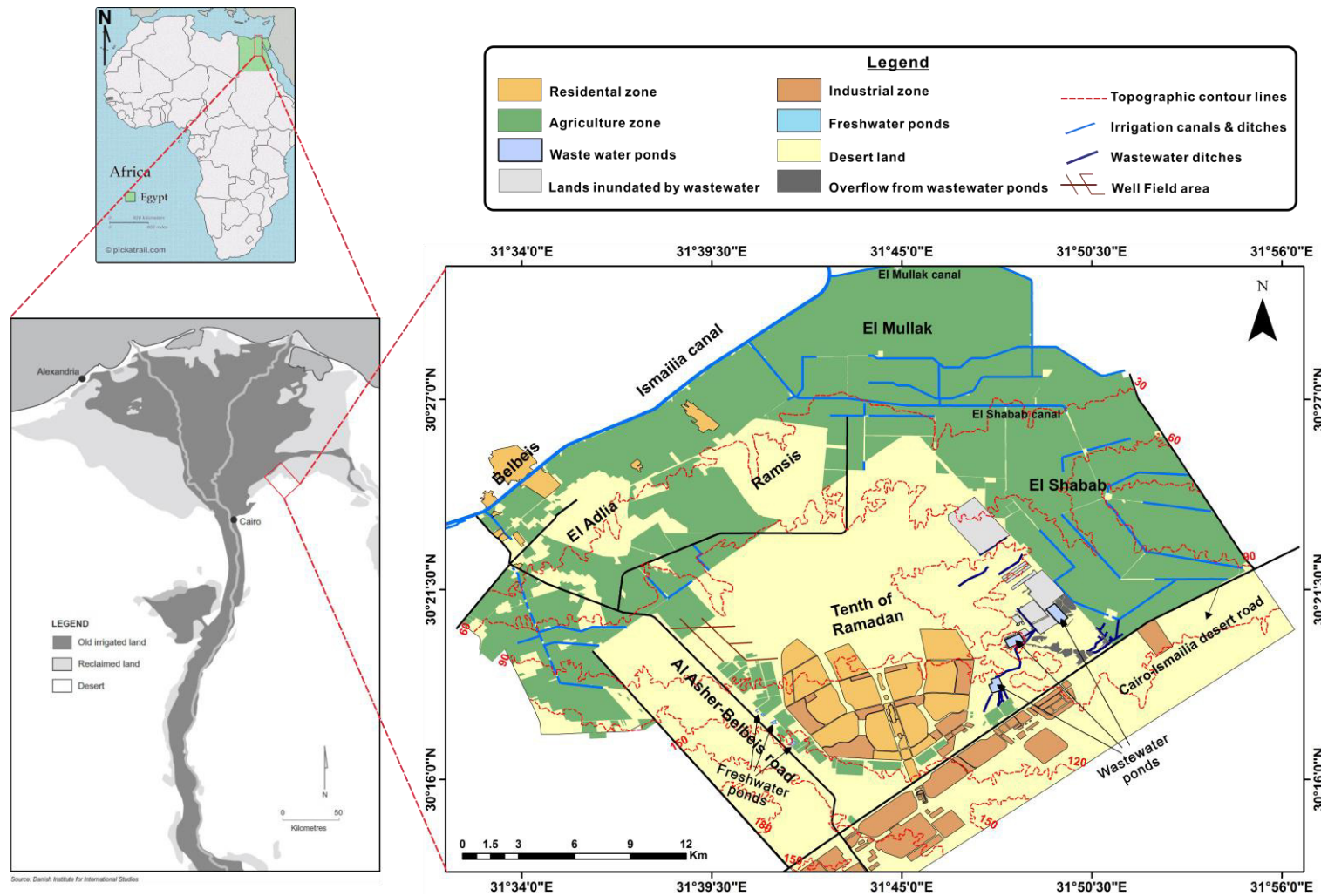


Fig. 2.1 Location map of the study area indicating the main land use divisions.

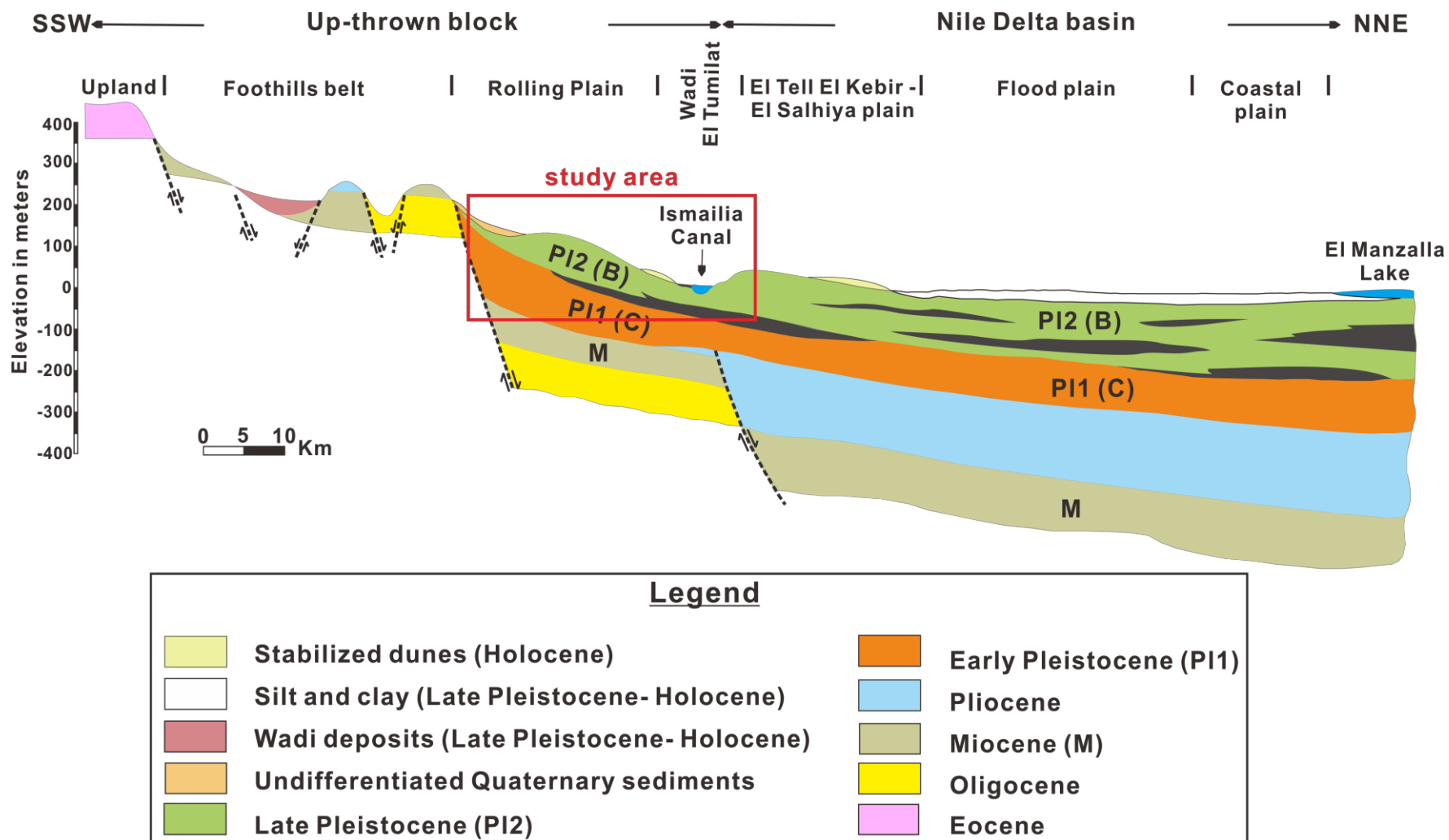


Fig. 2.2 A general SW-NE geologic cross section of the east Nile Delta. Modified after El-Shazly et al. (1975) (see Fig. 2.3 for the location).

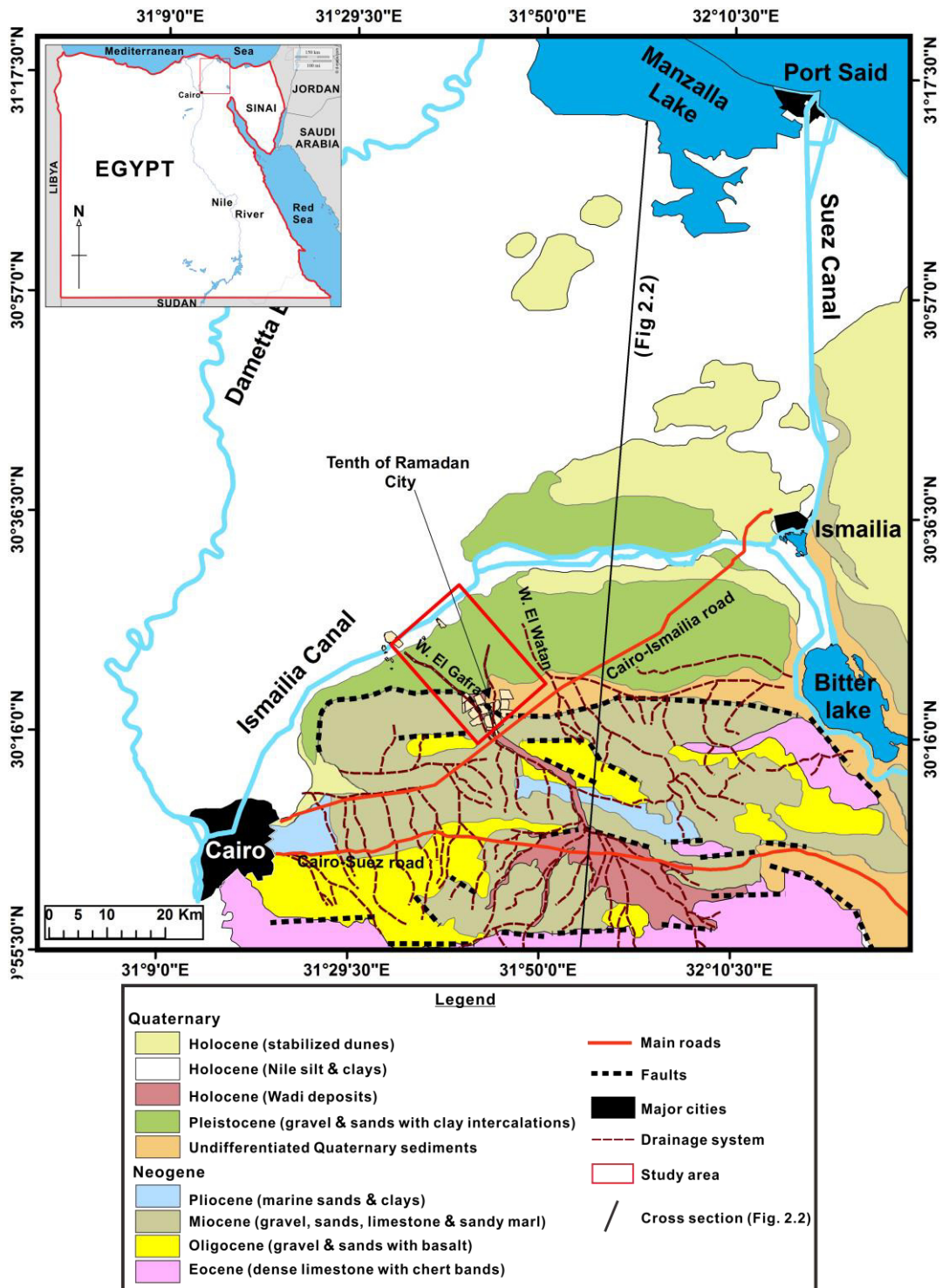


Fig. 2.3 Geologic map of the east Nile Delta, simplified and modified from CONOCO (1987) and Research Institute of Groundwater (1992).

Age	Nile Delta floodplain	Eastern desert fringe (the study area)
Holocene	Clay and silt up to 50 m (Nile Delta floodplain and coastal plain)	No deposits/dunes
Pleistocene	Sand and gravel up to 500 m thick (Nile Delta floodplain and coastal plain)	Sand and gravel up to 300 m thick (rolling plains)
Pliocene	Marine clays up to 1000 m thick	sandy/clayey deposits up to 100 m thick (foothills)
Miocene	Clays up to 1000 m thick	Detrital carbonates up to 120 m thick (foothills)
Oligocene	Lacustrine deposits	Basalt (El-Mokattam-Ataka upland) Fluviatile sands (El-Mokattam-Ataka upland)
Eocene		limestone (El-Mokattam-Ataka upland)


Legend	
	<p>Good aquifer</p> <p>Aquitard</p> <p>limited aquifer</p>

Fig. 2.4 Schematic correlation of rock units between the flood plain and the study area (modified after

Geirnaert and Laeven, 1992)

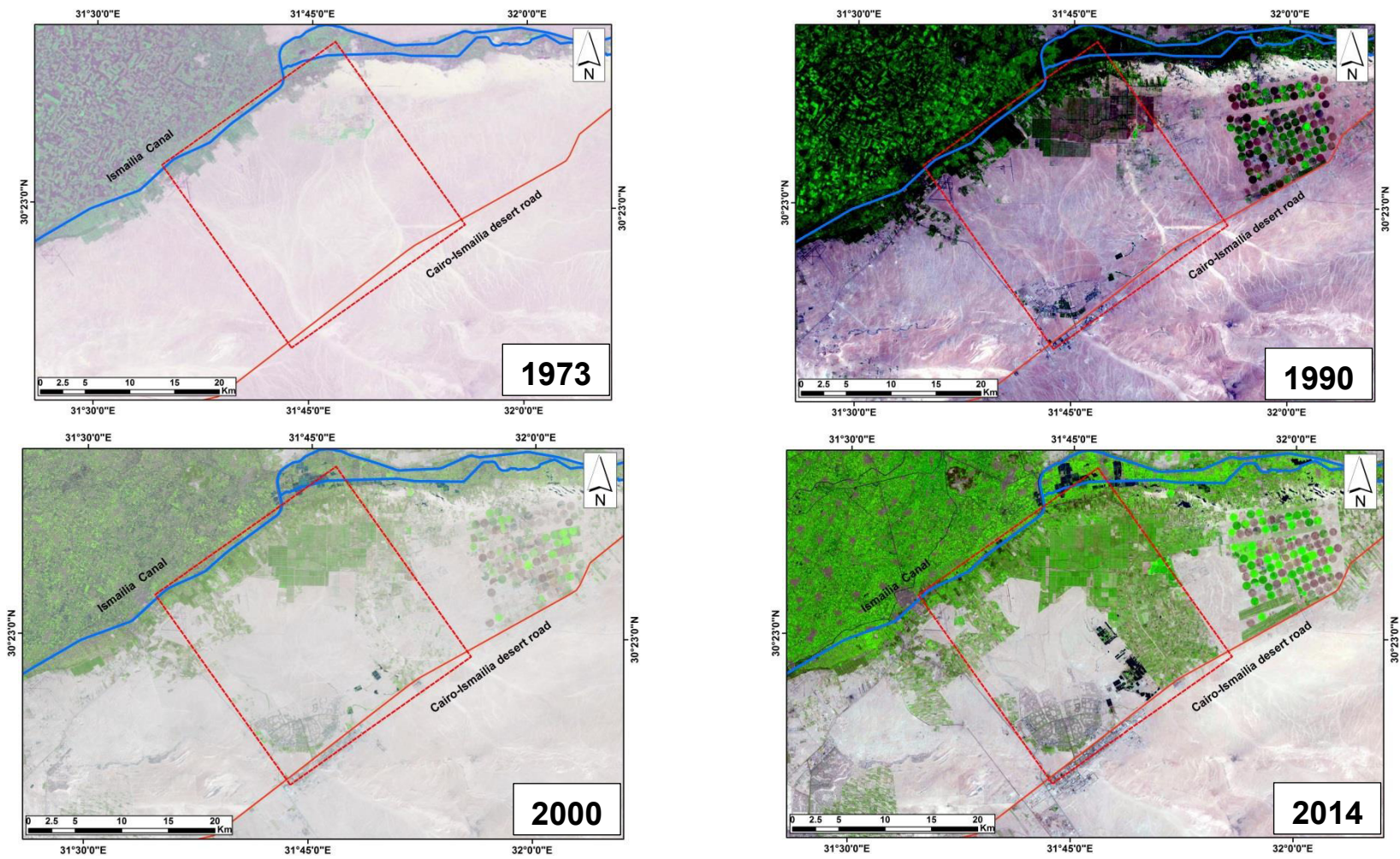


Fig. 2.5 Temporal changes of the Landsat images of the study area for the dates 1978, 1990, 2000, and 2014.



Fig. 2.6 Field photographs of the freshwater ponds located northwest of the Tenth of Ramadan city.

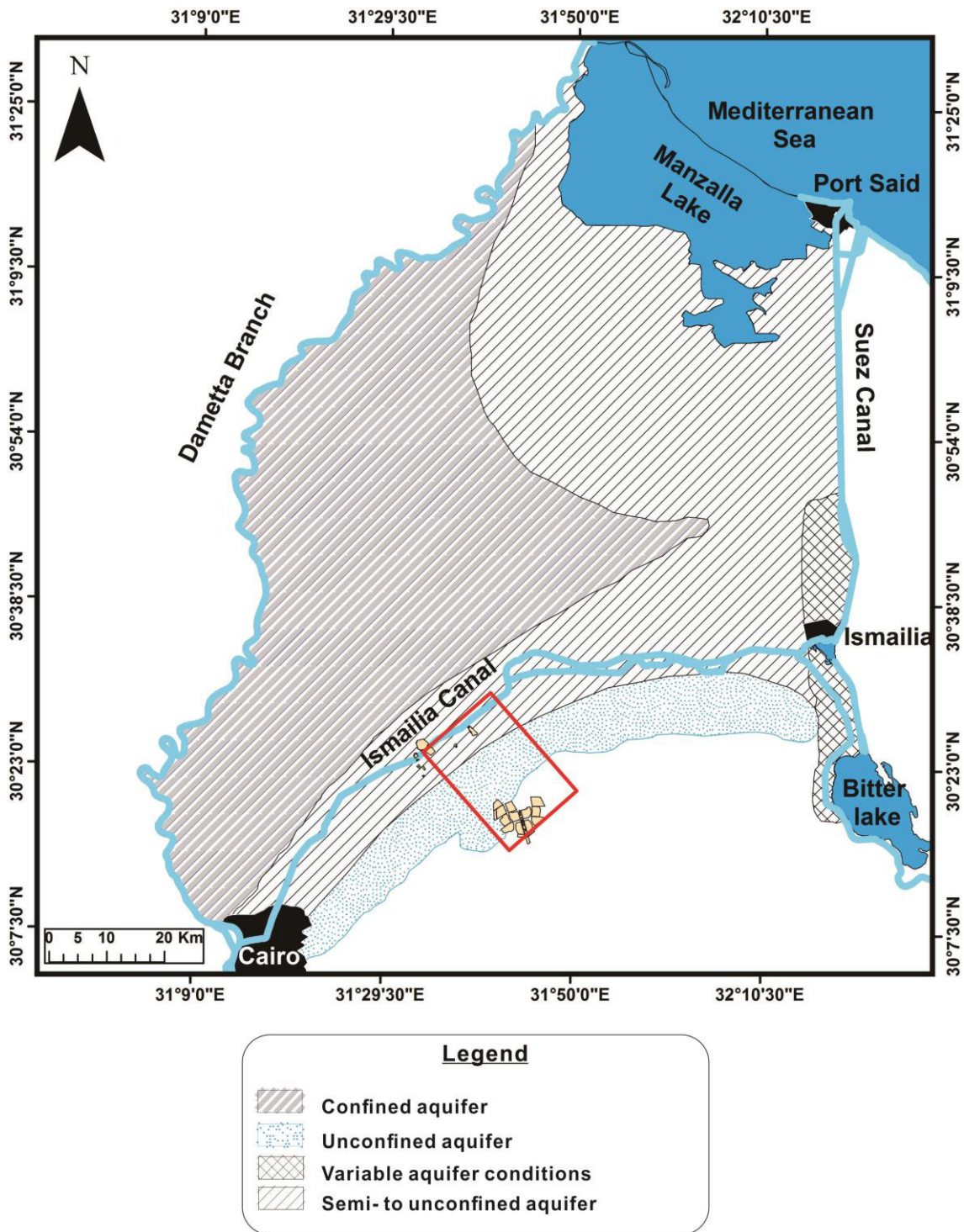


Fig. 2.7 Distribution of the confinement conditions in the Quaternary aquifer of the east Nile Delta, modified after Sallouma (1983).

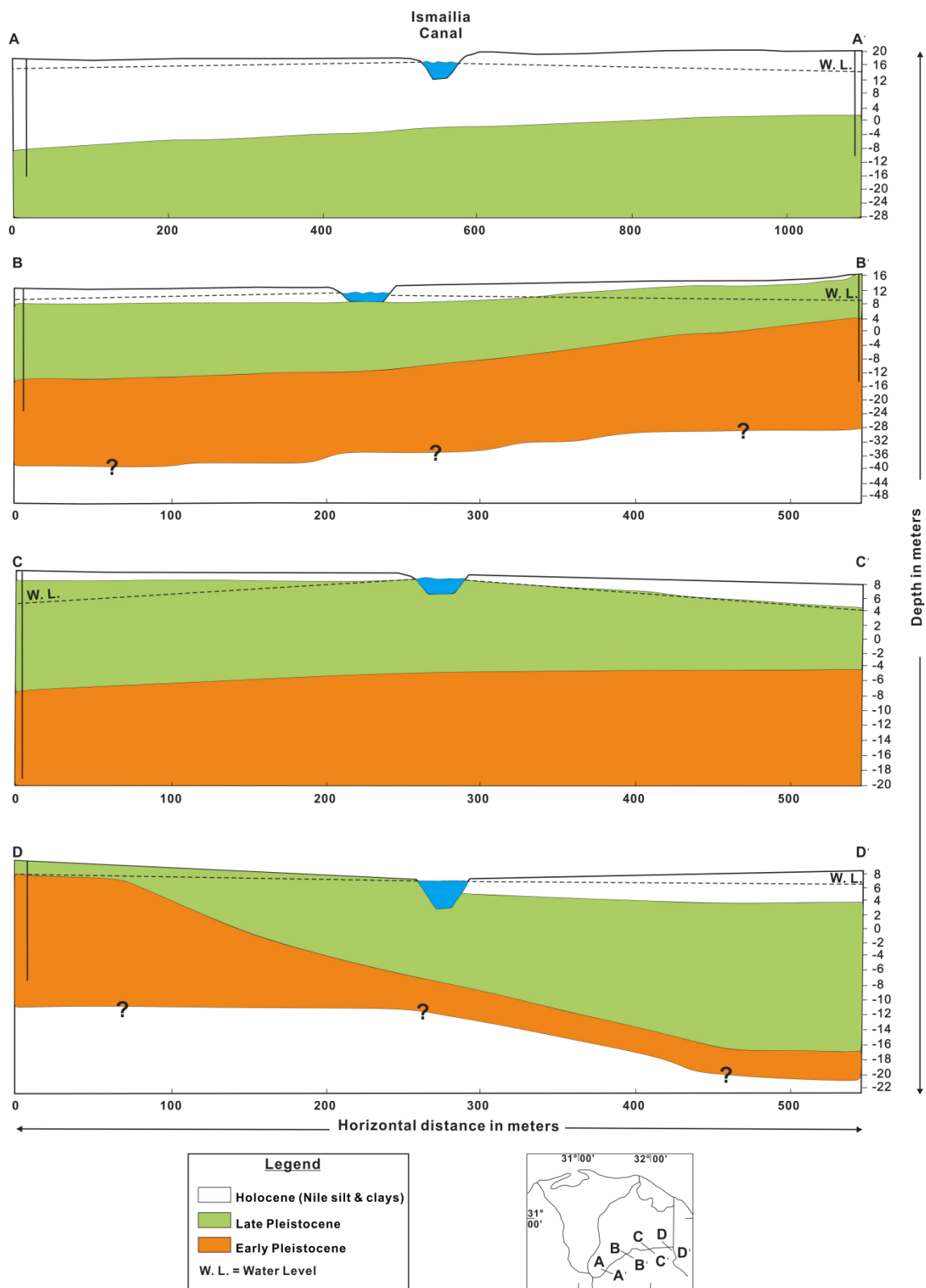


Fig. 2.8 Hydrogeological cross sections across the Ismailia Canal, modified after Sallouma (1983).

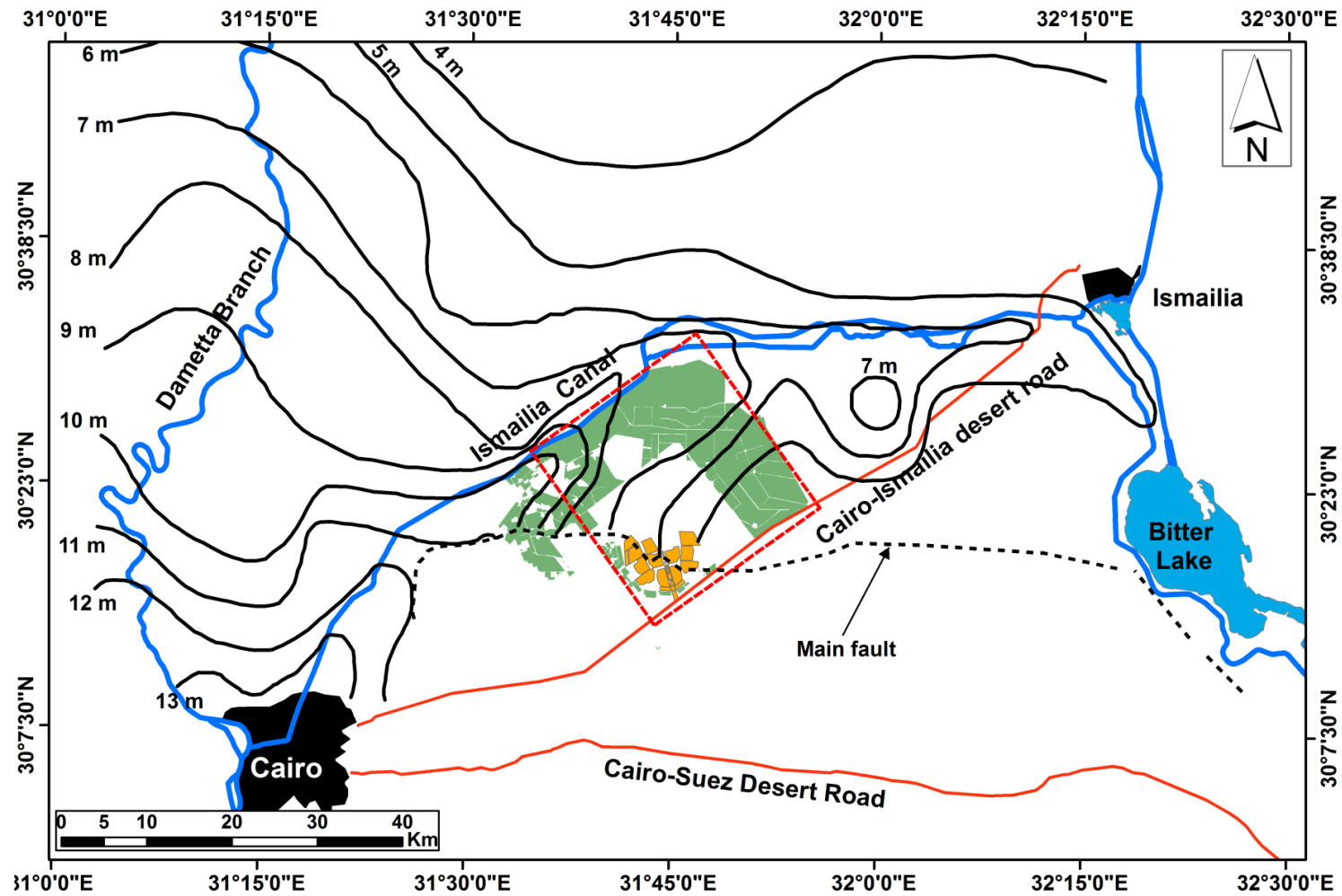


Fig. 2.9 Water table map of the Quaternary aquifer, south of the Ismailia Canal at year 2009. Modified after Misheloff (2010).

Table 2.1 Factors affecting the groundwater vulnerability in the Nile Delta (after Khater, 2002)

Thickness of the clay cap (m)	Vertical groundwater flow	Rate of recharge (mm/day)	Depth to groundwater from surface (m)	Groundwater vulnerability	Location
0	Downward	--	<5	High	Transition zone between old and reclaimed land
0-2	Downward	>1	5-15	High	Transition zone
0	Downward	<1	>15	Moderate-high	Desert fringes
0-10	Downward	<1	<5	Moderate-low	Flood plain and partially transition zone
>10	Downward	0.25-1	<5	Low	Flood plain
0-10	Upward	<25	<5	Low	North Delta (Flood plain)

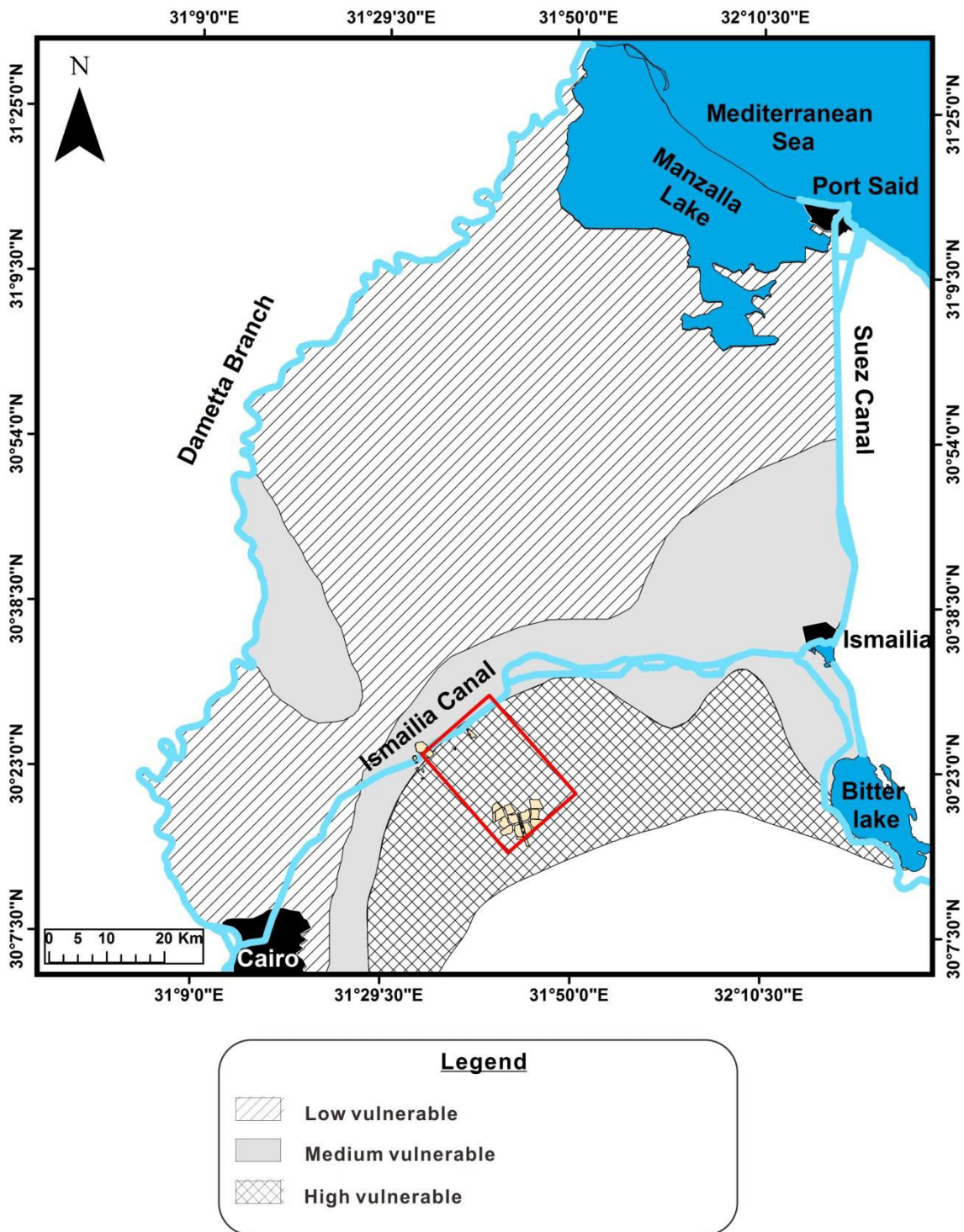


Fig. 2.10 Vulnerability map of the Quaternary groundwater aquifer in the east Nile delta, modified after Khater (2002).

(A)



(B)



(C)



Fig. 2.11 Field photographs of (A) wastewater pond No. 1, (B) wastewater pond No. 2, and (C) wastewater pond No. 3.

Table 2.2 The characteristics of raw, primary and secondary treated combined domestic and industrial wastewater, taken from El Monayeri et al. (2011).

Analysis	Raw wastewater	Primary treated wastewater	Secondary treated wastewater	Required wastewater characteristics according to law 48/1984
COD (ppm)	814-1,542	650-1,033	340-676	80
BOD (ppm)	420-780	260-620	190-300	60
TSS (ppm)	220-440	154-220	160-290	50

COD: Chemical Oxygen Demand

BOD: Biochemical Oxygen Demand

TSS: Total Suspended Solids

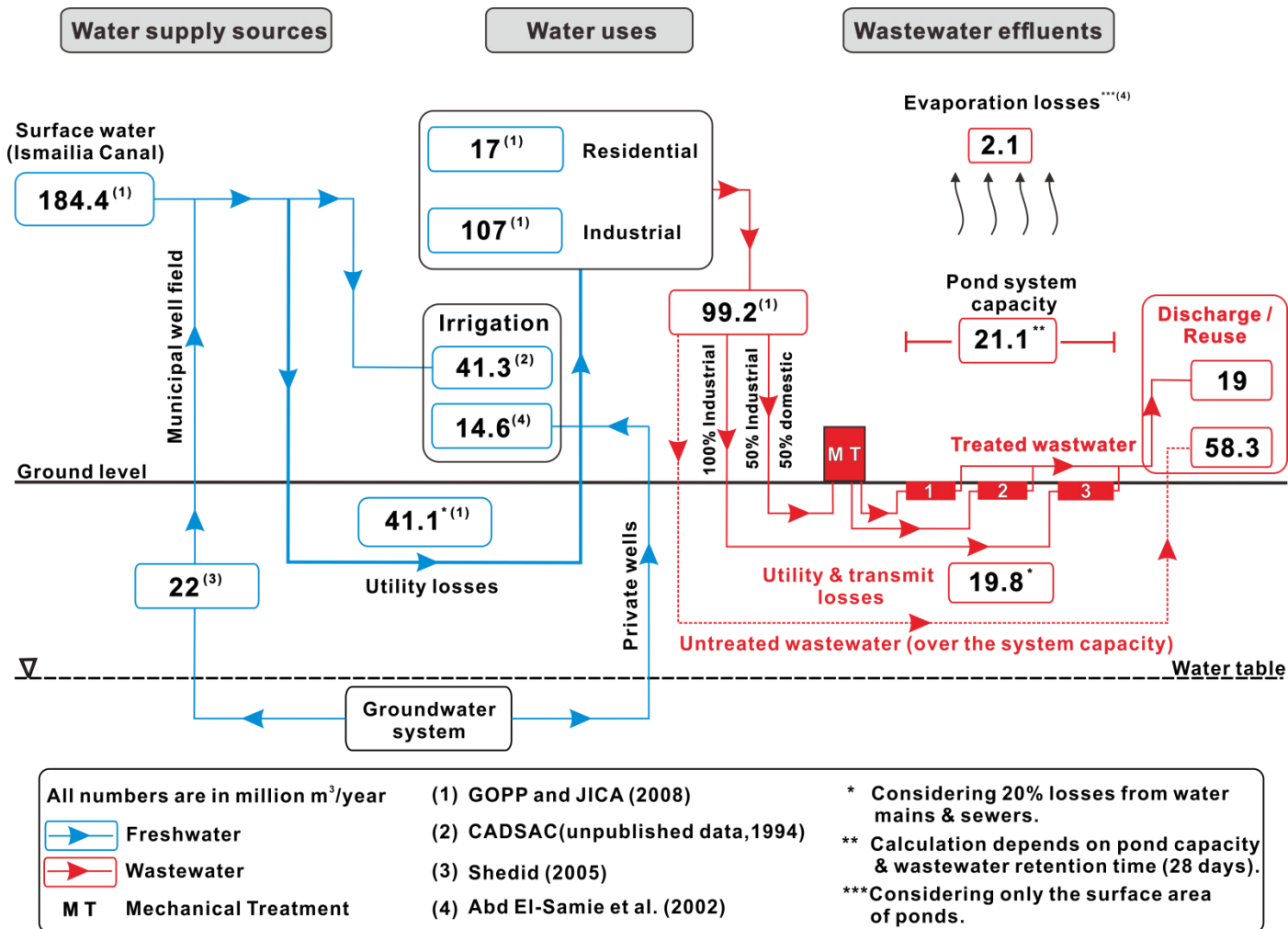


Fig. 2.12 Estimated water inflow and outflow for the Tenth of Ramadan city.



Fig. 2.13 A field photograph of the water-logging (raised soil-water levels) problem at the center of the Tenth of Ramadan city.

Table 2.3 Reclaimed area till 1990 in the eastern Nile Delta (Research Institute of groundwater/IWACO, 1991).

Reclaimed Area	Starting time	Average cultivated area (in square meters x 10⁵)
Salhiya	1982	588
El Shabab	1981	840
El Mullak	1964	462
Ramsis	1987	378
Khattara	1976	252

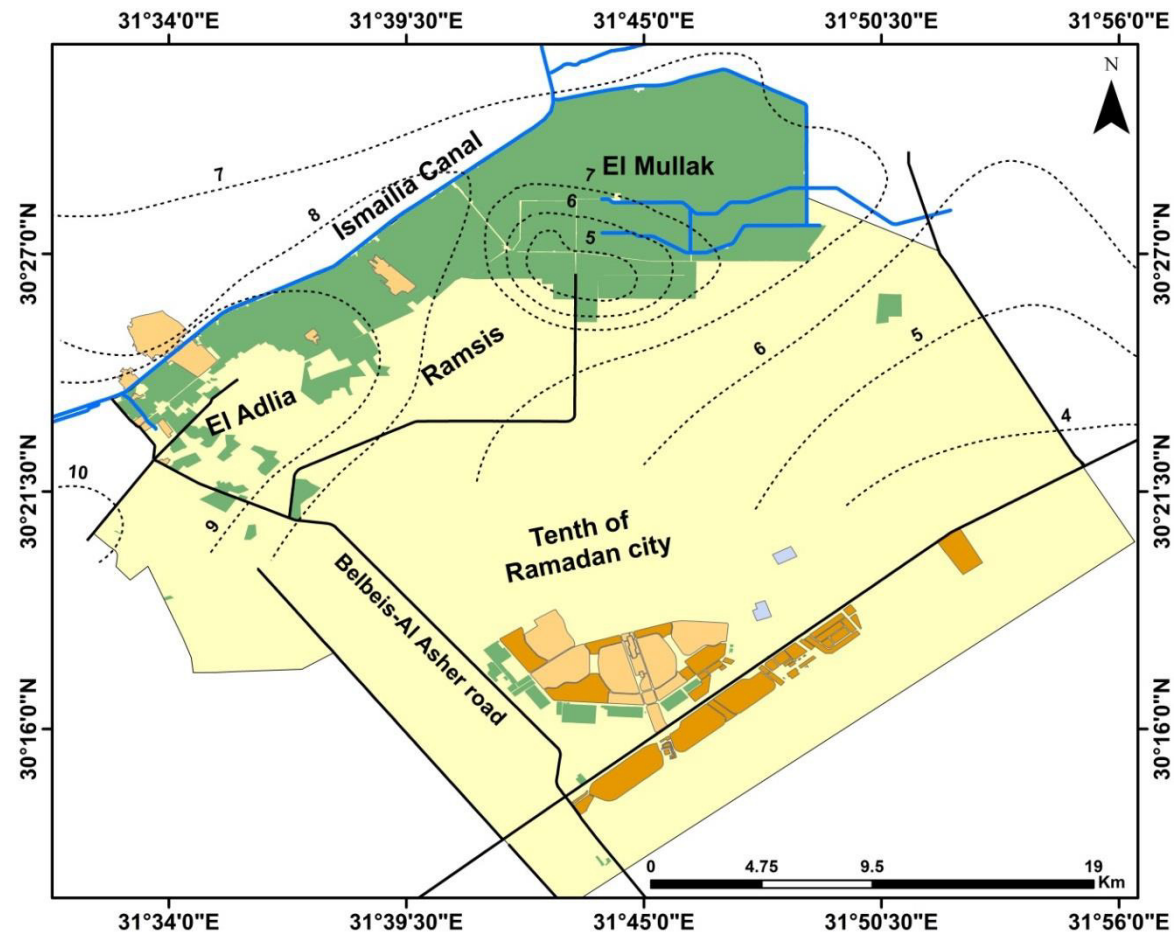


Fig. 2.14 Water table map of the Quaternary aquifer with the progress of land use in the study area at 1991, modified after Research Institute of groundwater

(1992)

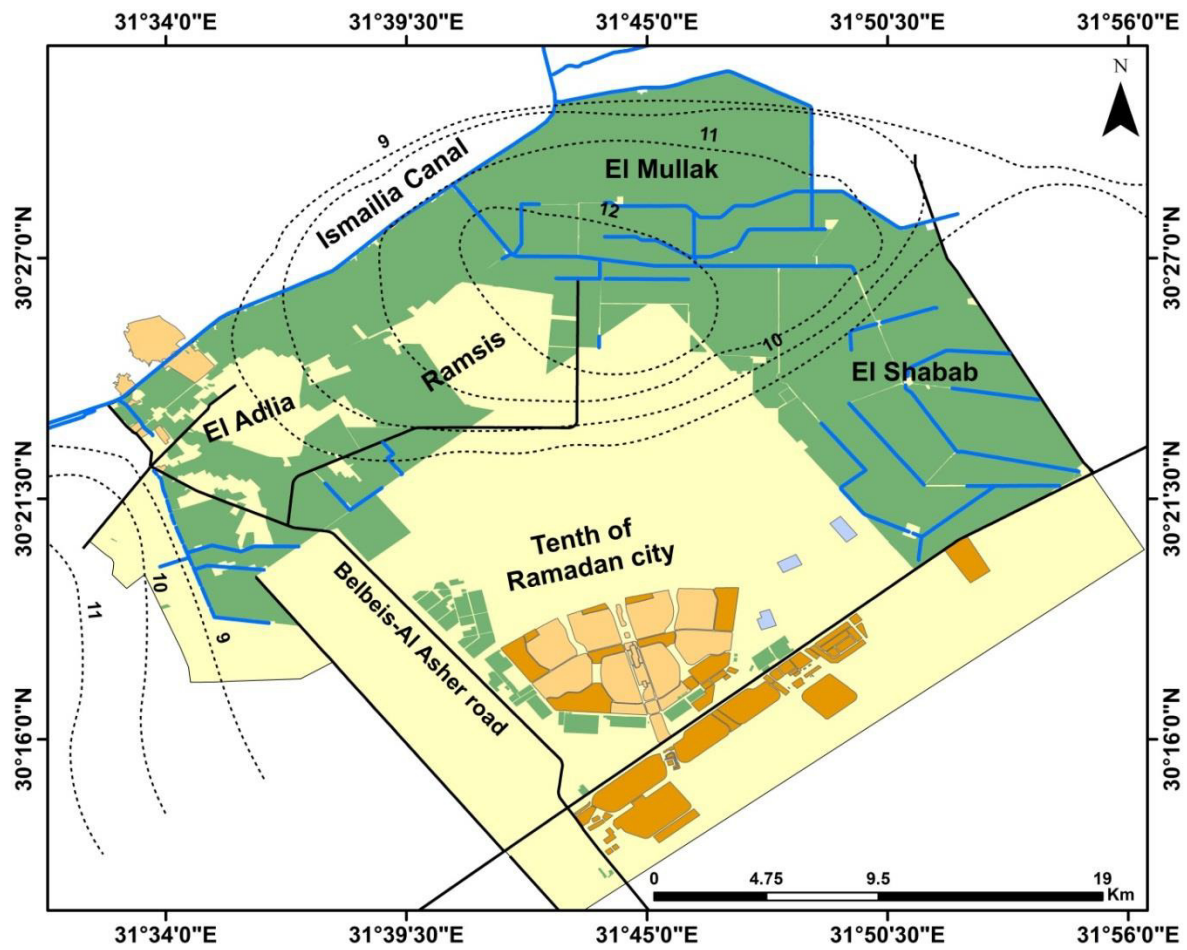


Fig. 2.15 Water table map of the Quaternary aquifer with the progress of land use in the study area at 2008, modified after Saleh (2009).

----- CHAPTER 3: METHODOLOGY AND DATA COLLECTION -----

3.1. OFFICE WORK

3.1.1. Gathering of data

The ability to properly study any groundwater system requires a solid understanding of the distribution, thickness, and quality of water aquifers. Such information were necessary to be collected prior to performing any fieldwork for the water sampling. Geology, hydrogeology, and surface geophysics data of the study area from various resources (El Shazly et al., 1975; Hefny et al., 1980; Ezz El Din, 1993; Gad, 1995; Abd El-Gawad, 1997; El-Haddad, 1996 and 2002) were revised to stand on the available subsurface information. Also, data, i.e., well logs, of the wells located at the well field area along with available reports from some well owners were integrated with the literature data to adequately map the Quaternary aquifer in the study area.

3.1.2. Analysis of borehole data

For the present study about 29 boreholes have been inventoried within the studied region and are presented in Appendix A. The locations of the boreholes are shown in Fig. 3.1. These boreholes have variable depths, with total depth values ranging from something about 20 to 30 m, along the Ismailia Canal, to over 300 m, along the Cairo-Ismailia desert road. Most boreholes, if not all, are completed in the Quaternary unit that is mainly composed of loose sand and gravels with some clay intercalations (El Shazly et al., 1975; Hefny et al., 1980). The analysis of data obtained from deep wells, over 300 m, revealed that the basal portion of the Quaternary deposits mostly rests unconformably on sandstones and sandy limestone, which are mostly belonging to the Miocene age (Hefny et al., 1980).

3.1.3. Delineation of aquifer boundaries

The stratigraphic succession and vertical distribution of the Quaternary and Miocene deposits across the study area were defined, based on the aforementioned lithological data, for each bore well and then correlated from one borehole to the next along two hydrogeologic cross sections to elucidate the

Quaternary and Miocene aquifer boundaries (Fig. 3.2). It is shown from these cross sections that the Quaternary aquifer is the main hydrogeologic unit and spreads all over the study area with a general increase of thickness towards the Ismailia canal while the Miocene aquifer is limited to the southern part of the study area as series of faulted structural highs (Fig. 3.2).

3.2. FIELD WORK

3.2.1. Water sampling

Samples were collected over two campaigns during August to September in both 2013 and 2014. Groundwater samples were collected from 69 wells which tap the Quaternary aquifer and five wells which tap the Miocene aquifer. In addition, three surface water samples were collected from the Ismailia canal, two samples from freshwater ponds, and 13 samples from the wastewater ponds (Fig. 3.3). About 14 samples from the Quaternary aquifer were collected at the same locations during the two campaigns and were used to check for the seasonal variations in groundwater chemical and isotopic characteristics.

3.2.2. Field measurements

For each field campaign, groundwater samples were collected from active municipal and private water supply wells after purging it for 15 to 20 min (Fig. 3.4) unless they were in continuous use. Coordinates and altitudes of the sampling sites were determined in the field with a GARMIN handheld global positioning system (GPS) at the well head, and the depths of wells were noted, where possible, from the well owner's records. Field parameters, i.e., electrical conductivity (EC), pH, and temperature (T), were measured using portable HORIBA probes (D-55 and D-54 models) (Fig. 3.4). The pH electrode was calibrated against pH 4, 7 and 10 standard solutions every seven days.

Field analyses were performed for the chemical constituents of which concentrations are susceptible to rapid change, i.e., alkalinity and redox sensitive species (e.g. NH_4^+ and NO_3^-), under atmospheric conditions (Jorstad, 2006). Samples for alkalinity were not filtered to prevent potential removal of inorganic carbon species (Jorstad, 2006). Alkalinity was determined in the field by titration

with 0.16 or 1.6 M H₂SO₄ in the presence of a bromocresol green-methyl red indicator using a HACH digital Titrator (Model 16900) (Fig. 3.4). Spectrophotometric analyses were performed in the field for NH₄⁺ and NO₃⁻ by using a HACH DR/890 spectrophotometer.

Samples for general ion chemistry analyses were collected once field parameters had stabilized. Sampled waters were filtered through 0.45 μm membrane filters and collected in two 50 ml polyethylene bottles after three repeated rinses. Samples are mainly filtered for several purposes; for example, to remove microorganisms in order to help preserve ambient analyte concentrations, and to remove suspended materials that interfere with specified analytical procedures, i.e., the IC system (Wilde et al., 2004-2009). Cation samples were preserved with a few drops of HNO₃ immediately after sampling. Acidification helps prevent precipitation, microbial activity, and sorption losses to the bottle walls. Unfiltered samples were collected for stable isotope analysis in 50 mL polyethylene bottles with poly-seal caps after three repeated rinses. No air bubbles were present in the samples, and bottles were kept from direct sunlight. No filtration is needed for stable isotope analysis since bacterial activity or suspended materials will not affect the measured values (IAEA, 2009). Selected well samples from the Quaternary and Miocene aquifers were analyzed for carbon-14 (¹⁴C) activity and δ¹³C to determine groundwater age. For this purpose, unfiltered water samples were collected in two 1000 mL high-density polyethylene bottles after rinsing three times. Following collection, the samples were sealed, labelled and stored in an ice-filled cooler, and transferred to refrigerator upon return from the field. All laboratory samples were analyzed within six months after sampling.

3.3. LABORATORY ANALYSES

3.3.1. Hydrochemistry

Major cations (Ca²⁺, Mg²⁺, Na⁺ and K⁺) and anions (Cl⁻ and SO₄²⁻) were analyzed following the USEPA method 300.1 (US Environmental Protection Agency, 1997) using a Dionex™ Ion Chromatograph (Model: DX 120) at the Environmental Science Center, The University of Tokyo, Japan.

Samples with high electrical conductivity ($>700 \mu\text{S}/\text{cm}$) were diluted before analysis to remain within the working range of the instrument ($< 100 \text{ mg}/\text{l}$). The ion balance errors for the analyses were within or less than $\pm 10\%$ except for some water samples. According to Hem (1989), Hounslow (1995) and other studies, a charge balance error within $\pm 10\%$ is considered to be acceptable. Observed precipitation in sample bottles before the analysis might be the cause of the charge imbalance.

3.3.2. Environmental tracers

3.3.2.1. Background

In hydrology, a tracer is a substance that marks the water itself or dissolved substances therein, and moves passively with the water or the solutes (Aeschbach-Hertig, 2006). That means, tracers need to be mobile, soluble and should not be strongly retarded by the soil or aquifer matrix (non-reactive or conservative) (Geyh, 2000). Environmental tracers include isotopes of hydrogen or oxygen in the water molecule, solute isotopes (e.g. C, N, S, etc.), and gas tracers (e.g. noble gases) that either dissolve into groundwater at recharge or accumulate in the subsurface from radioactive decay (Doyle, 2013). They can be categorized into two categories: natural and historical tracers (Scanlon et al., 2002). Natural tracers are tracers that are created or transported in the environment by natural processes, i.e., stable isotopes of oxygen and hydrogen, whereas historical tracers have been introduced to the environment by anthropogenic sources such as Chlorofluorocarbons (CFCs) (Scanlon et al., 2002; Healy, 2010; Doyle, 2013). The term "environmental tracers" is mainly used to distinguish them from "artificial tracers". The essential difference is that environmental tracers can be applied for studies on large spatial and temporal scales, whereas artificial are suitable for targeted studies of small scale processes, i.e., local tracers experiments using dyes, SF_6 , and so on (Aeschbach-Hertig, 2006).

The stable isotopes of oxygen, ^{16}O (99.7 %) and ^{18}O (0.2 %), and those of hydrogen, ^1H (99.9 %) and ^2H or deuterium; D (0.02 %), combine and produce water molecules of differing molecular mass (Geyh, 2000; Yoshida, 2002). These water molecules may be divided into light molecules ($^1\text{H}_2 \text{ }^{16}\text{O}$)

and heavy water molecules ($^1\text{HD } ^{16}\text{O}$ and $^1\text{H}_2 \text{ } ^{18}\text{O}$). Isotopes of water are ideal tracers for hydrological studies and they often form the foundation of a multi-tracer approach since they are a part of the water molecule itself ($\text{H}_2 \text{ } ^{18}\text{O}$ and $^1\text{HD } ^{16}\text{O}$), travel at the same rate as water, not retarded by interaction with aquifer materials or measurably altered by geochemical reactions, and vary temporally and spatially (Gibson et al., 2005; Liescheidt, 2012). This latter variation is caused by isotopic fractionation processes, which is the separation of isotopes by mass, due to a variance in reaction rates when water undergoes a phase change (Clark and Fritz, 1997). It is therefore possible to use stable isotope values to trace the origin of the water and evaluate the extent of mixing of groundwater with other resources since the isotopic composition of water changes only due to mixing of different water or due to fractionation (McGuire and McDonnel, 2007).

There is a strong relationship between the $\delta^{18}\text{O}$ and δD values of precipitation, which is reflected in the Meteoric Water Line (MWL) (Craig, 1961). This line, MWL, has been found, with some local variations, to be valid over large parts of the world (Geyh, 2000; Mazor, 2004) and expressed by the equation;

$$\delta \text{D} = 8 \delta^{18}\text{O} + 10$$

The meteoric water line is a convenient reference line for the understanding and tracing of local groundwater origins and movements (Mazor, 2004). Therefore, the deviations from the MWL could indicate various processes of isotopic exchange and fractionation (Geyh, 2000). The best known examples are departures due to evaporation observed in brines from sedimentary marine aquifers, exchange of oxygen between water molecules and silicate minerals (rock-water exchange processes) observed in geothermal systems, and mixing between meteoric groundwaters and seawater or paleowater (old groundwater) (Fig. 3.5) (Yurtsever, 1994; Geyh, 2000).

Mixing of water occurs at all stages of groundwater flow, from the attenuation of seasonal inputs in the recharge area, to the mixing of deep and shallow flow paths in the discharge area (Clark,

2015). Mixing is calculated from the concentrations of conservative species such as Cl^- , $\delta^{18}\text{O}$, and δD provided their concentrations are known for the different mixing endmembers (Clark, 2015). Other tracers, such as Ca^{2+} and Na^+ or HCO_3^- , SO_4^{2-} and their isotopes are less reliable due to non-conservative exchange or redox reactions (Clark, 2015). The relation between salinity and $\delta^{18}\text{O}$ or δD is also useful to highlight salinization pathways, i.e., leaching or dissolution, evaporative concentration or mixing of fresh water with saline water or seawater (Fig. 3.6) (Yurtsever, 1994; Geyh, 2000). For processes of leaching salt formations or mineral dissolution, the stable isotopic content of the water is not affected while the salinity of water increases (Yurtsever, 1994).

In addition to the use of H and O isotopes, Carbon-14 (^{14}C) is a naturally occurring radioactive isotope of carbon having a half-life of about 5,730 years (Mook, 1980). ^{14}C refers to the ratio of ^{14}C to total stable carbon (i.e., $^{14}\text{C}/(^{12}\text{C} + ^{13}\text{C})$) (Athanasopoulos, 2009). Since the early 1960s, ^{14}C present in groundwater as dissolved inorganic carbon (DIC) has been used in hydrologic studies to determine the time since recharge of older groundwater (Vogel and Ehgart, 1963). ^{14}C concentrations of the DIC in groundwater are reported in percent modern Carbon (pMC), where the modern activity of ^{14}C is set as 13.56 decays-per minute per gram of carbon (Kalin, 2000; Athanasopoulos, 2009). The reference (or, zero) year for this activity is 1950 AD (Kalin, 2000; Athanasopoulos, 2009). This reference year is considered to have an activity of 100 pMC; therefore with no possible mixing or dilution occurs, groundwater samples with an activity lower than 100 pMC are pre-1950 AD, and samples with an activity higher than 100 pMC are younger (Kalin, 2000; Athanasopoulos, 2009). ^{14}C is formed naturally by cosmic-ray bombardment of nitrogen in the upper atmosphere, where it rapidly oxidizes to $^{14}\text{CO}_2$, mixes into the lower atmosphere and is assimilated in the biosphere and hydrosphere (Kalin, 2000; Athanasopoulos, 2009). In addition to natural sources, ^{14}C also was produced by the atmospheric testing of nuclear weapons (Mook, 1980), and ^{14}C activities may exceed 100 pMC in areas where groundwater contains tritium from nuclear weapons tests (Izbicki and Michel, 2004). Carbon-14 activities are used to

determine the age (time since recharge) of groundwater on time scales ranging from recent to more than 20,000 years before present (Izbicki and Michel, 2004). Because ^{14}C is not part of the water molecule, its activity and interpreted ^{14}C ages may be affected by reactions between constituents dissolved in groundwater and aquifer materials (Izbicki and Michel, 2004). ^{13}C and ^{12}C , naturally occurring stable isotopes of carbon, play an important role in quantifying water-rock interactions in the case of ^{14}C age determination of groundwater (Geyh, 2000). Their ratio ($^{13}\text{C}/^{12}\text{C}$) also allows to identify the proportion of biogenic and carbonate CO_2 in water and to determine initial geological settings of the groundwater recharge (Geyh, 2000). ^{13}C data are expressed in delta notation (δ) as per mil (parts per thousand) differences relative to the ratio of ^{13}C to ^{12}C in standard Peedee Belemnite (PDB) (Gonfiantini, 1978 and 1984). Most marine carbonate rocks have $\delta^{13}\text{C} = -2$ to 0 ‰, whereas frequent values for organic material and CO_2 in soil are -28% to -20 ‰. Most plants have values around -23 ± 3 ‰, but certain plants have more positive values, around -12 ± 2 ‰ (Mazor, 2004).

Several studies have been conducted using multi-isotope study with hydrochemical analysis to understand the origin of variably mixed groundwater reservoirs (e.g. Gat and Gonfiantini, 1981; Clark and Fritz, 1997; Cook and Herczeg, 2000), to link groundwater recharge and salinization processes (e.g. Ma et al., 2005; Cartwright et al., 2007; Tweed et al., 2011), to relate groundwater recharge and salinity to geologic setting and structures (e.g. Morgan et al., 2006; Yuan et al., 2011), to show degradation of groundwater with increasing urbanization and agricultural demand (e.g. Ma et al., 2005; Négrel et al., 2011; Hamed et al., 2014), and to identify pollution risk resulting from inappropriate practices of wastewater handling and disposal in arid and vulnerable hydrogeologic settings that may give rise to groundwater recharge (e.g. Vanderzalm et al., 2011).

3.3.2.2. Analytical techniques

Stable isotopes of oxygen-18 (^{18}O) and deuterium (^2H) were analyzed in samples from the Ismailia canal, freshwater ponds, groundwater of the Quaternary aquifer, groundwater of the Miocene

aquifer, and wastewater. Samples were stored at room temperature in sealed bottles until the analysis at the hydrology laboratory, Kumamoto University, Kumamoto, Japan. $\delta^2\text{H}$ and $\delta^{18}\text{O}$ were measured by Isotope Ratio Mass Spectrometry (Thermo Fisher scientific, Delta V Advantage), using equilibration method with CO_2 for $\delta^{18}\text{O}$ (Epstein and Mayeda, 1953) and H_2 in the presence of platinum (Pt) catalyst for $\delta^2\text{H}$ (Ohsumi and Fujino 1986; Horita et al., 1989). Analytical error was estimated to be better than $\pm 0.05 \text{ ‰}$ and $\pm 0.5 \text{ ‰}$, for ^{18}O and ^2H , respectively. Both $\delta^{18}\text{O}$ and $\delta^2\text{H}$ values were reported relative to Vienna Standard Mean Ocean Water (VSMOW) (Coplen, 1995).

Samples for carbon-14 (^{14}C) activity and $^{13}\text{C}/^{12}\text{C}$ ratios ($\delta^{13}\text{C}$) were kept chilled until analysis at Beta Analytic, Inc., U.S.A. The ^{14}C activity and $\delta^{13}\text{C}$ of the water samples were derived from the dissolved inorganic carbon (DIC) using National Electrostatics Corporation (NEC) 250 keV Single Stage Accelerator Mass Spectrometer (SSAMS) coupled with a Thermo DeltaPlus, gasbench. 12M phosphoric acid was placed into a vessel within a closed chemistry line and the entire line was evacuated of all air. Water sample was introduced into the acid to evolve CO_2 from all DIC species present. The solution (water+acid) was then agitated and pumped on until no further CO_2 evolution was observed. Upon completion, the solution was verified to be pH 1 or lower to ensure complete capture of all DIC as CO_2 for the analysis. $\delta^{13}\text{C}$ was measured on CO_2 created during the process of converting DIC to CO_2 during ^{14}C sample preparation. CO_2 was then graphitized over cobalt catalyst to provide the target for the AMS. ^{14}C analysis was performed on graphite after CO_2 samples were reduced to this state. Uncertainties were lower than $\pm 0.4 \text{ pMC}$ and $\pm 0.1 \text{ ‰}$ for ^{14}C and $\delta^{13}\text{C}$ measurements, respectively.

3.4. MULTIVARIATE STATISTICAL ANALYSIS.

3.4.1. Background

The information gathered through many variables can be handled using multivariate techniques (Laaksoharju, 1999). Multivariate methods typically analyze three or more variables, and compared with univariate analysis, explain more variation in a data set (Nolan, 1999). Principal component analysis

(PCA) and hierarchical cluster analysis (HCA) are the two most commonly used multivariate approaches. PCA is a useful method in data reduction, manipulation, and visualization of complex data systems, where patterns and data similarities are not well understood (Stauffer et al., 1985; Melloul and Collin, 1992; Valder et al., 2012). PCA reduces a large data set to a few independent, composite variables (principal components) that explain much of the variance of the original data (Puckett and Bricker, 1992). Extracted components are linear combinations of the original variables (Helsel and Hirsch, 1992). Component loadings show the degree of correlation between the original variables and each principal component. The greater is the loading (regardless of sign), the greater is the correlation (Nolan, 1999). Variables that are highly correlated with a principal component are considered to represent a particular process influencing the data. Interpreting principal components, however, is a subjective process (Puckett and Bricker, 1992; Nolan, 1999). Component scores show the influence of a principal component on individual samples. Information on which samples are influenced by a given process can be obtained by plotting the scores in relation to x- and y-axes representing extracted components (Nolan, 1999). The composite variables and associated scores yield insight into the data that could not be easily obtained by analyzing one explanatory variable at a time (Nolan, 1999).

From the mathematical perspective, if you have P variables X_1, X_2, \dots, X_P measured on a sample of n objects, then the i^{th} principal component, Z_i , can be written as a linear combination of the original variables (Cornish, 2007; Lei, 2013);

$$Z_i = a_{i1} X_1 + a_{i2} X_2 + a_{i3} X_3 + \dots + a_{ip} X_p$$

The principal components are chosen such that the first one, $Z_1 = a_{11} X_1 + a_{12} X_2 + a_{13} X_3 + \dots + a_{1p} X_p$ accounts for as much of the variation in the data as possible and subject to the following constraint that $a_{11}^2 + a_{12}^2 + \dots + a_{1p}^2 = 1$ (Cornish, 2007)

The second principal component $Z_2 = a_{21} X_1 + a_{22} X_2 + a_{23} X_3 + \dots + a_{2p} X_p$ is chosen such that its variance is as high as possible. A similar constraint is applied that $a_{21}^2 + a_{22}^2 + \dots + a_{2p}^2 = 1$

(Cornish, 2007). The second component is chosen such that it is uncorrelated with the first component. The remaining principal components are chosen in the same way (Cornish, 2007).

HCA aims to classify a sample of objects on the basis of a set of measured variables into a number of different groups such that similar subjects are placed in the same group (cluster) (Cornish, 2007), where the within-group variance is as small as possible, and the differences between the clusters can be large (Templ et al., 2008; King, 2014). Two main HCA procedures are agglomerative methods and divisive methods. In agglomerative HCA, most commonly applied methods and used in this study, each observation starts as an individual cluster. The first step is then to group the two “closest” (most similar) clusters into one cluster, resulting in one less cluster. This process is done repeatedly until all observations have been grouped into one cluster (Cornish, 2007; King, 2014) and this allows a hierarchy of clusters to be established from the bottom up (Mooi and Sarstedt, 2011). There are various measures to express (dis)similarity between pairs of objects. A straightforward way to assess two objects’ proximity is by drawing a straight line and getting the distance between them (Mooi and Sarstedt, 2011). This type of distance is referred to as the Euclidean distance (or straight-line distance) and is most commonly used (Güler et al., 2002; Mooi and Sarstedt, 2011). To express the Euclidean distance mathematically, suppose we have P variables X_1, X_2, \dots, X_P measured on a sample of n objects, the observed data for object i can be referred to as $x_{i1}, x_{i2}, \dots, x_{ip}$ while the observed data for j object as $x_{j1}, x_{j2}, \dots, x_{jp}$. Then the Euclidean distance between these two objects can be written as (Cornish, 2007; Mooi and Sarstedt, 2011):

$$d_{ij} = \sqrt{(x_{i1} - x_{j1})^2 + (x_{i2} - x_{j2})^2 + \dots + (x_{ip} - x_{jp})^2}$$

The squared Euclidean distance is simply derived by squaring the Euclidean distance equation. In addition to the distance or similarity measure, the clustering algorithm should also be decided. The clustering algorithm describes the procedure used to determine which clusters are the most similar to each other (Townend, 2002; King, 2014). The main methods used to determine which clusters should be joined at each stage are; single-linkage method (Sneath, 1957), complete linkage method (Sorensen, 1948),

average linkage method (Sokal and Michener, 1958), centroid method (Sokal and Michener, 1958), and Ward's method (Ward, 1963). The first four linkage methods are all based on a similar principle: there is a chain of similarity leading to whether or not a case is added to a cluster. The rules governing this chain differ from one linkage method to another (Field, 2000). Ward's method, used in this study, has a different and complex approach that does not combine the two most similar objects successively or depend on single measurement of similarity (Field, 2000; Mooi and Sarstedt, 2011; King, 2014). Instead, those objects whose merger increases the overall within-cluster variance to the smallest possible degree, are combined (Mooi and Sarstedt, 2011). This method tends to produce clusters of roughly equal size, because the smaller clusters usually have a smaller sum of squares (Cornish, 2007; King, 2014). Ward's method is sensitive to outliers (Hair et al., 2006; Cornish, 2007), but it is still commonly applied to hydrochemical studies (Güler et al. 2002; Raiber et al. 2012; King, 2014) as it reduces the within group variance (Gong et al., 2008; Mooi and Sarstedt, 2011; King, 2014).

Recent studies have confirmed the usefulness of multivariate analysis techniques for evaluation and interpretation of groundwater quality data sets (e.g. Singh et al., 2009), providing insight into the hydrological processes (e.g. Mohapatra et al., 2011; Ghesquière, 2015), identifying critical water quality issues and possible sources of pollution/polluting processes (e.g. Rao et al., 2010), and interaction of river water/groundwater and groundwater mixing (e.g. Long and Valder, 2011; Valder et al., 2012; King et al., 2014).

3.4.2. Checking the Data adequacy

Principal component analysis (PCA) and hierarchical cluster analysis (HCA) were conducted using XLSTAT (Version 2015.4.01.20780). Two tests were used for the adequacy of the interest of the implementation of the PCA on a dataset: the Bartlett's sphericity test and the Kaiser-Meyer-Olkin (KMO) index. Bartlett's test of sphericity is a statistical test of the correlation matrix to determine if the variables are significantly correlated (Hair et al., 2006; King, 2014). The KMO statistically analyses partial

correlations between variables and compares them to the simple correlations for the same variables (Spicer, 2004; King, 2014). If the KMO index is high (≈ 1), the PCA can act efficiently; if KMO is low (≈ 0), the PCA is not relevant (Rakotomalala, 2013). The results from KMO test (0.76) and Bartlett's test of sphericity (<0.05) confirmed that PCA can be applied on the dataset consisting of nine selected physical-chemical (EC, Na^+ , Mg^{2+} , Ca^{2+} , HCO_3^- , Cl^- , and SO_4^{2-}) and isotopic ($\delta^{18}\text{O}$ and $\delta^2\text{H}$) variables.

3.4.3. Statistical treatment of the dataset

The raw data were used for the PCA because the correlation matrix has the effect of standardizing the data (DOE, 2012) while it was standardized for the HCA. The standardized data are obtained by subtracting the mean of the distribution from each data and dividing by the standard deviation of the distribution (Davis, 1986). A common criterion (Kaiser normalization) for determining the number of principal components to consider for further analysis is those having an eigenvalue greater than one (Kaiser, 1960). The Varimax rotation was also applied in order to reduce the overlap between original variables and maximize the variance in each principal component (Davis, 1986). The Ward linkage method and Squared Euclidean distance measurement were considered for the HCA, as they are effective in cluster determination in water studies (Güler et al., 2002).

3.5. REFERENCES

- Abd El-Gawad, A. M., 1997. Shallow geophysical exploration for defining the water occurrences in the area east of the Nile Delta, Egypt. Unpublished PhD Thesis, Fac. of Sci., Ain Shams Univ., Egypt. 410 p.
- Aeschbach-Hertig, W., 2006. Physics of Aquatic Systems II (isotope hydrology). Lecture notes, Heidelberg University, available online <http://www.iup.uni-heidelberg.de/institut/forschung/groups/aquasys/WAH/lehre/material/Chap1%20Introduction.pdf> accessed on December 6th, 2015.
- Athanasopoulos, P., 2009. Using stable isotopes to develop a regional hydrogeological model and characterize nitrate sources in groundwater. MSc Thesis, College of Graduate Studies and Research, University of Saskatchewan, Saskatchewan, available online <http://ecommons.usask.ca/bitstream/handle/10388/etd-08272009-114503/PanaMScThesis2009.pdf> accessed on December 3rd, 2015.
- Cartwright, I., Hannam, K., Weaver, T.R. 2007. Constraining flow paths of saline groundwater at basin margins using hydrochemistry and environmental isotopes: Lake Cooper, Murray Basin, Australia. *Aust. J. Earth Sci.*, 54, 1103–1122.
- Chambers, J. M., Cleveland, W. S., Kleiner, B., Tukey, P. A., 1983. *Graphical Methods for Data Analysis*: PWS-Kent Publishing Co., Boston, 395 p.
- Chen, K., Jiao, J.J., Huang, J., Huang, R., 2007. Multivariate statistical evaluation of trace elements in groundwater in a coastal area in Shenzhen, China. *Environ. Pollut.* 147 (3), 771–780.
- Clark, I., 2015. *Groundwater Geochemistry and Isotopes*. CRC press.
- Clark, I., Fritz, P., 1997. *Environmental Isotopes in Hydrogeology*. Lewis, Boca Raton. FL. 328 p.
- Cook, P., Herczeg, A.L. (Eds.) 2000. *Environmental Tracers in Subsurface Hydrology*, Kluwer academic publishers, New York, 529 p.

- Coplen, T. B., 1995. Discontinuance of SMOW and PDB. *Nature* 375, 285.
- Cornish, R., 2007. Cluster analysis. In statistics. Available online at <http://www.statstutor.ac.uk/resources/uploaded/clusteranalysis.pdf> accessed on January 5th, 2016.
- Cornish, R. 2007. Principal component analysis. In statistics. Available online at <http://www.statstutor.ac.uk/resources/uploaded/principle-components-analysis.pdf> accessed on January 5th, 2016.
- Craig, H., 1961. Standard for reporting concentrations of deuterium and oxygen-18 in natural waters. *Science*, 133, 1833-1834.
- Davis, J. C., 1986. *Statistics and data analysis in geology*. John Wiley and sons Inc., New York.
- DOE (U.S. Department of Energy), 2012. Multivariate statistical analysis of water chemistry in evaluating the origin of contamination in Many Devils Wash, Shiprock, New Mexico, LMS/SHP/S09257, ESL-RPT-2012-03, Office of Legacy Management, Grand Junction, Colorado, December. Available online http://energy.gov/sites/prod/files/S09257_ChemOrigin.pdf accessed on August 30th, 2015.
- Doyle, J., 2013. Integrating environmental tracers and groundwater flow modeling to investigate groundwater sustainability, Gibsons, BC. MSc Thesis, Faculty of Science, university of British Columbia, available online <http://hdl.handle.net/2429/45015> accessed on December 3rd, 2015.
- El-Haddad , I. M., 1996. Groundwater Sources and Soil Evaluation for the Tenth of Ramadan City Area and its Surroundings, Egypt. Unpublished MSc Thesis, Fac. Sci., Mansoura Univ., Mansoura, Egypt, 199 p.
- El-Haddad I. M., 2002. Hydrogeological studies and their environmental impact on future management and sustainable development of the new communities and their surroundings, east of the Nile Delta, Egypt. Unpublished PhD Thesis, Faculty Sci., Mansoura Univ., 435p.
- El-Shazly, E.M., Abdel Hady, M.A., El-Shazly, M.M., El-Ghawaby, M.A., El-Kassas, I. A., Salman, A.B.,

- Morsi, M.A., 1975. Geological and Groundwater Potential Studies of El-Ismailia Master Plan Study Area. Rem. Sens. Res. Project, Acad. Sci. Res. and Techn., Cairo, Egypt, 24 p.
- Englert, A., 2003. Measurement, Estimation and Modelling of Groundwater Flow Velocity at Krauthausen Test Site. PhD Thesis, Publikationsserver der RWTH Aachen University, available online at <http://d-nb.info/968913598/34> accessed on January 20th, 2016.
- Ezz El-Din, H., 1993. Geophysical and sedimentology studies on the Heliopolis aquifer, Cairo-Ismailia desert road. Unpublished MSc Thesis, Fac. of Sci., Ain Shams Univ., Egypt, 228 p.
- Epstein, S., Mayeda, T., 1953. Variation of O-18 content of waters from natural sources. *Geochim Cosmochimica Acta*, 4, 213–224.
- Farnham, I.M., Johannesson, K.H., Singh, A.K., Hodge, V.F., Stetzenbach, K.J., 2003. Factor analytical approaches for evaluating groundwater trace element chemistry data. *Anal. Chim. Acta*, 490 (1–2), 123–138.
- Field, A. P., 2000. Cluster analysis. In: postgraduate statistics. Available online at <http://www.statisticshell.com/docs/cluster.pdf> accessed on January 5th, 2016.
- Gad, M. I., 1995. Hydrogeological studies for groundwater reservoirs, east of Tenth of Ramadan City and vicinities, Unpublished MSc Thesis, Fac. Sci., Ain Shams Univ., Egypt, 187 p.
- Gat, J. R., Gonfiantini, R., (Eds) 1981. Stable Isotope Hydrology; Deuterium and Oxygen-18 in the Water Cycle. IAEA Technical Report Series #210, Vienna. 337 p.
- Geyh, M. 2000. Groundwater, saturated and unsaturated zone. In: Mook, W.G.(ed.), Environmental isotopes in the hydrological cycle; principles and applications. IHP-V, Technical Documents in Hydrology, No. 39, IV, UNESCO, Paris, 196 pp.
- Ghesquière, O., Walter, J., Chesnaux, R., Rouleau, A. 2015. Scenarios of groundwater chemical evolution

- in a region of the Canadian Shield based on multivariate statistical analysis. *J. Hydrol.: Regional Studies*,4, 246-266.
- Gibson, J. J., Edwards, T. W. D., Birks, S. J., St Amour, N. A., Buhay, W. M., McEachern, P., Wolfe, B. B., Peters, D. L. 2005. Progress in isotope tracer hydrology in Canada: *Hydrological Processes*,19: 303-327, DOI 10.1002/hyp.5766.
- Gonfiantini, R., 1978. Standards for stable isotope measurements in natural compounds: *Nature*, 217, 534–536.
- Gonfiantini, R., 1984. Advisory group meeting on stable isotope reference samples for geochemical and hydrological investigations, Vienna, 19–21 September 1983, Report to Director General, International Atomic Energy Agency, Vienna.
- Gong, H., Hu, Z., Zhao, W., Wang, Y., Gong, Z., 2008. Three Dimensional Groundwater Virtual Reality System and Its Spatial Database. In: *International Geoscience and Remote Sensing Symposium (IGARSS)*, 2008, 2007 IEEE International Geoscience and Remote Sensing Symposium, IGARSS 2007, edited, 4741-4744.
- Güler, G., Thyne, G., McCray, J., Turner, A. 2002. Evaluation of graphical and multivariate statistical methods for classification of water chemistry data. *Hydrogeol. J.*, 10, 455-474.
- Hair, J. F., Black, W. C., Babin, B. J., Anderson, R. E., Tatham, R. L., 2006. *Multivariate data analysis*, sixth edition. New Jersey: Pearson Prentice Hall.
- Hamed, Y., Ahmadi, R., Demdoum, A., Bouri, S., Gargouri, I., Dhia, H. B., Al-Gamal, S., Laouar, R., Choura, A. 2014. Use of geochemical, isotopic, and age tracer data to develop models of groundwater flow: A case study of Gafsa mining basin-Southern Tunisia, *J. Afr. Earth Sci.*, 100, 418–436.
- Healy, R.W., 2010. Chemical Tracer Methods. In: Healy, R.W., with contributions by Scanlon, B.R., *Estimating Groundwater Recharge*. Cambridge University Press, United Kingdom, 136-165 pp.

- Hefny, K., Farid, M.S., Morsi, A., Khater, A.R., El-Ridi, M.R, Khalil, Z.B., Atwa, A. Attia, D., 1980. Groundwater Studies for the Tenth of Ramadan City. Unpublished internal rept., Research Institute for Groundwater, Ministry of Public works and Water Researches, El Kanater, Cairo, Egypt, 54 p.
- Helsel, D.R., and R.M. Hirsch. 1992. Statistical methods in water resources. Elsevier, New York
- Hem, J. D. 1989. Study and interpretation of the chemical characteristics of natural water (3rd ed.), US Geological Survey Water-Supply Paper 2254, 263 p.
- Horita, J., Ueda, A., Mizukami, K. and Takatori, I. 1989. Automatic δD and $\delta^{18}O$ analyses of multi water samples using H_2 and CO_2 -water equilibration methods with a common equilibration set-up. Appl. Radiat. Isot., 40, 801-805.
- Hounslow, A. W., 1995. Water Quality Data: Analysis and Interpretation, CRC Lewis publishers, Boca Raton, FL., 397 p.
- IAEA (International Atomic Energy Agency), 2009. Groundwater sampling procedures for isotope hydrology. Available online at <http://www-naweb.iaea.org/naweb/ih/documents/other/2014%20ENG%20Gw%20Sampling%20booklet%20-%20separate%20pages.pdf> accessed on January 21th, 2016.
- Izbicki, J.A., Michel, R.L. 2004. Movement and Age of Ground Water in the Western Part of the Mojave Desert, Southern California, USA. U.S.G.S. Water Resources Investigations Report 03-4314, p. 42.
- Jorstad, L.B., 2006. Analysis of variation in inorganic contaminant concentration and distribution in a landfill leachate plume: Astrolabe Park, Sydney, Australia. PhD Thesis, The University of New South Wales, Sydney. Available online http://www.unsworks.unsw.edu.au/primo_library/libweb/action/diDisplay.do?vid=UNSWORKS&docId=unsworks_877&fromSitemap=1&afterPDS=true accessed on December 8th, 2015.
- Kaiser, H.F., 1960. The application of electronic computers to factor analysis, Educ. Psychol. Meas., 20, 141–151.

- Kalin, R. M., 2000. Radiocarbon dating of groundwater systems. In "Environmental Tracers in Subsurface Hydrology", P. G. Cook and A. L. Herczeg, eds., 111-144. Kluwer Academic Publishers: Boston.
- King, A. C., 2014. The Cressbrook Creek alluvial aquifer system, Southeast Queensland : hydrochemistry and isotopes to determine hydrological processes and response to floods. PhD Thesis. Queensland University of Technology. Available online <http://eprints.qut.edu.au/78443/> accessed January 5th, 2016.
- King, A.C., Raiber M., Cox M.E. 2014. Multivariate statistical analysis of hydrochemical data to assess alluvial aquifer–stream connectivity during drought and flood: Cressbrook Creek, southeast Queensland, Australia. *Hydrogeol. J.*, 22(2), 481–500.
- Laaksoharju, M., Tullborg, E.-L., Wikberg, P., Wallin, B., Smellie, J., 1999. Hydrogeochemical conditions and evolution at the Äspö HRL, Sweden. *Applied Geochemistry*, 14, 835-859.
- Leech, N.L., Barrett, K.C., Morgan, G.A. 2015. Exploratory Factor Analysis and Principal Components Analysis. In: Leech, N.L., et al. (eds.) *IBM SPSS for intermediate statistics: use and interpretation*, 5th ed., Routledge: New York, 68-83.
- Lei, L., 2013. Assessment of Water Quality Using Multivariate Statistical Techniques in the Ying River Basin, China. Master thesis, University of Michigan, 52 p. available online <http://babel.hathitrust.org/cgi/pt?id=mdp.39015089709169> accessed on January 5th, 2016.
- Liescheidt, R.M., 2012. Using the O and H stable isotopes to track sources of water in constructed wetlands. Master thesis, 76 p. available online http://geo.illinoisstate.edu/ewpeter/documents/Liescheidt_Thesis_2012.pdf accessed on November 24th, 2015.
- Long A.J., Valder J.F. 2011. Multivariate analyses with end-member mixing to characterize groundwater flow: wind cave and associated aquifers. *J. Hydrol*, 409 (1), 315–327.

- Ma, J.Z., Wang, X.S., Edmunds, W.M. 2005. The characteristics of ground-water resources and their changes under the impacts of human activity in the arid Northwest China — a case study of the Shiyang River Basin *J. Arid Environ.*, 61, 277–295.
- Mazor, E., 2004. *Chemical and isotopic groundwater hydrology: the applied approach*, 3rd ed. Marcel Dekker, Inc., New York.
- McGarigal, K., 2000. *Analysis of Environmental Data Conceptual Foundations: Data Exploration , Screening & Adjustments*. Lecture notes, University of Massachusetts Amherst, Massachusetts. Available online at <http://www.umass.edu/landeco/teaching/ecodata/schedule/exploratory.pdf> accessed on January 19th, 2016.
- McGuire ,K., McDonnel, J., 2007. Stable isotope tracer in watershed hydrology, Chapter 11. In: Michener RH, Lajtha K (eds) *Stable Isotopes in Ecology and Environmental Science*, vol 41, 2nd edn. Blackwell Publishing, 375–449.
- Melloul, A. , Collin, M. 1992. The ‘principal components’ statistical method as a complementary approach to geochemical methods in water quality factor identification; application to the Coastal Plain aquifer of Israel. *J. Hydrol.*, 140, 49–73.
- Mohapatra P.K., Vijay R., Pujari P.R., Sundaray S.K., Mohanty B.P. 2011. Determination of processes affecting groundwater quality in the coastal aquifer beneath Puri City, India: a multivariate statistical approach. *Water Science and Technology*, 64(4), 809-817.
- Mooi, E., Sarstedt, M. 2011. Cluster analysis. In: Mooi, E., Sarstedt, M. (Eds.), *A Concise Guide to Market Research: The Process, Data, and Methods Using IBM SPSS Statistics*, Springer-Verlag Berlin Heidelberg, pp. 237–284.
- Mook, W.G., 1980. The dissolution-exchange model for dating of groundwater with ¹⁴C., in Fritz, P., and Fontes, J.C., (eds.), *Handbook of Environmental Isotopes Geochemistry*, Elsevier, Amsterdam, 1, 50–74.

- Morgan, K. , Jankowski, J. , Taylor, G., 2006. Structural controls on groundwater flow and groundwater salinity in the Spicers Creek catchment, Central West region, New South Wales. *Hydrol. Process.*, 20 , 2857–2871.
- Négrel, P., Pauwels, H., Dewandel, B., Mascré, C., Gandolfi, JM., Ahmed, S. 2011. Understanding groundwater systems and their functioning through the study of stable water isotopes in a hard-rock aquifer (Maheshwaram watershed, India) *J. Hydrol.*, 397, 55–70.
- Nolan. B.T. 1999. Nitrate behavior in ground waters or the Southeastern USA . *J. Environ. Qual.* 28(5): 1518-1527.
- Ohsumi, T. and Fujino, H. 1986. Isotope exchange technique for preparation of hydrogen gas in mass spectrometric D/H analysis of natural waters. *Anal. Sci.*, 2, 489-490.
- Puckett, L.J., and O.P. Bricker. 1992. Factors controlling the major ion chemistry of streams in the Blue Ridge and Valley and Ridge physiographic provinces of Virginia and Maryland. *Hydrolog. Proc.* 6:79-98.
- Rakotomalala, R., 2013. Didacticiel - Études de cas (in English). Available online http://eric.univ-lyon2.fr/~ricco/tanagra/fichiers/en_Tanagra_KMO_Bartlett.pdf accessed on January 6th, 2016.
- Rao, Y. R. S., Keshari, A. K. , Gosain, A. K. 2010. Evaluation of regional groundwater quality using PCA and geostatistics in the urban coastal aquifer, East Coast of India. *International Journal of Environment and Waste Management* 5 (1–2), 163–180.
- Sanford, R.F., Pierson, C.T., Crovelli, R.A., 1993. An objective replacement method for censored geochemical dat. *Math.Geol.* 25(1), 59-80.
- Scanlon, B.R., Healy, W.H., Cook, P.G., 2002. Choosing appropriate techniques for quantifying groundwater recharge. *Hydrogeology Journal*, 10, 18-39.
- Shapiro, S. S., Wilk, M. B., 1965. An analysis of variance test for normality (complete sampels),

- Biometrika, 52 , 591–611.
- Singh, S. K., Singh, C. K., Kumar, K. S., Gupta, R., Mukherjee, S. 2009. Spatial-temporal monitoring of groundwater using multivariate statistical techniques in Bareilly District of Uttar Pradesh, India. *J. Hydrology and Hydromechanics*, 57 (1), 45–54.
- Sneath, P. H. A., 1957. The application of computers to taxonomy. *Journal of General Microbiology*, 17, 201–226.
- Sokal, R. R., and Michener, C. D., 1958. A statistical method for evaluating systematic relationships. *University of Kansas Science Bulletin*, 38, 1409–1438.
- Sorensen, T., 1948. A method of establishing groups of equal amplitude in plant sociology based on similarity of species content and its application to analyses of the vegetation on Danish commons. *Biologiske Skrifter*, 5, 1–34.
- Spicer, J., 2004. What Makes a Difference?. In: Spicer, J, (Ed.) *Making Sense Multivariate Data: An Intuitive Approach*, SAGE Publications, Inc. Thousand Oaks, USA. https://uk.sagepub.com/sites/default/files/upm-binaries/5079_Spicer_Chapter_1.pdf. Accessed on January 6th, 2016.
- Stauffer, D. F., Garton, E. O., Steinhorst, R. K. 1985. A comparison of principal component from real and random data. *Ecology*, 66, 1693-1698.
- Stevens, Graham J., 2015. Natural Dissipation of MTBE in Groundwater at UST Sites Following the Connecticut Ban in 2004. Master's Theses. P. 716. http://digitalcommons.uconn.edu/gs_theses/716 accessed on January 18th, 2016.
- Templ, M., Filzmoser, P. , Reimann, C., 2008. Cluster analysis applied to regional geochemical data: Problems and possibilities. *Applied Geochemistry* 23 (8): 2198-2213. DOI: 10.1016/j.apgeochem.2008.03.004.

- Townend, J., 2002. Practical statistics for environmental and biological scientists: John Wiley and Sons Ltd.
- Tweed, S., Leblanc, M., Cartwright, I., Favreau, G., Leduc, C., 2011. Arid zone groundwater recharge and salinisation processes; an example from the Lake Eyre Basin, Australia, *J. Hydrol.*, 408, 257-275.
- US Environmental Protection Agency, 1997. The Determination of Inorganic Anions in Water by Ion Chromatography, USEPA, Method 300.1, Cincinnati, OH, 1997.
- Valder, J.F., Long, A.J., Davis, A.D., Kenner, S.J., 2012. Multivariate statistical approach to estimate mixing proportions for unknown end members. *J. Hydrol.* ,460–461, 65–76
- Vanderzalm, J.L., Jeuken, B.M., Wischusen, J.D.H., Pavelic, P., Le Gal La Salle, C., Knapton, A., Dillion, P.J. 2011. Recharge sources and hydrogeochemical evolution of 5 groundwater in alluvial basins in arid central Australia. *Journal of Hydrology*, 6 397(1-2): 71-82.
- Ward, J.H., Jr. 1963. Hierarchical Grouping to Optimize an Objective Function. *Journal of the American Statistical Association*, 58, 236–244.
- Wilde, F.D., Radtke, D.B., Gibs, Jacob, and Iwatsubo, R.T., eds., 2004 with updates through 2009, Processing of water samples (ver. 2.2): U.S. Geological Survey Techniques of Water-Resources Investigations, book 9, chap. A5, April 2004, available at <http://pubs.water.usgs.gov/twri9A5/>. accessed on December 8th, 2015.
- Yoshida, N. 2002. Fundamentals of hydrogen and oxygen isotopes in hydrology, in: Yoshida, N. (Ed.), *Hydrogen and Oxygen Isotopes in Hydrology*, UNESCO, 153-179.
- Yuan, R., Song, X., Zhang, Y., Han, D., Wang, S., Tang, C. 2011. Using major ions and stable isotopes to characterize recharge regime of a fault-influenced aquifer in Beiyishui River Watershed, North China Plain. *J. Hydrol.*, 405, 512–521.
- Yurtsever, Y., 1994. Role of environmental isotopes in studies related to salinization processes and salt

water intrusion dynamics In: Proceedings of the 13th saltwater intrusion meeting, Calgary, Italy, 5–10 June 1994, 177–185.

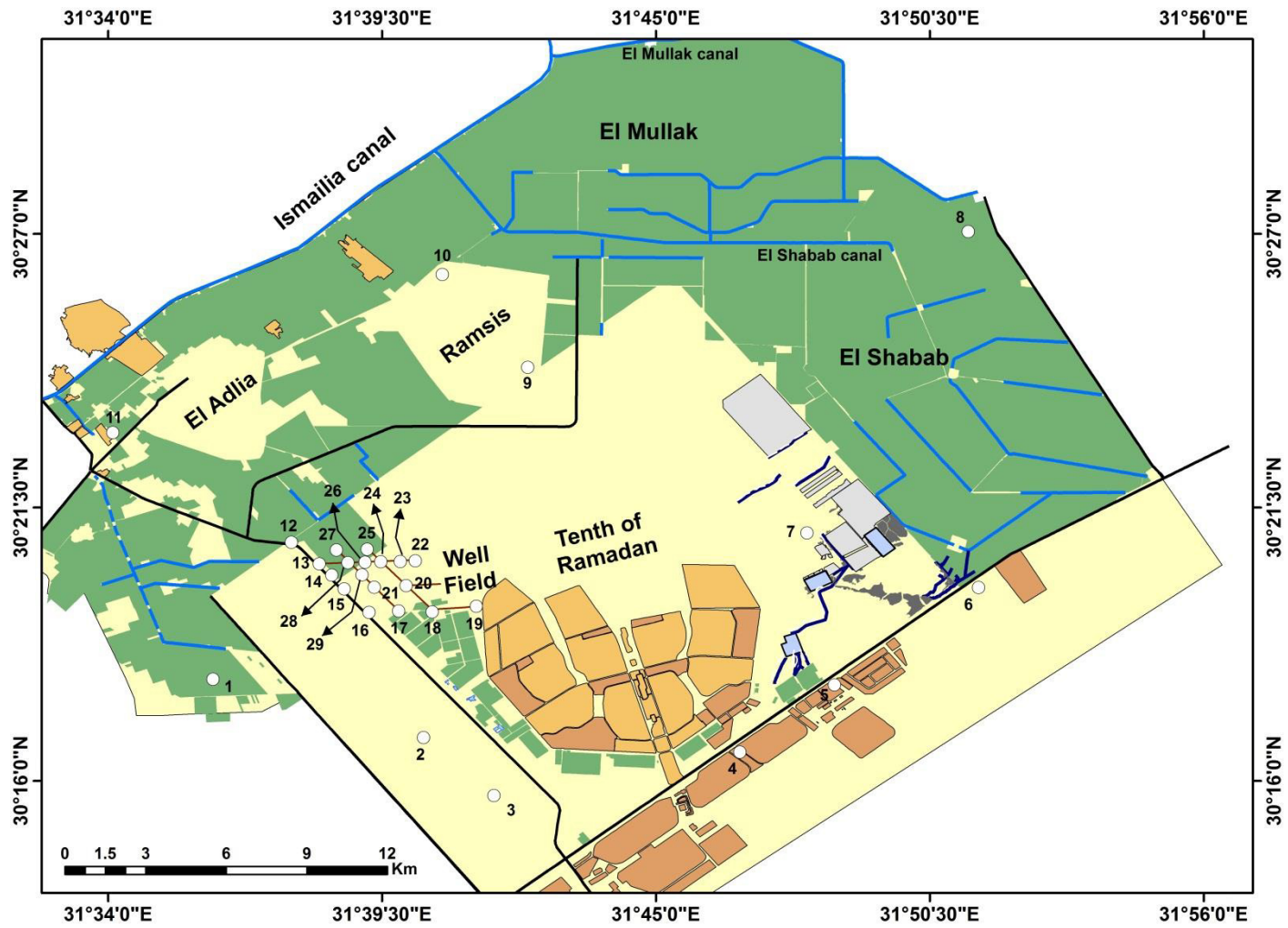


Fig. 3.1 Location map of the available boreholes with lithologic data in the study area.

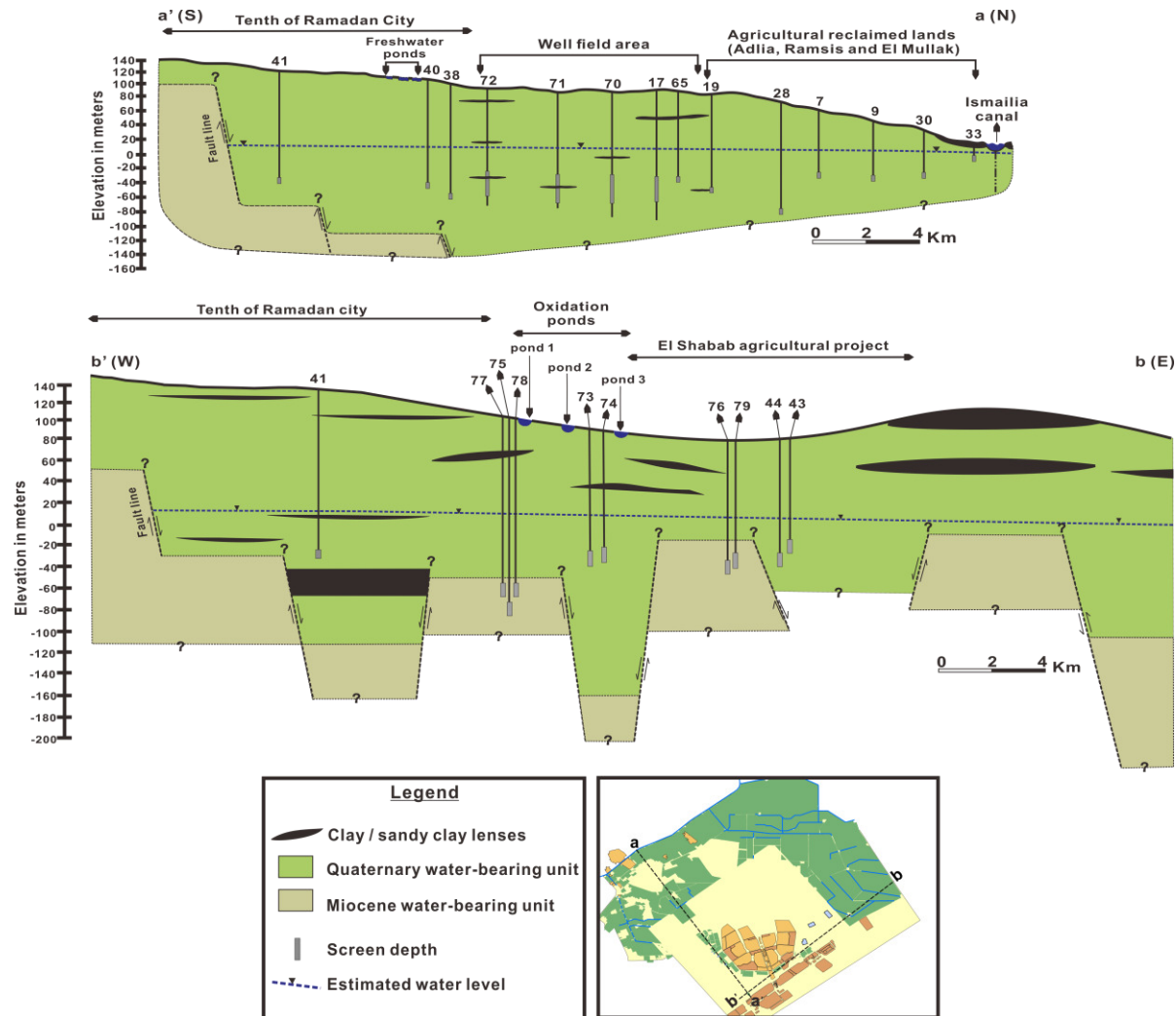


Fig. 3.2 Schematic drawings of the subsurface hydrogeological conditions of the study area.

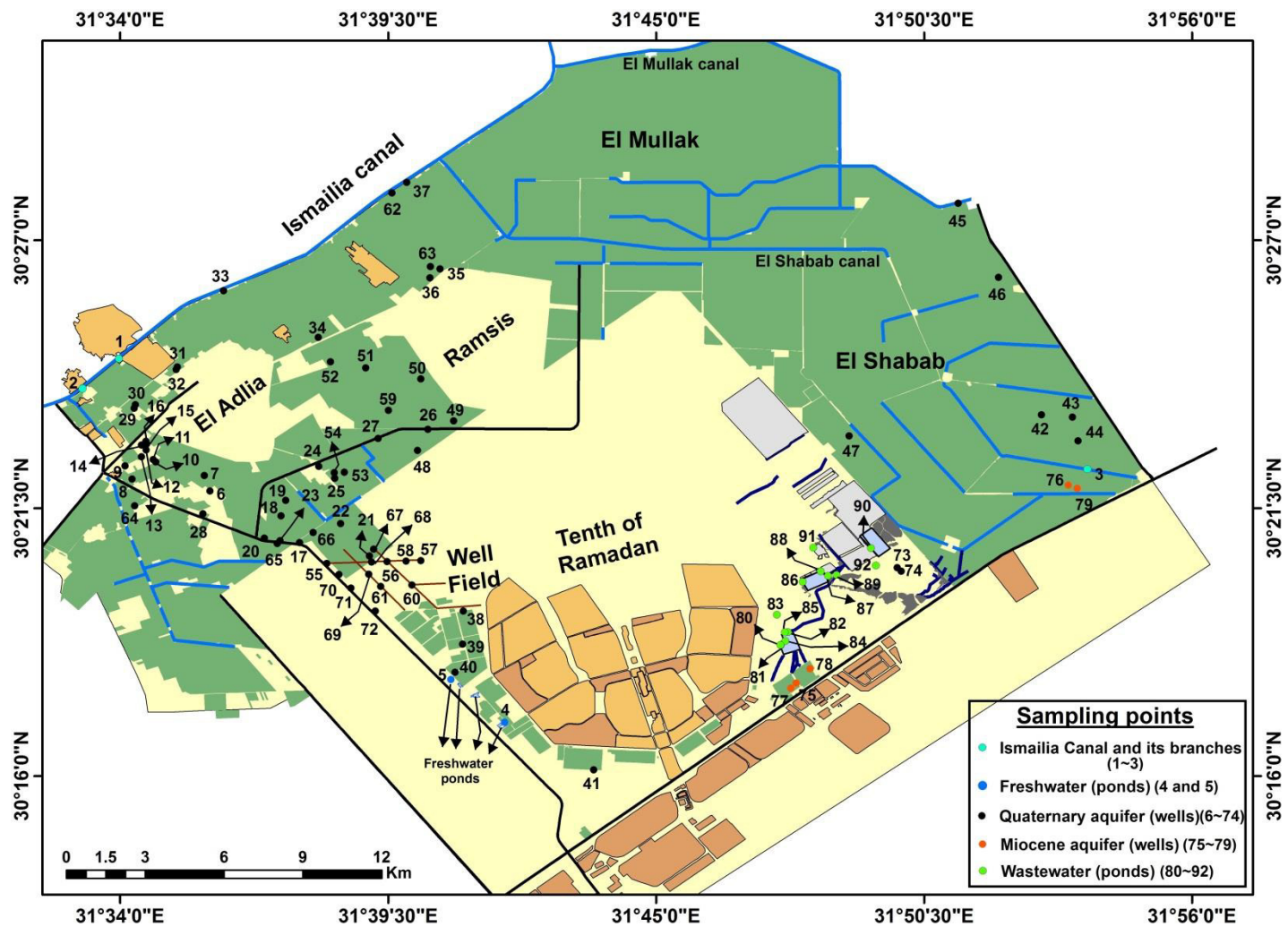


Fig. 3.3 Location map of the sampling points.



Active groundwater wells sampled from the study area



In-situ field measurements (pH, EC, and T)



Office measurements (e.g. alkalinity and spectrophotometric analyses)

Fig. 3.4 Flowchart of field and office measurements after each sampling day.

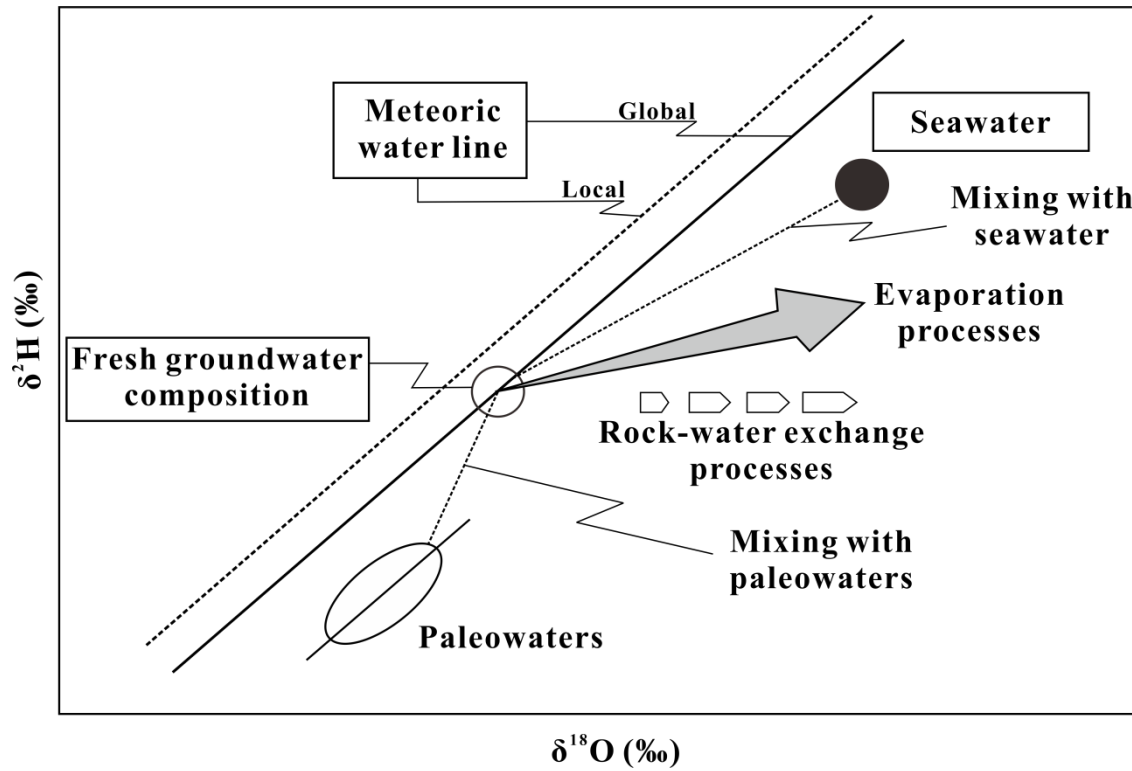


Fig. 3.5 Various processes which shift the $\delta^{18}\text{O}$ and $\delta^2\text{H}$ values from the meteoric water line (MWL). Modified after Yurtsever (1994) and Geyh (2000).

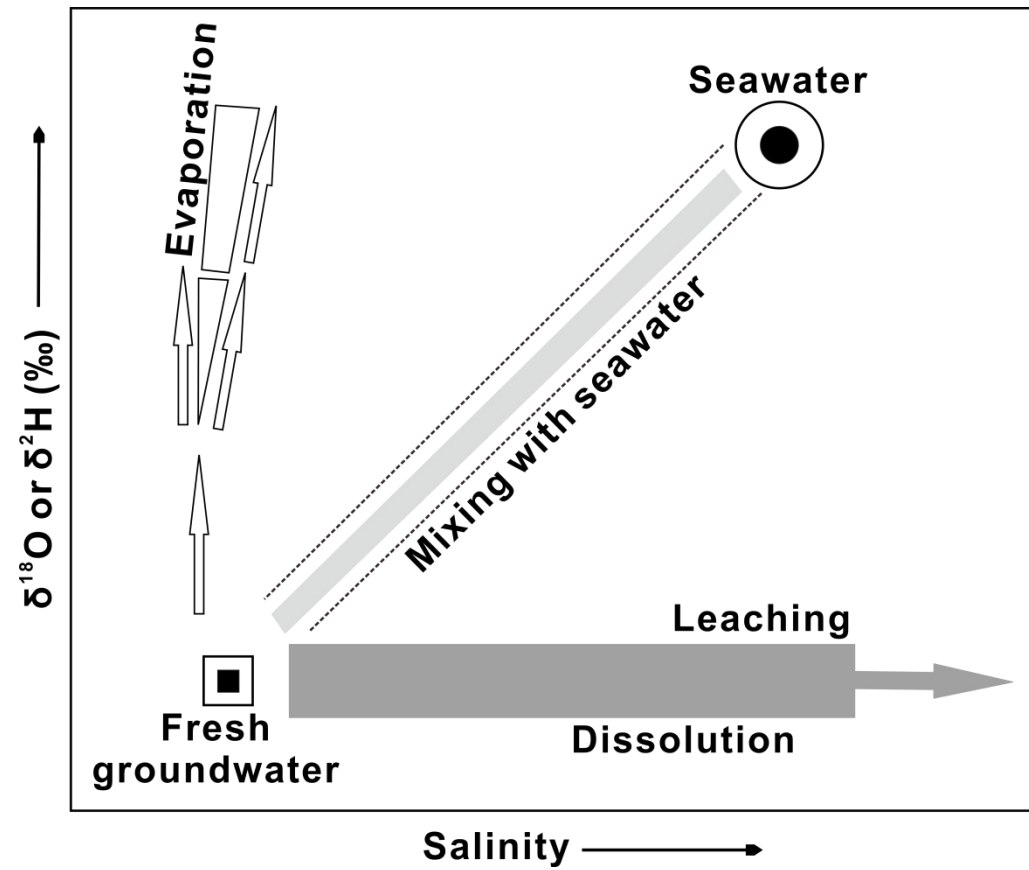


Fig. 3.6 Stable isotope composition ($\delta^{18}\text{O}$ or $\delta^2\text{H}$) versus salinity for the identification of different salinization processes: mixing of fresh water and seawater, dissolution of salt and leaching, and evaporation. Modified after Yurtsever (1994) and Geyh (2000).

----- CHAPTER 4: RESULTS -----

Generally, no major temporal changes could be observed in the chemical pattern of the groundwater samples in the Quaternary aquifer (Table 4.1; Fig. 4.1). Although some exceptions to this general finding were observed in the anomalous depletion of potassium (K^+) concentration during 2014 campaign (Fig. 4.1) that might be related to an analytical error. Also, local changes in the concentration of some ions, i.e., Na^+ , and SO_4^{2-} , observed at site Nos. 39 and 54 might be related to site-specific conditions or an analytical error. The average $\delta^{18}O$ composition (-1.15 ‰) of first campaign is similar to that of the second campaign average isotopic values (-1.05 ‰) with standard deviations 1.28 ‰ and 1.30 ‰ for first and second campaigns, respectively. The same is observed for δ^2H . Based on that, seasonal effect on groundwater samples of the Quaternary aquifer was very small and can be ignored.

4.1. CONVENTIONAL HYDROCHEMICAL ANALYSIS

Major ion concentration, nutrient constituents (NH_4^+ and NO_3^-), and stable isotopic composition from the four groups of samples, i.e., surface water (Ismailia Canal, irrigation canals and freshwater ponds), groundwater in the Quaternary aquifer, groundwater in the Miocene aquifer, and wastewater from the wastewater ponds, are shown in Table 4.2. The chemical and isotopic composition of the River Nile, and the Ismailia Canal, changed temporally in response to the construction of the Aswan High Dam, completed in 1970, which collects water in the upper part of the Nile watershed by the Lake Nasser (El Bakri et al., 1992; Nada et al., 2002; Nada, 2013). According to the previous researchers (El Bakri et al., 1992; Clark and Fritz, 1997; Hussein and Moussa, 2012), the pre-1970 groundwater, recharged mainly by the Nile River, is depleted in $\delta^{18}O$ and δ^2H , plotted along or near the GMWL, and relatively similar to the mean values of precipitation in the Nile headwaters (Addis Ababa) whereas the post-1970 groundwater are more enriched due to intensive evaporation from the Lake Nasser. Available chemical and isotopic data of the old Nile water before 1970 (Matthess, 1982; Khalil and Hanaa, 1984; Awad et al., 1994; Sadek and Abd El-Samie, 2001) are also presented in Table 4.2.

A Piper diagram is presented in Fig. 4.2. This diagram is useful in screening and sorting large numbers of chemical data to aid in rapid determinations of similarities and differences among water samples (Piper, 1944). Water from the Ismailia Canal, water from fresh water ponds, and the old Nile water were characterized by $\text{Ca}^{2+}\text{-HCO}_3^-$ water type which showed low electric conductivity (EC) ranging in between 320 $\mu\text{S/cm}$ to 501 $\mu\text{S/cm}$ (Table 4.2). The pH of the surface water (Ismailia Canal and fresh water ponds) were alkaline (from 7.8 to 8.4). Based on the Piper's classification, four water types can be distinguished in the groundwater of the Quaternary aquifer. The first type, $\text{Ca}^{2+}\text{-HCO}_3^-$ water, is plotted in the same field with the Ismailia canal and freshwater ponds. Samples from this type are located along the main course of the Ismailia canal, i.e., sample Nos. 33 and 37 (Fig. 3.3). The second type is classified as mixed $\text{Na}^+, \text{Ca}^{2+}\text{-HCO}_3^-$ water type and is found within three kilometers from the canal course, i.e., sample Nos. 31, 32, and 62 (Fig. 3.3). Both aforementioned types have EC values less than 1000 $\mu\text{S/cm}$ (Table 4.2 ; Fig. 4.3). The third type is mixed $\text{Ca}^{2+}, \text{Mg}^{2+}\text{-Cl}^-, \text{SO}_4^{2-}$ water type and is found in El Adlia area, i.e., sample Nos. 12, 13, 16 (Fig. 3.3). The EC of the latter varied from 500 $\mu\text{S/cm}$ to 1779 $\mu\text{S/cm}$ (Table 4.2 ; Fig. 4.3). The fourth type, majority of the water samples from the Quaternary aquifer, is distributed over the rest of the region and described as $\text{Na}^+\text{-Cl}^-$ or $\text{Na}^+\text{-Cl}^-, \text{SO}_4^{2-}$ waters. The increase of EC is observed in the last type from the north and northwest ($< 1000 \mu\text{S/cm}$), i.e., the well field area and close (3 to 6 kilometer distance) to the Ismailia canal, to south and southeast ($> 6000 \mu\text{S/cm}$) at El Shabab agricultural area (Fig. 4.3). However, some groundwater samples with high EC values were also found south of the Ismailia canal, i.e., sample No. 9, 11, 34, and 63, and north of the well field area, i.e., sample Nos. 17, 22, 66, and 67 (Fig. 4.3). The pH conditions of the groundwater samples from the Quaternary aquifer ranged from near neutral (6.6) to alkaline (8.2). Near neutral pH conditions are located in wells nearby the wastewater ponds. Groundwater samples of the Miocene aquifer are dominated by $\text{Na}^+\text{-Cl}^-$ water type while wastewater samples have $\text{Na}^+\text{-Cl}^- (\text{HCO}_3^-, \text{SO}_4^{2-})$ water type. In comparison with samples of the Quaternary aquifer, the groundwater samples of the Miocene aquifer exhibit elevated

concentrations of Na^+ and Cl^- , depleted HCO_3^- , near neutral (6.8) to slightly alkaline (7.6) pH conditions, and high EC values up to 11530 $\mu\text{S}/\text{cm}$ (Table 4.2). Wastewater samples were enriched in HCO_3^- compared with the sample from the Ismailia canal and groundwater of the Miocene and Quaternary aquifers. The pH varied from acidic (6.46) in pond 3 to alkaline (9.29) in pond 1, while EC ranged from 774 $\mu\text{S}/\text{cm}$ to 3440 $\mu\text{S}/\text{cm}$ for pond 1 (domestic wastewater), from 832 $\mu\text{S}/\text{cm}$ to 2390 $\mu\text{S}/\text{cm}$ for pond 2 (mixed domestic and industrial wastewater), from 1514 $\mu\text{S}/\text{cm}$ to 3070 $\mu\text{S}/\text{cm}$ for pond 3 (industrial wastewater) (Table 4.2).

Dissolved concentrations of nitrogen compounds (as NO_3^- and NH_4^+) are shown in Table 4.2. Overall, the main form of nitrogen compounds present in the groundwater of the Miocene and Quaternary aquifers is nitrate, while ammonia, up to 60 mg/l, was dominant in wastewater (Table 4.2). The nitrate concentrations in groundwater of the Quaternary aquifer varied from less than 1 mg/l at the well field area to about 50 mg/l at El Shabab agricultural area (Tables 4.2).

4.2. CONVENTIONAL STABLE-ISOTOPIC ANALYSIS

The relationships between $\delta^2\text{H}$ and $\delta^{18}\text{O}$ are shown in Fig. 4.4 for groundwater samples collected from the Quaternary and Miocene aquifers, surface water from the Ismailia Canal, freshwater ponds, and wastewater from the ponds along with the global meteoric water line (GMWL) (Craig, 1961). There has been no systematic monitoring of $\delta^2\text{H}$ and $\delta^{18}\text{O}$ in precipitation at Cairo station (50 km southwest from the study area) to define the local meteoric water line (LMWL). The calculated weighted means of $\delta^{18}\text{O}$ and $\delta^2\text{H}$ for local precipitation (1987-2003) at Cairo station based on Global Network for Isotopes in Precipitation (GNIP) data, were a -4.2‰ and -23.1‰, respectively (Fig. 4.4). Data of the water in the Ismailia Canal by previous researchers (Hamza et al., 1987; Abd El-Samie et al., 2002), wastewater (Abd El-Samie et al., 2002; Khalil et al., 2015), and groundwater in the Miocene aquifer (Abd El-Samie et al., 2002), and the old Nile water (Awad et al., 1994; Sadek and Abd El-Samie, 2001) are also shown in Fig. 4.4 for reference.

A wide range, from -2.41 to 2.71‰ for $\delta^{18}\text{O}$ and from -18 to 24.4‰ for $\delta^2\text{H}$, is observed in groundwater of the Quaternary aquifer (Table 4.2). The majority of groundwater samples from the Quaternary aquifer are plotted in the range from -2.2 to -0.2‰ for $\delta^{18}\text{O}$ and from -7 to 6‰ for $\delta^2\text{H}$ while groundwater samples from wells in the eastern part, i.e., El Shabab agricultural area, are shifted to the heavier $\delta^{18}\text{O}$ and are lined in a linear trend, i.e., sample Nos. 42 to 47 (Fig. 4.4). Groundwater samples from the Miocene aquifer show depleted isotopic signature, less than -29.9 and -4.05‰ for $\delta^2\text{H}$ and $\delta^{18}\text{O}$, respectively, compared with the groundwater from the Quaternary aquifer (Fig. 4.4). Samples from wastewater ponds have the most enriched isotopic signatures (from 18.2 to 32 ‰ for $\delta^2\text{H}$ and from 2.4 to 3.11 ‰ for $\delta^{18}\text{O}$), higher than the other surface water samples (from 19 to 21.2 ‰ for $\delta^2\text{H}$ and from 1.80 to 2.47 ‰ for $\delta^{18}\text{O}$), possibly due to evaporation.

Spatially, heavier (less negative) isotope values of the groundwater in the Quaternary aquifer were observed nearby the Ismailia canal and the freshwater ponds while lighter (more negative) values were recorded in the southern part of the study area, i.e., along the Cairo-Ismailia desert road (Fig. 4.5). Also, the distribution of $\delta^{18}\text{O}$ showed a relative depletion of stable isotope values in the well field area and some wells, i.e., 17, 18, and 66, in the agricultural areas northward of the well field. Heavier isotope values are also characterized for groundwater samples in El Shabab agricultural area (Fig. 4.5).

4.3. MULTIVARIATE STATISTICAL ANALYSIS

4.3.1. Data preparation and analysis

Due to small range of pH and temperature (T), these two variables were excluded from the multivariate analysis. Minor solutes (NO_3^- and NH_4^+), $\delta^{13}\text{C}$, and ^{14}C were also not considered due to missing data (not measured) of most of the samples. Potassium (K^+) was excluded from the analyses because it was below detection limits for a large number of samples (about 54 % of the samples). Such data are not appropriate for many multivariate techniques as noted by Sanford et al. (1993) and Güler et al. (2002). Samples with missing data values, i.e., Nos. 10, 11, 27, 33, and 37, were not included in the

multivariate analysis. Samples with ion balance error above 10 %, i.e., Nos. 2, 3, 4, and 5, were rejected as they were supposed to miss important ions. Finally, the dataset used in this analysis constitutes a data matrix of 82 sampling points by nine selected physical-chemical (EC, Na⁺, Mg²⁺, Ca²⁺, HCO₃⁻, Cl⁻, and SO₄²⁻) and isotopic ($\delta^{18}\text{O}$ and $\delta^2\text{H}$) variables.

Because PCA is based on correlations, the variables should be related to each other (in pairs) in a linear or even monotonically relationship (Leech et al., 2015). The relationship can be assessed among variables with matrix scatterplots, as shown in Fig 4.6. From Fig. 4.6, most of the variables are linearly or at least monotonically related to one another. Also, because many statistical techniques, including PCA, assume multivariate normally distributed data, it is important to ensure that the data reflect this pattern. The distributions of nine variables, used for PCA, were evaluated for normality distribution through graphical displays such as quantile-quantile plot (Q-Q plot) (Fig. 4.7), and through descriptive statistics of the data, such as central tendency (mean and median) and dispersion (standard deviation and skewness) (Table 4.3). The Q-Q plot depicts the sample quantiles on the x axis against the theoretical quantiles from a normal distribution of the same sample size on the y axis (Chambers et al., 1983). If the data are from a perfectly normal distribution, the data will lie on a diagonal straight line while departures from the diagonal indicate deviations from a normal distribution (McGarigal, 2000). Also, skewed distributions show up nicely as deviations from the line at the tails (McGarigal, 2000). From the Q-Q plots (Fig. 4.7), the variables were generally found to be positively skewed with deviations from the diagonal line at the tails. The skewness coefficients are tabulated in Table 4.3 for each variable. The distributions of all variables, except deuterium ($\delta^2\text{H}$), were positively skewed. The calculated skewness is significant and sufficiently large since the absolute values of skewness coefficients are higher than two times their standard errors (Table 4.3). In addition to the previous graphical and statistical tests of normality, the data were also analyzed by running a Shapiro-Wilk test, using XLSTAT, to further test the normality of the data. The Shapiro-Wilk test (Shapiro and Wilk, 1965) uses the hypothesis testing format to determine if a

normal distribution could be used to describe the data or not. The null hypothesis (H_0) states that the distribution function $F(x)$ is a normal distribution function whereas the alternative hypothesis (H_a) states $F(x)$ is non-normal. Shapiro-Wilk test calculates a test parameter (W), which is presented together with a probability of finding samples, with a worse match, with a normal distribution than the studied data set (Englert, 2003). This probability gives the significance level at which the normality of the data set is acceptable from a statistical point of view (Englert, 2003). With a α level of 0.05, the null-hypothesis would be rejected and the sample would be determined not to be normally distributed if the probability of the outcome (p-value) is less than 0.05 (Stevens, 2015). Conversely, if the p-value is greater than the α level, the null hypothesis cannot be rejected and the sample may be normally distributed (Stevens, 2015). As shown in [Table 4.4](#), the p-value from the Shapiro-Wilk test clearly does not support a normal distribution with the results for all variables less than 0.0001. This is less than the α level of 0.05, and therefore, the null-hypothesis would be rejected and the sample would be determined not to be normally distributed. Based on the shape of the Q-Q plots, skewness coefficients, and Shapiro-Wilk tests for each variable, it was determined that non-parametric statistical techniques, Spearman's rank correlation, were necessary for calculating the correlation matrix, used as input for the PCA. Because of the different variable units and ranges in the concentrations of each, a correlation matrix was used so that each variable is normalized to unit variance and therefore contributed equally to the PCA (Farnham et al., 2003; Chen et al., 2007; Ghesquière et al., 2015). [Tables 4.5 and 4.6](#) provide the Spearman's rank correlation coefficients and probability (p) values, respectively, for the analyzed parameters.

4.3.2. Hierarchical cluster analysis (HCA)

The HCA was performed on the standardized groundwater dataset of the Quaternary aquifer (64 samples) by Ward's method as amalgamation rule using squared Euclidean distance as similarity measure. [Fig. 4.8](#) shows the dendrogram, a more effective way of showing the clusters, obtained from HCA of the groundwater samples in the Quaternary aquifer. The vertical scale represents the measure of

similarity that is used to define the similarities between the sample points while the sample points are along the horizontal axis. The phenon line, an arbitrary line that defines clusters in Fig. 4.8, was drawn across the dendrogram at a linkage distance of about 42. Samples with linkage distance lower than 42 are therefore grouped into the same cluster. Based on the dendrogram and a linkage distance of 42, four major clusters were identified. Samples from clusters 1 and 2 are linked to the other two clusters 3 and 4 at an elevated distance (284.41), indicating that groundwater samples in clusters 1 and 2 are clearly distinct from the groundwater samples of clusters 3 and 4. Clusters 3 and 4 have the lower linkage distance (about 71) of the four clusters (Fig. 4.8), therefore, has the greater similarity between the clusters. It can be expected that the geochemistry of the groundwater samples of cluster 3 would have similarities with the ones of cluster 4. From the dendrogram, more than half (59%) of the samples were classified to cluster 1. In order to conduct detailed analysis, cluster 1 was divided into four subclusters (Fig. 4.8). The clusters were identified spatially by reclassifying the location map of the study area with the clusters (Fig. 4.9).

4.3.3. Principal component analysis (PCA)

PCA was applied to determine the variables that best represent the variations among four clusters identified using HCA, and to explore the relationships among the clusters in the groundwater of the Quaternary aquifer and other water groups in the study area, i.e., the Ismailia Canal, groundwater in the Miocene aquifer, wastewater from the wastewater ponds, and the old Nile water. As can be seen from the Spearman's correlation matrix (Table 4.5), EC, Na⁺, Mg²⁺, Ca²⁺, Cl⁻, and SO₄²⁻ show relatively moderate to strong correlations with one another ($r = 0.569-0.956$). Weak to moderate negative correlations are apparent between HCO₃⁻ and all the variables, but moderate positive correlations with $\delta^2\text{H}$ and $\delta^{18}\text{O}$. EC, Na⁺, Cl⁻, and SO₄²⁻ exhibit negative weak to moderate correlations with $\delta^2\text{H}$ and $\delta^{18}\text{O}$. A statistically significant strong positive correlation between $\delta^2\text{H}$ and $\delta^{18}\text{O}$ was also found ($r = 0.948$). In addition, the Spearman's correlation coefficients determined that specific variables were not statistically significant at the $\alpha = 0.05$ level of significance, i.e., Mg²⁺ with both $\delta^2\text{H}$ and $\delta^{18}\text{O}$, and Ca²⁺ with $\delta^{18}\text{O}$

(Tables 4.5 and 4.6). The correlations shown in Table 4.5 are translated into Principal Components (PCs) by calculating eigenvalues (Table 4.7). The number of significant principal components (PCs) was determined based on Kaiser Normalization Criterion (Kaiser, 1960). Two principal components, with eigenvalues larger than one, accounted for 80.9 % of the total variance in the data, are regarded as significant (Table 4.7). Thereafter, Varimax rotation was performed on extracted two significant PCs to improve the interpretation of PCA, as it increased the absolute values of larger loadings and reduced the absolute values of smaller loadings within each component (Lei, 2013). Table 4.8 summarizes the PCA results after rotation, including the loadings, the eigenvalues, the amount of variance explained by each PC, and the cumulative variance. The PC loadings were sorted according to the criteria of Liu et al. (2003), i.e., strong, moderate, and weak, corresponding to the absolute loading values of more than 0.75, 0.75–0.50 and 0.50–0.30, respectively. As shown in Table 4.8, first principal component (PC1) represents the largest proportion, i.e., 53.1 % of the total variance within the dataset. It is associated with strong positive weightings of EC, Na⁺, SO₄²⁻, Cl⁻, Ca²⁺, and Mg²⁺ and negative weak weightings of HCO₃⁻. The second principal component (PC2), which explains 27.8% of the total variance within the dataset, exhibits strong positive weightings of δ¹⁸O and δ²H, moderate positive weighting of HCO₃⁻, and negative weightings for Cl⁻ (Table 4.8). The correlations between the nine variables (Table 4.5) determine which variables contribute the most to the formation of the PCs (Table 4.3); high correlations (± 0.6 or greater) will be grouped together by the PC while low correlations will not have high loadings on the same PC. The loadings of the nine variables on PCs (Table 4.8) are also depicted graphically in the correlation circle shown in Figure 4.10. The loadings of these variables for PC1 and PC2 plot very close together, suggesting that the processes that impact these variables' concentrations and variability in the groundwater are similar (Iranmanesh et al., 2014). The EC contributes significantly to the PC1. EC represents the contributions of all the constituents in the groundwater samples therefore, the PC1 may be termed “salinity factor of groundwater”. The δ¹⁸O, δ²H, and HCO₃⁻ contribute to the PC2.

Concentrations of these variables are controlled by the interaction and mixing of groundwater with different water sources, surface water from the Ismailia Canal and/or groundwater from the Miocene aquifer. Hence, The PC2 might be termed “groundwater mixing”.

Fig. 4.11 shows the scores of the groundwater samples from the Quaternary aquifer and other water groups on PCA space (PC1 vs. PC2). There appears to be reasonable statistical discrimination between the four major clusters as defined by HCA. The four clusters of the groundwater in the Quaternary aquifer occupy different areas in PCA space (Fig. 4.11). Most of the samples from clusters 1 along with the old Nile River water are in quadrants 1 and 4. Cluster 2 samples, except for sample No. 59, and water from the Ismailia Canal are plotted in quadrant 1. Most of the samples assigned to cluster 3 are plotted in quadrant 3. Cluster 4 samples are in quadrant 2 and have higher positive PC1 scores. Groundwater samples from the Miocene aquifer are positioned in quadrant 3 whereas wastewater samples are located in quadrants 1 and 2 with high positive PC2 scores (Fig. 4.11).

4.3.4. Re-evaluation of conventional hydrochemical and isotopic analyses

As illustrated above, the use of conventional techniques, Piper diagram and $\delta^{18}\text{O}$ - $\delta^2\text{H}$ plot proved to have limitations compared with the multivariate methods for partitioning water chemistry and isotopic data of the Quaternary aquifer into distinct clusters that may be significant in the hydrogeologic context, i.e., different recharge sources and mixing processes. HCA classified the 64 groundwater samples of the Quaternary aquifer into four major clusters and four subclusters using nine variables (Fig. 4.8). Statistical summaries of the variables under each cluster were introduced in Table 4.9 and combined with graphical techniques, i.e., Piper (Fig. 4.12) and Stiff (Fig. 4.13) diagrams to provide efficient hydrochemical and isotopic evaluation of the four major clusters defined for the groundwater of the Quaternary aquifer.

As shown in Table 4.9, subcluster 1.1 (n= 5) has low EC (average 956 $\mu\text{S}/\text{cm}$) as indicated by very small Stiff diagram size (Fig. 4.13) and is spatially distributed within El Adlia area (Fig. 4.9). From

the Piper diagram (Fig. 4.12), this subcluster is plotted closer to surface water from the Ismailia Canal and the Old Nile water. Subcluster 1.2 (n= 8) have elevated Na^+ , Cl^- , and SO_4^{2-} concentrations and slightly higher EC (average 1764 $\mu\text{S}/\text{cm}$) than subcluster 1.3 (n= 14) (average 1335 $\mu\text{S}/\text{cm}$) (Table 4.9 and Fig. 4.13). Subcluster 1.2 is distributed in El Adlia to Ramsis areas while subcluster 1.3 at the well field area (Fig. 4.9). Subcluster 1.4 (n= 11) is characterized by elevated concentrations of Na^+ , Cl^- , and SO_4^{2-} and high EC (average 2950 $\mu\text{S}/\text{cm}$) (Table 4.9 and Fig. 4.13) compared to the other subclusters. $\delta^{18}\text{O}$ and $\delta^2\text{H}$ are progressively increased in the following sequence, subclusters 1.3 to 1.4 to 1.2 to 1.1 (Table 4.9), i.e., from the well field area to the El-Adlia area. Groundwater samples assigned to cluster 2 (n= 8) are plotted close to water from the Ismailia Canal in the Piper diagram (Fig. 4.12) and spatially found along and within four kilometers from the Ismailia Canal and near the freshwater ponds (Fig. 4.9). This cluster is characterized by high HCO_3^- concentration (average 241 mg/l) and most enriched $\delta^{18}\text{O}$ and $\delta^2\text{H}$ (Table 4.9). Cluster 3 (n= 10) and cluster 4 (n= 8) have considerably elevated Na^+ , Cl^- and SO_4^{2-} concentrations, and very high average EC values, i.e., 3610 $\mu\text{S}/\text{cm}$ and 6100 $\mu\text{S}/\text{cm}$, respectively (Table 4.9 and Fig. 4.13), compared to the first two clusters. Additionally, cluster 3 is more depleted in $\delta^{18}\text{O}$ and $\delta^2\text{H}$ relative to cluster 4 (Table 4.9) and projected together on the Piper diagram close to the groundwater of the Miocene aquifer (Fig. 4.12). Samples from the latter two clusters (clusters 3 and 4) are spatially located north of the well field area, El Adlia and Ramsis areas, neighboring the groundwater wells of the Miocene aquifer in the south of the study area, and in El-Shabab area adjacent to the wastewater ponds (Fig. 4.9). Although NO_3^- is not considered in the HCA but it is found to be variant between four clusters (Table 4.9) and therefore could be used to further characterize each cluster. Subcluster 1.3 has the lowest nitrate concentrations (average 2.6 mg/l) compared to cluster 4 (average 36.6 mg/l) (Fig. 4.14).

From $\delta^{18}\text{O}$ - $\delta^2\text{H}$ plot (Fig. 4.15), the isotopic composition of subcluster 1.1 has a narrow range of $\delta^{18}\text{O}$ (-0.87 to -0.53‰) and $\delta^2\text{H}$ (1 to 3.7‰) values. It is plotted very close to the old Nile water component (Fig. 4.15). According to their relative alignment in Fig 4.15, subcluster 1.2 is slightly

enriched in $\delta^{18}\text{O}$ (-1.44 to -0.46‰) and $\delta^2\text{H}$ (-6.3 to 3.2‰) than subcluster 1.3 (-1.74 to -1.38‰ for $\delta^{18}\text{O}$, -6.8 to -2.3‰ for $\delta^2\text{H}$). Samples from subcluster 1.4 are plotted in a wide range from -1.76 to -0.04‰ for $\delta^{18}\text{O}$ and from -6.5 to 6.9‰ for $\delta^2\text{H}$. Highly enriched values of cluster 2, from 0.49 to 2.71‰ for $\delta^{18}\text{O}$ and from 10.5 to 24.4‰ for $\delta^2\text{H}$, are plotted near the surface water from the Ismailia canal and freshwater ponds. Highly depleted values of cluster 3, from -2.41 to -0.47‰ for $\delta^{18}\text{O}$ and from -18 to 3.1‰ for $\delta^2\text{H}$, were shifted toward the groundwater samples from the Miocene aquifer. Samples from cluster 4 were found to be shifted to the heavier $\delta^{18}\text{O}$ and were aligned in a linear trend (Fig. 4.15).

Measured ^{14}C activities for groundwater samples from nine wells in the Quaternary aquifer ranged from 42 to 80 percent modern carbon (pMC) (Table 4.10). ^{14}C activity was highest for cluster 2, followed by subclusters 1.2 and 1.4, then subcluster 1.3. Groundwater sampled from the Miocene aquifer (sample No. 71) had a low ^{14}C activity of 35 pMC. ^{14}C activities of cluster 3 samples were in between those of subcluster 1.3 and of the Miocene aquifer (Table 4.10). Measured $\delta^{13}\text{C}$ of groundwater samples from wells in the Quaternary aquifer ranged from -11.8 to -5.4‰ (Table 4.10). The $\delta^{13}\text{C}$ values were more depleted in subclusters 1.2, 1.3 and 1.4, and cluster 2, than those in cluster 3. The $\delta^{13}\text{C}$ value of the groundwater from the Miocene aquifer was -8.2‰ (Table 4.10).

A summary table (Table 4.11) is presented for the main physical, hydrochemical, and isotopic characteristics of the defined four clusters for the groundwater in the Quaternary aquifer and the other water groups, i.e., the old Nile water, water from the Ismailia Canal, groundwater in the Miocene aquifer, and wastewater. It is apparent from Table 4.11 that some (sub) clusters, i.e., subcluster 1.1 and cluster 2, have relative similarity in hydrochemical and isotopic characteristics to the old Nile water and water from the Ismailia Canal, respectively. The same also could be applied on clusters 3 and 4 as they have similar physical and hydrochemical characteristics to the groundwater of the Miocene aquifer but more enriched stable isotopic composition.

4.4. REFERENCES

- Abd El-Samie, S.G., Sadek, M.A., Mahmoud, N.S., 2002. Assessment of groundwater pollution from the oxidation ponds in Tenth of Ramadan city, using isotopic techniques and hydrogeological modeling. Arab J. Nucl. Sci. appl., 35, 35-47.
- Awad, M. A., Farid, M. S., Hamza, M. S. 1994. Studies on the recharge of the aquifer systems in the southern portion of the Nile Delta using radioisotopes and hydrochemistry, Isotope Rad. Res., 28(1), 17-25.
- Clark, I. D., and Fritz, P. 1997. Environmental Isotopes in Hydrogeology. Lewis Publishers, Boca Raton, FL, 328 p.
- Craig, H., 1961. Isotopic variations in meteoric waters. Sci., 133, 1702-1703.
- El Bakri, A, Tantawi, M.A., Blavoux, B., Dray, M., 1992. Sources of water recharge identified by isotope in El Minya Governorate (Nile Valley, Middle Egypt). In Proceeding of International Symposium on Isotope Techniques in Water Resources Development 1991, IAEA, Vienna, 643-645.
- Hamza, M. S., Aly, A. I. M., Swailem, F. M., Nada, A., 1987. Environmentally stable isotopes and groundwater recharge in the eastern Nile delta. Int. J. Water Resour. D., 3, 228-232.
- Hussein, M. F., Moussa, L. 2012. Water management in the System of the River Nile in Egypt assisted by isotopic and geochemical data. In: Proc. 1st Int. Conf. on Integrative Sciences and Sustainable Development of Rivers, Lyon, France, 26 – 28 June 2012. <http://www.graie.org/ISRivers/actes/pdf2012/3C404-128HUS.pdf> Accessed on June 7th, 2015.
- Iranmanesh, A., Locke II, R.A., Wimmer, B.T., 2014. Multivariate statistical evaluation of groundwater compliance data from the Illinois Basin–Decatur Project. Energy Procedia, 63, 3182-3194 . <http://dx.doi.org/10.1016/j.egypro.2014.11.343>
- Kaiser, H.F., 1960. The application of electronic computers to factor analysis, Educ. Psychol. Meas., 20, 141–151.

- Khalil, J.B., Hanna, F.S., 1984. Changes in the quality of the Nile water in Egypt during the twenty-five years, 1954-1979. *Irrig. Sci.*, 5:1-13, DOI 10.1007/BF00275033.
- Lei, L., 2013. Assessment of Water Quality Using Multivariate Statistical Techniques in the Ying River Basin, China. Master thesis, University of Michigan, 52 p. available online <http://babel.hathitrust.org/cgi/pt?id=mdp.39015089709169> accessed on January 5th, 2016.
- Liu, C.W., Lin, K.H., Kuo, Y.M., 2003. Application of factor analysis in the assessment of groundwater quality in a blackfoot disease area in Taiwan. *Sci. Total Environ.*, 313, 77–89.
- Matthess G., 1982. *The Properties of Groundwater*. John Wiley, New York.
- Nada, A. A., Hussein, M. F., Forehlich, K. 2002. Climatic changes and isotopic content along the River Nile Valley. In: *proc. Int. Symp. on the Study of the Environmental Change using Isotope Techniques*, IAEA Vienna, 23-27 April 2001, IAEA, Vienna, 413-414.
- Nada, A. A., 2013. Applications of environmental isotopes in hydrological studies along the River Nile Valley, Egypt. In: *proc. Int. Symp. on Isotopes in Hydrology, Marine Ecosystems and Climate Change Studies*, Monaco, 27 March – 1 April 2011, IAEA Vienna, 1580, 137-144.
- Piper, A., 1944. A graphic procedure in geochemical interpretation of water analysis. *Trans. Am. Geophys. U.*, 914–928.
- Sadek, M.A., Abd El-Samie, S.G., 2001. Pollution vulnerability of the Quaternary aquifer near Cairo, Egypt, as indicated by isotopes and hydrochemistry. *Hydrogeology J.*, 9, 273–281.

Table 4.1 Chemical and isotopic data of 14 groundwater samples collected from the Quaternary aquifer over two campaigns (2013 and 2014).

ID	Sampling campaign	*Well depth (m)	T (°C)	pH	EC (µS/cm)	Cations (mg/l)				Anions (mg/l)			Isotopes	
						Na ⁺	K ⁺	Mg ²⁺	Ca ²⁺	HCO ₃ ⁻	Cl ⁻	SO ₄ ²⁻	δ ² H (‰)	δ ¹⁸ O (‰)
17	2014	150	28.5	7.1	4300	701	ND	25	103	175	852	673	-2.9	-1.25
	2013		27.7	7.5	4020	715	19	31	151	150	1019	573	-2.3	-1.28
24	2014	120	27.3	7.5	1788	352	ND	3	24	150	301	241	-6.3	-1.44
	2013		26.1	7.9	1960	371	9	12	37	265	413	209	-6.4	-1.62
25	2014	114	27.5	7.4	1759	326	8	6	19	229	319	183	-6.2	-1.53
	2013		27.4	7.9	1658				NM				-6.0	-1.75
26	2014	120	30.4	7.5	2120	370	ND	10	56	197	331	397	0.3	-0.81
	2013		27.4	7.9	1830	333	7	10	46	167	320	289	0.6	-1.12
35	2014	105	26.5	7.8	2140	398	ND	3	21	254	219	449	11.2	0.49
	2013		26.0	7.7	2300	461	27	7	51	246	246	499	10.5	0.54
36	2014	105	26.0	7.9	1591	346	ND	2	13	219	222	365	2.5	-0.55
	2013		26.0	7.9	2040	409	6	9	41	230	290	362	3.1	-0.59
38	2014	160	29.1	7.9	2060	373	3	2	17	198	351	149	-6.8	-1.74
	2013		27.8	7.8	2510	450	6	10	67	201	686	184	-7.2	-1.85
39	2014	160	29.3	7.8	3030	611	ND	15	63	170	716	705	-6.5	-1.76
	2013		28.9	7.8	3040	574	16	12	64	185	791	235	-6.8	-1.70
40	2014	160	27.3	8.1	1338	282	ND	1	6	190	189	252	23.6	2.69
	2013		27.4	8.0	1509	309	5	2	24	203	256	261	23.9	2.49

41	2014	165	29.5	7.3	3870	605	ND	74	203	117	933	528	-13.1	-2.32
	2013		28.4	7.3	4460	613	19	92	251	117	1305	531	-14.5	-2.54
53	2014	92	27.6	7.8	2030	381	ND	12	88	131	481	217	-0.6	-0.91
	2013		25.8	7.9	2050	368	3	12	68	145	495	184	-1.3	-1.26
54	2014	110	27.3	7.9	1531	292	ND	4	16	205	219	165	-5.2	-1.71
	2013		25.9	7.8	2990	563	9	18	72	219	573	459	-4.5	-1.49
61	2014	150	27.9	8.0	774	229	ND	1	7	189	154	98	-5.3	-1.56
	2013		27.9	8.2	989	219	2	2	30	205	158	106	-6.1	-1.92
73	2014	110	29.0	6.6	3420	946	ND	76	309	65	1685	547	-18.0	-2.41
	2013		27.5	7.7	7130	1038	21	71	403	48	2318	520	-16.4	-2.08
Average	2014				2267	444	5	17	67	177	498	355	-2.3	-1.06
	2013				2749	494	11	22	100	183	682	339	-2.3	-1.16
Standard deviation	2014				1012	199	2	25	87	49	423	199	10.1	1.31
	2013				1579	244	7	27	109	58	594	159	10.1	1.28

* Well depth information was obtained from the available well logs (e.g., well field area) and from the well owners.

EC: Electric Conductivity, T: Temperature, ND: Not Detected, NM: Not Measured

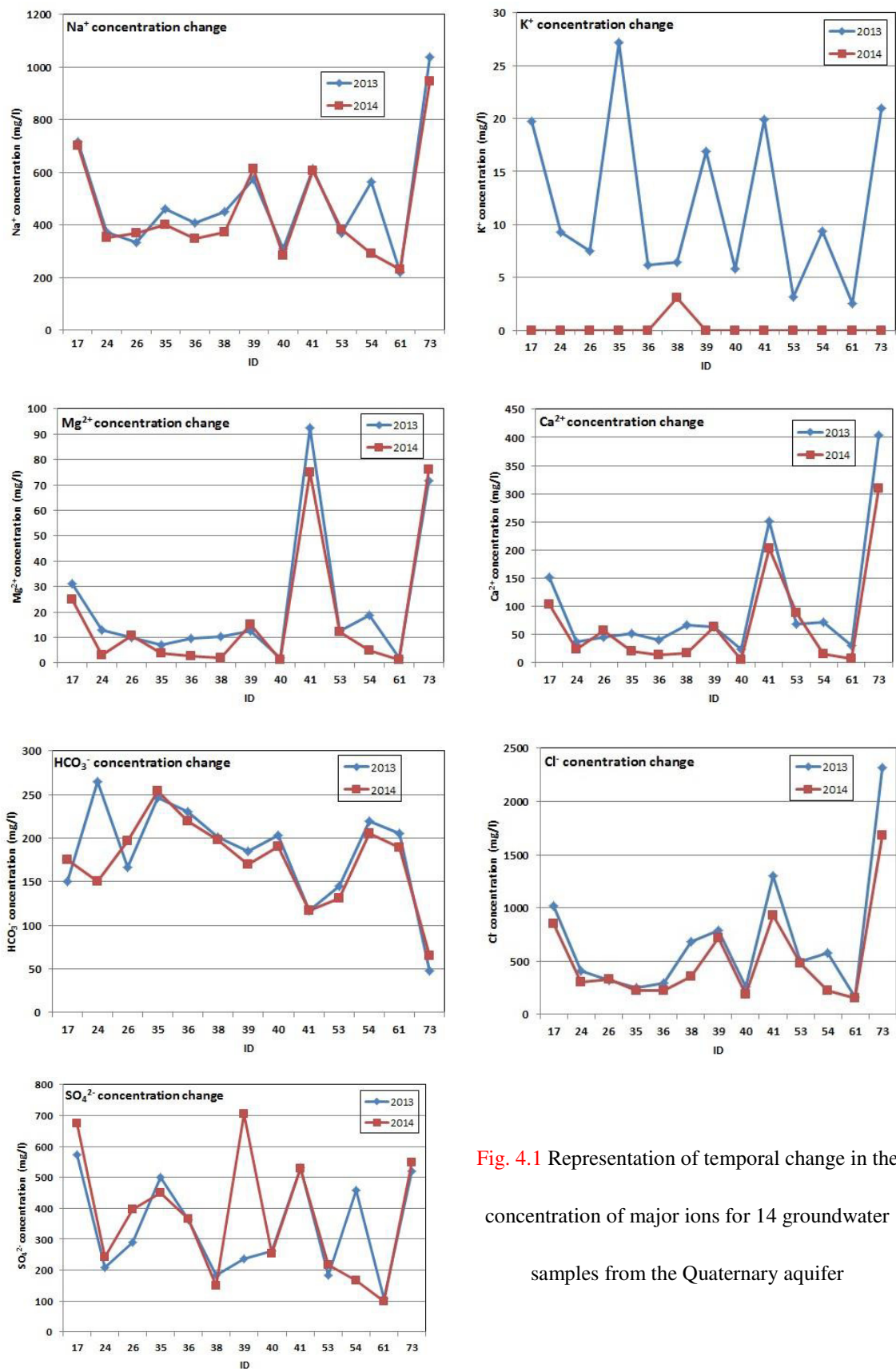


Fig. 4.1 Representation of temporal change in the concentration of major ions for 14 groundwater samples from the Quaternary aquifer

Table 4.2 Field-measured parameters, hydrochemical and isotopic characteristics of water samples.

ID	Water group	*Well depth (m)	T (°C)	pH	EC (µS/cm)	Cations (mg/l)					Anions (mg/l)				Isotopes		Cluster/subcluster category
						Na ⁺	K ⁺	Mg ²⁺	Ca ²⁺	NH ₄ ⁺	HCO ₃ ⁻	Cl ⁻	SO ₄ ²⁻	NO ₃ ⁻	δ ² H (‰)	δ ¹⁸ O (‰)	
1	Ismailia		29.1	8.3	409	36	8	11	37	ND	138	25	52	0.9	19.0	2.07	
2	Canal		29.0	8.1	358	23	3	4	62	NM	126	15	25	NM	20.0	2.00	
3	El Shabab Canal		30.6	8.4	342	24	4	7	56	NM	120	15	25	NM	20.2	1.80	
4	Fresh water		29.6	8.3	380	24	5	7	59	NM	128	23	30	NM	21.2	2.47	
5	ponds		32.8	7.8	501	27	5	10	49	NM	122	24	34	NM	20.5	2.04	
6		45	28.9	7.9	748	157	ND	14	30	ND	160	96	307	3.1	1.0	-0.82	Subcluster 1.1
7		84	28.3	7.5	3060	413	10	30	102	NM	184	577	466	NM	-0.9	-0.95	Subcluster 1.4
8		80	27.3	7.4	2400	321	11	35	103	NM	172	504	386	NM	6.9	-0.04	Subcluster 1.4
9		80	26.7	7.4	3710	620	ND	28	89	NM	182	578	816	NM	4.0	-0.45	Subcluster 1.4
10	Quaternary	70	38.4	7.4	1328	133	27	20	42	ND	166	180	167	2.0	NM	NM	Unclassified
11	Aquifer	60	26.1	7.1	3650	1006	ND	47	152	NM	207	843	1249	NM	NM	NM	Unclassified
12		90	27.1	7.5	899	65	15	21	53	NM	134	99	114	NM	3.3	-0.61	Subcluster 1.1
13		90	27.0	7.3	507	54	10	16	42	ND	153	68	49	3.1	2.9	-0.87	Subcluster 1.1
14		90	26.6	7.2	1564	205	1	15	35	ND	130	228	245	9.8	3.7	-0.71	Subcluster 1.1
15		90	26.2	7.3	1064	111	ND	18	57	NM	148	145	161	NM	3.3	-0.53	Subcluster 1.1

16		95	26.2	7.2	1779	250	48	82	130	NM	130	321	771	NM	3.1	-0.53	Cluster 3
17		150	28.5	7.1	4300	701	ND	25	103	ND	175	852	673	15.9	-2.9	-1.25	Subcluster 1.4
18		120	31.8	7.4	2790	454	ND	26	117	ND	160	686	176	4.8	-2.4	-1.30	Subcluster 1.4
19		130	30.3	7.1	2780	870	ND	126	230	1	140	1610	558	24.7	-0.8	-0.98	Cluster 3
20		130	27.5	7.3	5050	930	ND	34	130	10	174	1021	1041	28.3	-0.8	-0.98	Cluster 4
21		150	29.5	7.4	2270	389	ND	67	97	5	167	701	141	11.0	-4.1	-1.50	Subcluster 1.4
22		150	27.4	7.0	3440	843	ND	47	164	ND	142	1144	521	30.4	-1.7	-0.99	Cluster 3
23		130	27.1	7.4	2730	617	ND	2	32	4	194	490	673	19.2	1.0	-0.61	Subcluster 1.4
24		120	27.3	7.4	1788	352	ND	3	24	NM	150	301	241	NM	-6.3	-1.44	Subcluster 1.2
25		114	27.5	7.4	1759	326	8	6	19	ND	229	319	183	5.1	-6.2	-1.53	Subcluster 1.3
26	Quaternary Aquifer	120	30.4	7.5	2120	370	ND	10	56	4	197	331	397	11.3	0.3	-0.81	Subcluster 1.2
27		130	34.3	7.4	1945	314	ND	8	44	NM	157	466	153	NM	NM	NM	Unclassified
28		115	26.8	7.5	5450	1234	ND	37	151	ND	233	1004	1726	47.0	-1.6	-0.95	Cluster 4
29		60	24.9	7.2	2680	340	ND	36	106	3	240	362	513	10.9	10.5	0.60	Cluster 2
30		60	23.7	7.2	1628	287	ND	29	94	NM	277	260	391	NM	14.2	1.28	Cluster 2
31		30	24.9	7.7	687	107	ND	7	23	ND	223	31	38	14.8	24.2	2.71	Cluster 2
32		30	24.1	7.6	733	140	13	6	24	NM	248	35	57	NM	23.3	2.61	Cluster 2
33		15	26.2	7.6	576	40	2	10	51	ND	164	41	44	13.8	NM	NM	Unclassified
34	60	25.0	7.1	5750	1445	ND	46	217	ND	274	1137	1928	27.0	6.4	0.37	Cluster 4	
35	105	26.5	7.8	2140	398	ND	3	21	NM	254	219	449	NM	11.2	0.49	Cluster 2	
36	105	26.0	7.9	1591	346	ND	2	13	2	219	222	365	5.8	2.5	-0.55	Subcluster 1.2	
37	18	26.9	7.3	792	64	1	16	73	ND	266	49	38	11.6	NM	NM	Unclassified	
38	160	29.1	7.9	2060	373	3	2	17	1	198	351	149	6.6	-6.8	-1.74	Subcluster 1.3	

39		160	29.3	7.8	3030	611	ND	15	63	2	170	716	705	11.8	-6.5	-1.76	Subcluster 1.4
40		160	27.3	8.1	1338	282	ND	1	6	8	190	189	252	8.6	23.6	2.69	Cluster 2
41		165	29.5	7.3	3870	605	ND	74	203	ND	117	933	528	24.8	-13.1	-2.32	Cluster 3
42		180	28.5	6.9	7720	1306	ND	47	220	ND	64	1626	1116	22.7	-0.8	-0.10	Cluster 4
43		120	28.4	7.4	7820	1416	ND	45	244	5	76	1359	1535	39.7	0.5	0.17	Cluster 4
44		135	27.9	7.3	7530	1602	ND	75	383	ND	76	1547	2881	50.6	-9.3	-1.02	Cluster 4
45		110	26.8	7.5	2920	547	ND	5	135	1	202	488	528	11.6	-5.5	-0.72	Subcluster 1.4
46		120	27.8	7.3	4610	955	ND	24	91	ND	163	843	1135	30.1	-3.5	-0.51	Cluster 4
47		120	27.7	7.4	4870	1088	ND	18	77	13	179	899	1447	47.1	2.0	0.37	Cluster 4
48		140	27.9	7.9	2350	553	ND	16	56	ND	187	744	241	2.4	0.2	-0.99	Subcluster 1.4
49	Quaternary Aquifer	116	28.1	7.9	1223	255	ND	3	14	NM	192	200	108	NM	2.1	-0.60	Subcluster 1.2
50		105	27.5	7.8	2660	491	ND	82	180	NM	174	397	884	NM	2.8	-0.53	Cluster 3
51		110	27.1	7.5	3870	777	ND	83	175	NM	174	596	1253	NM	2.0	-0.47	Cluster 3
52		110	27.2	7.4	2050	476	ND	16	38	24	188	471	485	3.2	1.2	-0.46	Subcluster 1.2
53		92	27.6	7.8	2030	381	ND	12	88	NM	131	481	217	NM	-0.6	-0.91	Subcluster 1.2
54		110	27.3	7.9	1531	292	ND	4	16	ND	205	219	165	1.4	-5.2	-1.71	Subcluster 1.3
55		150	27.9	8.1	1660	394	ND	1	12	2	167	301	223	3.1	-1.6	-1.15	Subcluster 1.2
56		150	28.7	8.2	1210	258	ND	1	11	ND	187	224	120	1.4	-4.4	-1.56	Subcluster 1.3
57		150	28.5	7.7	1708	309	ND	6	33	ND	187	290	167	0.4	-4.4	-1.38	Subcluster 1.3
58	150	28.3	8.0	1228	228	ND	8	40	ND	166	218	95	1.5	-4.2	-1.53	Subcluster 1.3	
59	120	27.9	7.5	2890	538	ND	12	60	ND	164	432	520	7.7	0.2	-0.90	Subcluster 1.4	
60	150	28.2	7.9	1137	237	ND	3	46	3	190	195	94	1.5	-4.9	-1.43	Subcluster 1.3	
61	150	27.9	8.0	774	229	ND	1	7	NM	189	154	98	NM	-5.3	-1.56	Subcluster 1.3	

62		20	23.8	7.6	795	97	8	9	50	NM	222	34	83	NM	24.4	2.64	Cluster 2
63		100	23.8	7.5	4030	751	8	13	135	NM	274	466	1146	NM	13.0	1.06	Cluster 2
64		85	26.7	7.8	1652	319	11	16	63	NM	180	341	249	NM	3.2	-0.60	Subcluster 1.2
65		130	31.4	7.9	1514	288	3	4	38	NM	173	305	161	NM	-2.4	-1.49	Subcluster 1.3
66		150	28.2	7.6	4100	738	20	28	165	NM	145	1174	580	NM	-2.2	-1.32	Cluster 3
67	Quaternary Aquifer	150	28.6	7.5	4230	551	19	80	218	NM	162	1311	407	NM	-5.6	-1.46	Cluster 3
68		150	28.1	7.6	1479	308	4	6	77	NM	192	380	160	NM	-4.4	-1.62	Subcluster 1.3
69		155	28.1	8.2	1209	243	3	4	39	NM	206	230	126	NM	-5.3	-1.69	Subcluster 1.3
70		160	28.2	8.1	682	275	5	2	30	NM	200	275	138	NM	-3.4	-1.62	Subcluster 1.3
71		157	28.1	8.0	814	291	9	4	49	NM	201	396	160	NM	-4.4	-1.68	Subcluster 1.3
72		160	27.9	8.1	1586	312	7	6	49	NM	185	332	157	NM	-2.3	-1.39	Subcluster 1.3
73		110	29.0	6.6	3420	946	ND	76	309	5	65	1685	547	6.1	-18.0	-2.41	Cluster 3
74		110	29.1	6.8	5950	1112	ND	116	396	ND	70	2035	653	6.4	-16.9	-2.11	Cluster 3
75	Miocene Aquifer	180	27.9	7.5	8880	1161	ND	114	401	11	97	1793	865	15.7	-34.4	-4.59	
76		120	28.2	7.5	5760	1530	ND	139	502	ND	62	2616	1725	16.6	-29.9	-4.05	
77		160	28.3	7.4	4900	1259	ND	150	551	ND	89	2410	793	16.7	-32.7	-4.31	
78		160	27.9	6.8	8420	1084	42	126	537	NM	68	2993	690	NM	-31.8	-4.45	
79		120	27.9	7.6	11530	1667	66	95	675	NM	44.8	4307	670	NM	-33.5	-4.46	
80	Wastewater Pond 1		31.6	9.2	3440	599	33	24	68	ND	380	696	373	1.4	32.0	5.46	
81			35.4	8.6	774	276	20	6	71	NM	384	284	79	NM	22.4	2.86	
82			30.4	8.0	2160	345	38	9	64	NM	468	409	63	NM	23.4	3.11	
83			21.7	7.2	2320	329	34	7	62	NM	216	391	56	NM	21.3	2.54	
84			27.6	7.9	1135	345	36	12	63	NM	472	443	61	NM	23.4	3.08	

85	Pond 1	29.7	7.6	2710	375	44	19	170	NM	322	391	526	NM	NM	NM
86		28.3	6.7	1592	271	17	1	17	14	342	274	107	1.5	20.6	2.4
87	Pond 2	30.7	8.0	1526	219	25	8	68	NM	350	254	45	NM	NM	NM
88		31.7	8.2	2390	333	39	16	63	NM	396	416	73	NM	NM	NM
89		31.2	8.0	832	236	22	1	67	NM	362	312	35	NM	NM	NM
90	Pond 3	30.6	6.4	2400	466	30	9	45	60	294	331	696	1.4	18.2	2.27
91		27.6	8.0	1514	228	24	9	66	NM	336	259	58	NM	NM	NM
92		29.8	6.9	3070	492	58	19	60	NM	468	706	50	NM	NM	NM
R1					11.7		8.8	15.8		56.5	3.4	39.6			
R2	Old Nile			320	16.79	2.7	18.3	46		126.88	11.71	19.2		4.3	-0.6
R3	water				17	4	9	27		128	10	12			
R4					27	4	10	28		132	18	10			

* Well depth information was obtained from the available well logs (e.g., well field area) and from the well owners.

EC: Electric Conductivity, T: Temperature, ND: Not Detected, NM: Not Measured

R1: (Matthess, 1982), R2: (Awad et al., 1994; Sadek & Abd El-Samie, 2001), R3 & R4: (Khalil & Hanaa, 1984)

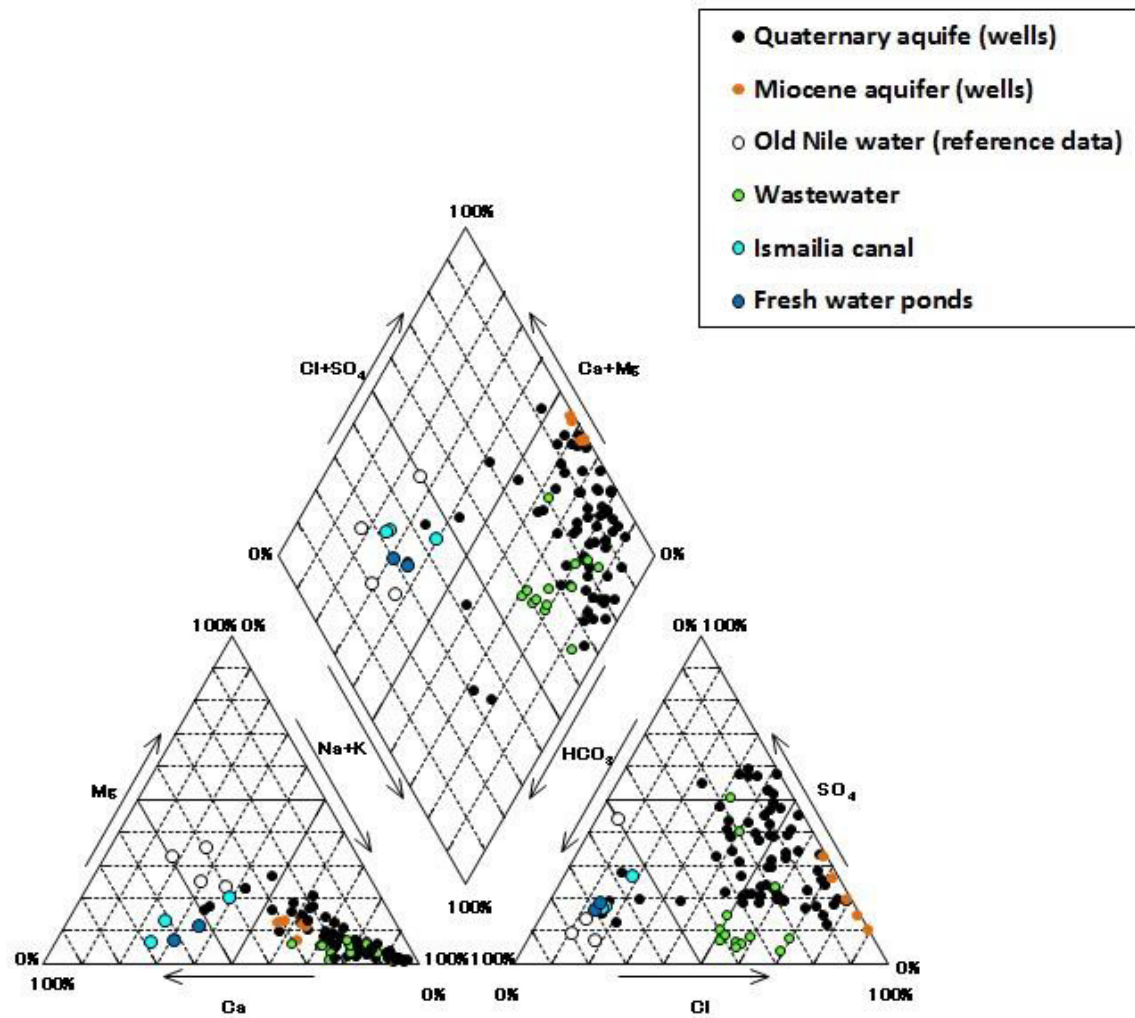


Fig. 4.2 Piper diagram for the different water groups in the study area.

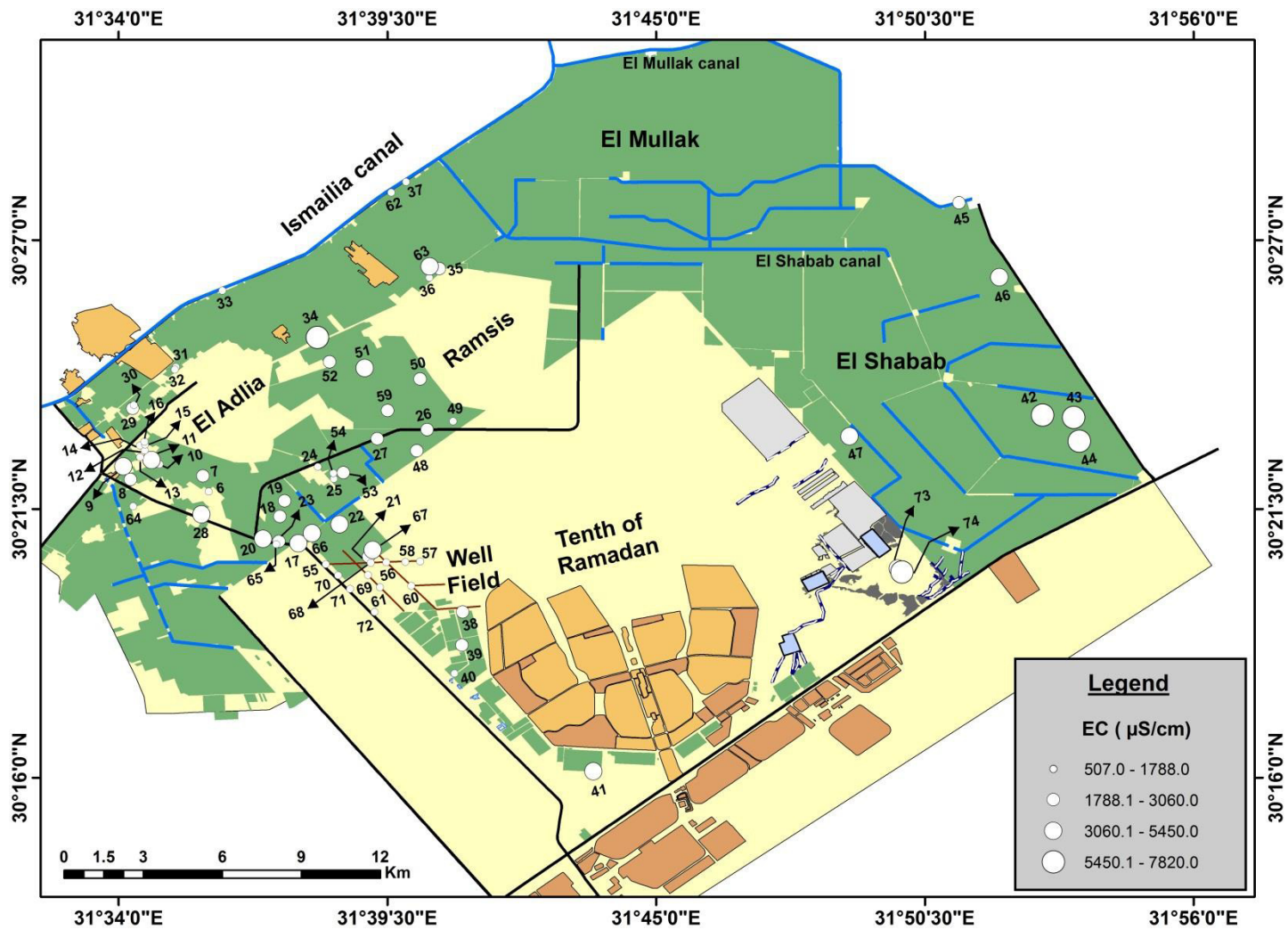


Fig. 4.3 Spatial EC distribution of the Quaternary aquifer in the area of study.

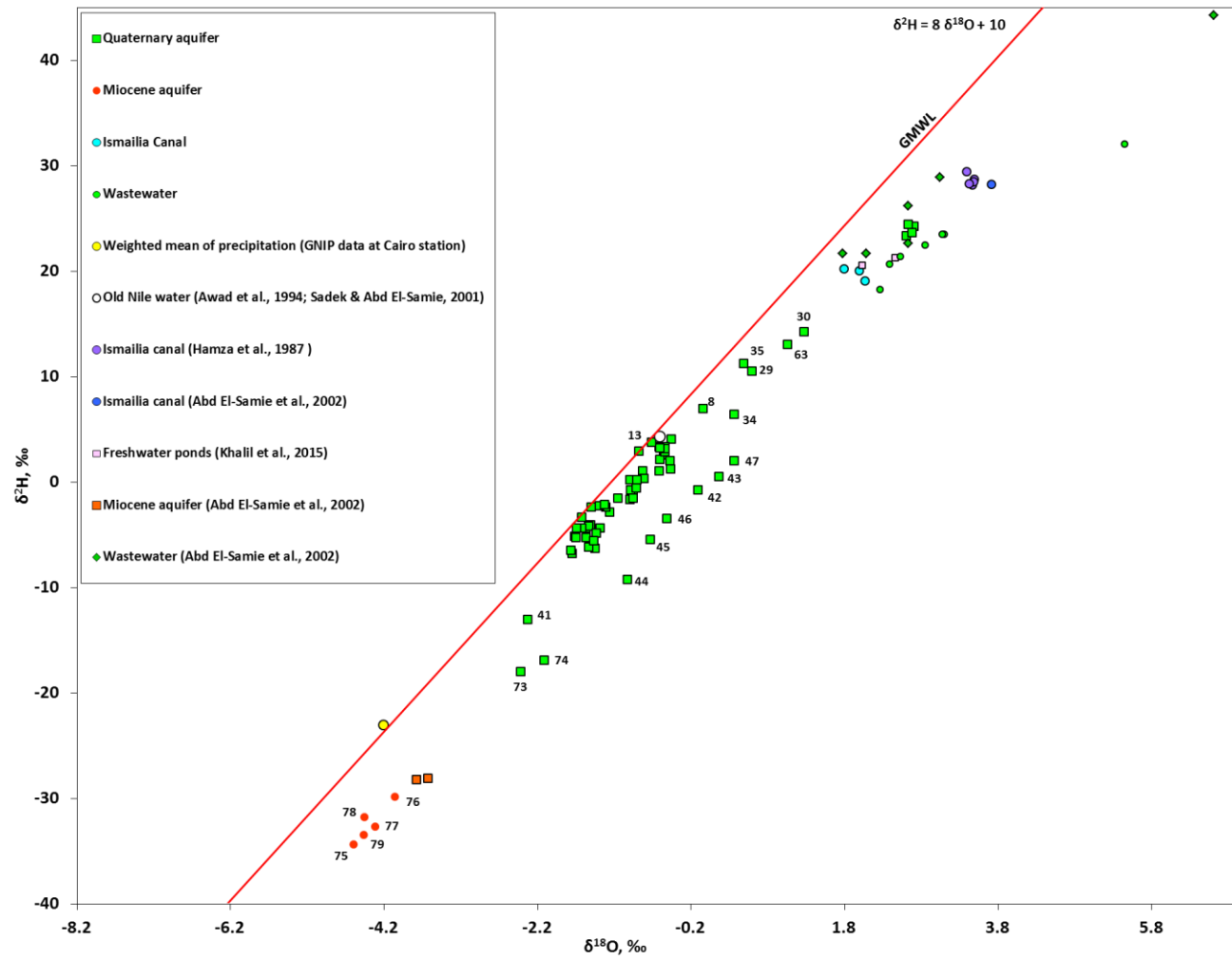


Fig. 4.4 $\delta^2\text{H}$ - $\delta^{18}\text{O}$ diagram of groundwater from the Quaternary and the Miocene aquifers, surface water and waste water from the ponds.

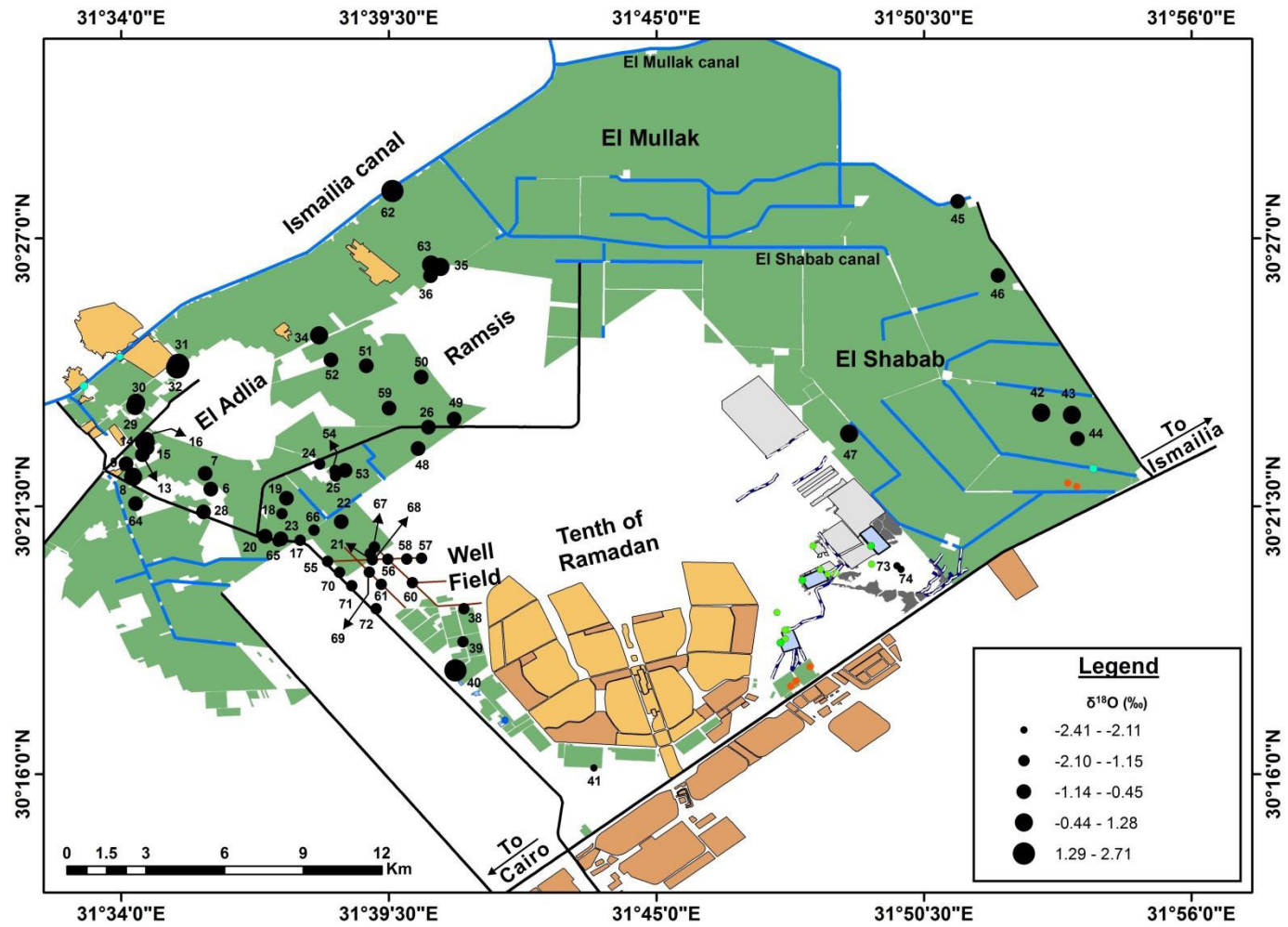


Fig. 4.5 Spatial $\delta^{18}\text{O}$ distribution of the Quaternary aquifer in the area of study.

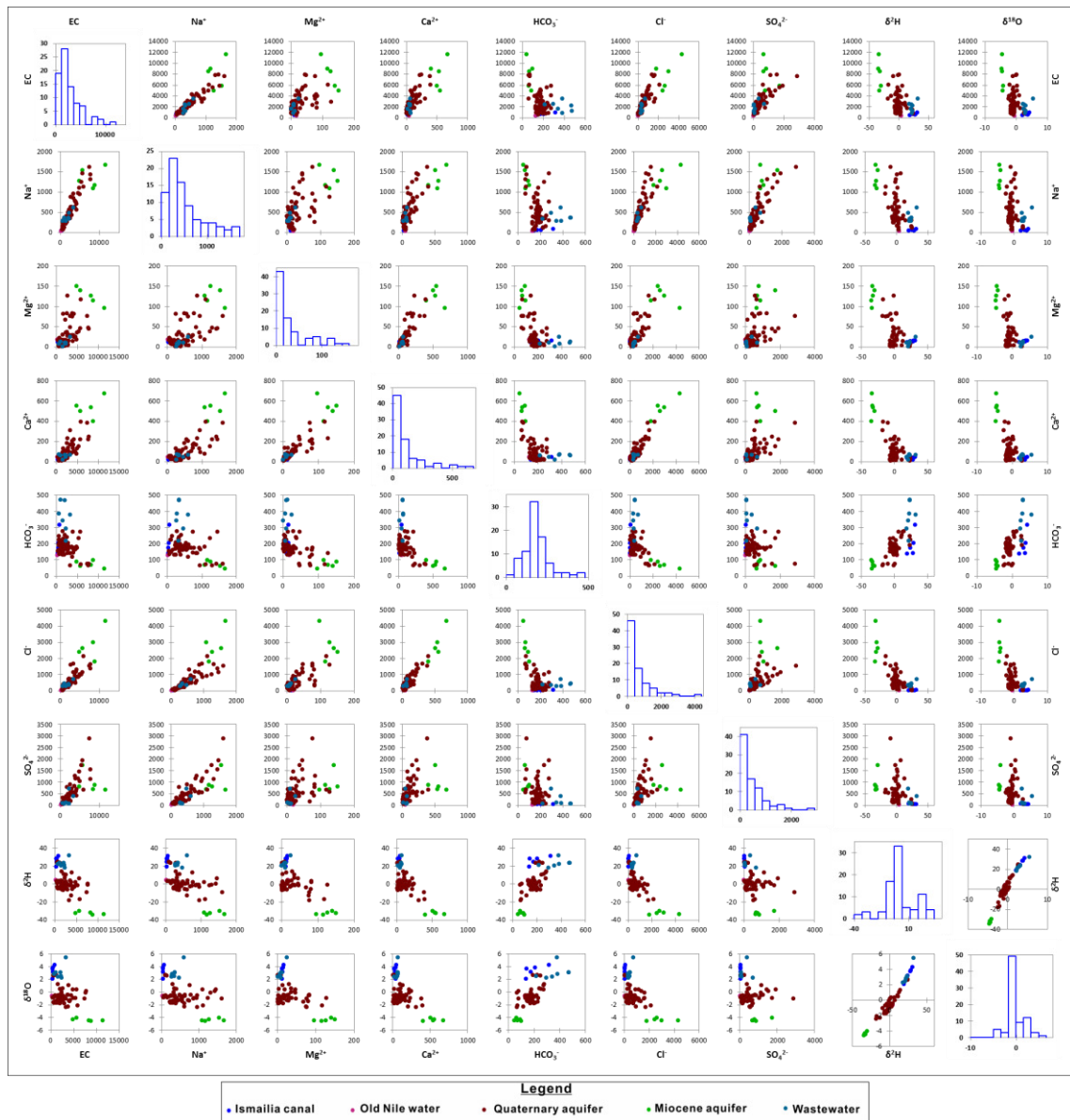


Fig. 4.6 Scatterplot matrix of nine variables for different water groups, i.e., Quaternary and Miocene aquifers, water from the Ismailia canal, old Nile water, and wastewater.

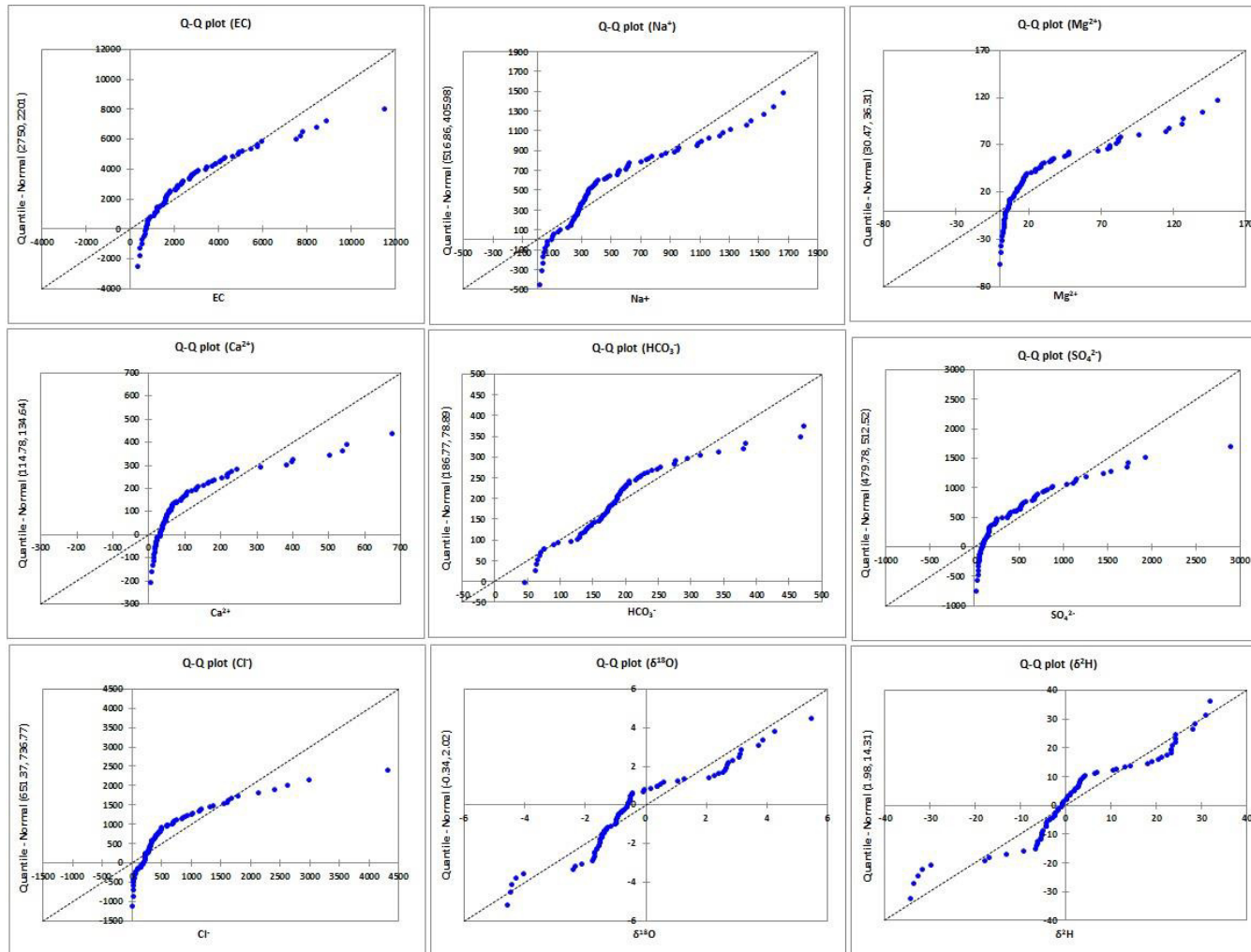


Fig. 4.7 Q-Q plot of the nine variables used for PCA

Table 4.3 Descriptive statistics for the 82 samples from the Quaternary and Miocene aquifers, Water from the Ismailia canal, the old Nile water, and wastewater.

Statistic	EC	Na ⁺	Mg ²⁺	Ca ²⁺	HCO ₃ ⁻	Cl ⁻	SO ₄ ²⁻	δ ² H	δ ¹⁸ O
Nbr. of observations	82	82	82	82	82	82	82	82	82
Minimum	320	16	1	6	44	11	19	-34.4	-4.59
Maximum	11530	1667	150	675	472	4307	2881	32.0	5.46
Median	2090	361	15	62	179	385	279	0.2	-0.82
Mean	2749	516	30	114	186	651	479	1.9	-0.34
Variance (n)	4845182	164817	1318	18129	6223	542832	262672	204.7	4.09
Standard deviation (n)	2201	405	36	134	78	736	512	14.3	2.02
Skewness	2	1	2	2	1	3	2	-0.2	0.58
Standard error of skewness	0.3	0.3	0.3	0.3	0.3	0.3	0.3	0.3	0.3

Table 4.4 Shapiro-Wilk test for normality for nine variables of the dataset

Variables	Shapiro-Wilk test*	
	Test parameter (W)	P-value
EC	0.842	< 0.0001
Na ⁺	0.872	< 0.0001
Mg ²⁺	0.750	< 0.0001
Ca ²⁺	0.704	< 0.0001
HCO ₃ ⁻	0.889	< 0.0001
Cl ⁻	0.732	< 0.0001
SO ₄ ²⁻	0.782	< 0.0001
δ ² H	0.919	< 0.0001
δ ¹⁸ O	0.912	< 0.0001

* alpha (α) value for Shapiro - Wilk test is 0.05

Table 4.5 Spearman's correlation coefficients of the variables measured for 82 samples from the Quaternary and Miocene aquifers, Water from the Ismailia canal, the old Nile water, and wastewater.

Variables	EC	Na ⁺	Mg ²⁺	Ca ²⁺	HCO ₃ ⁻	Cl ⁻	SO ₄ ²⁻	δ ² H	δ ¹⁸ O
EC	1	0.956	0.642	0.770	-0.328	0.927	0.878	-0.444	-0.296
Na ⁺	0.956	1	0.569	0.722	-0.288	0.942	0.871	-0.474	-0.326
Mg ²⁺	0.642	0.569	1	0.875	-0.555	0.668	0.593	-0.183	-0.132
Ca ²⁺	0.770	0.722	0.875	1	-0.437	0.821	0.667	-0.313	-0.214
HCO ₃ ⁻	-0.328	-0.288	-0.555	-0.437	1	-0.381	-0.317	0.490	0.479
Cl ⁻	0.927	0.942	0.668	0.821	-0.381	1	0.784	-0.529	-0.413
SO ₄ ²⁻	0.878	0.871	0.593	0.667	-0.317	0.784	1	-0.370	-0.236
δ ² H	-0.444	-0.474	-0.183	-0.313	0.490	-0.529	-0.370	1	0.948
δ ¹⁸ O	-0.296	-0.326	-0.132	-0.214	0.479	-0.413	-0.236	0.948	1

Values in bold are different from 0 with a significance level alpha=0.05

Table 4.6 P-values of the calculated Spearman's correlation coefficients

Variables	EC	Na ⁺	Mg ²⁺	Ca ²⁺	HCO ₃ ⁻	Cl ⁻	SO ₄ ²⁻	δ ² H	δ ¹⁸ O
EC	0	0.000	0.000	0.000	0.003	0.000	0.000	0.000	0.007
Na ⁺	< 0.0001	0	< 0.0001	< 0.0001	0.009	< 0.0001	< 0.0001	< 0.0001	0.003
Mg ²⁺	< 0.0001	< 0.0001	0	< 0.0001	< 0.0001	< 0.0001	< 0.0001	0.100	0.237
Ca ²⁺	< 0.0001	< 0.0001	< 0.0001	0	< 0.0001	< 0.0001	< 0.0001	0.004	0.054
HCO ₃ ⁻	0.003	0.009	< 0.0001	< 0.0001	0	0.000	0.004	< 0.0001	< 0.0001
Cl ⁻	< 0.0001	< 0.0001	< 0.0001	< 0.0001	0.000	0	< 0.0001	< 0.0001	0.000
SO ₄ ²⁻	< 0.0001	< 0.0001	< 0.0001	< 0.0001	0.004	< 0.0001	0	0.001	0.033
δ ² H	< 0.0001	< 0.0001	0.100	0.004	< 0.0001	< 0.0001	0.001	0	< 0.0001
δ ¹⁸ O	0.007	0.003	0.237	0.054	< 0.0001	0.000	0.033	< 0.0001	0

Values in bold are different from 0 with a significance level alpha=0.05

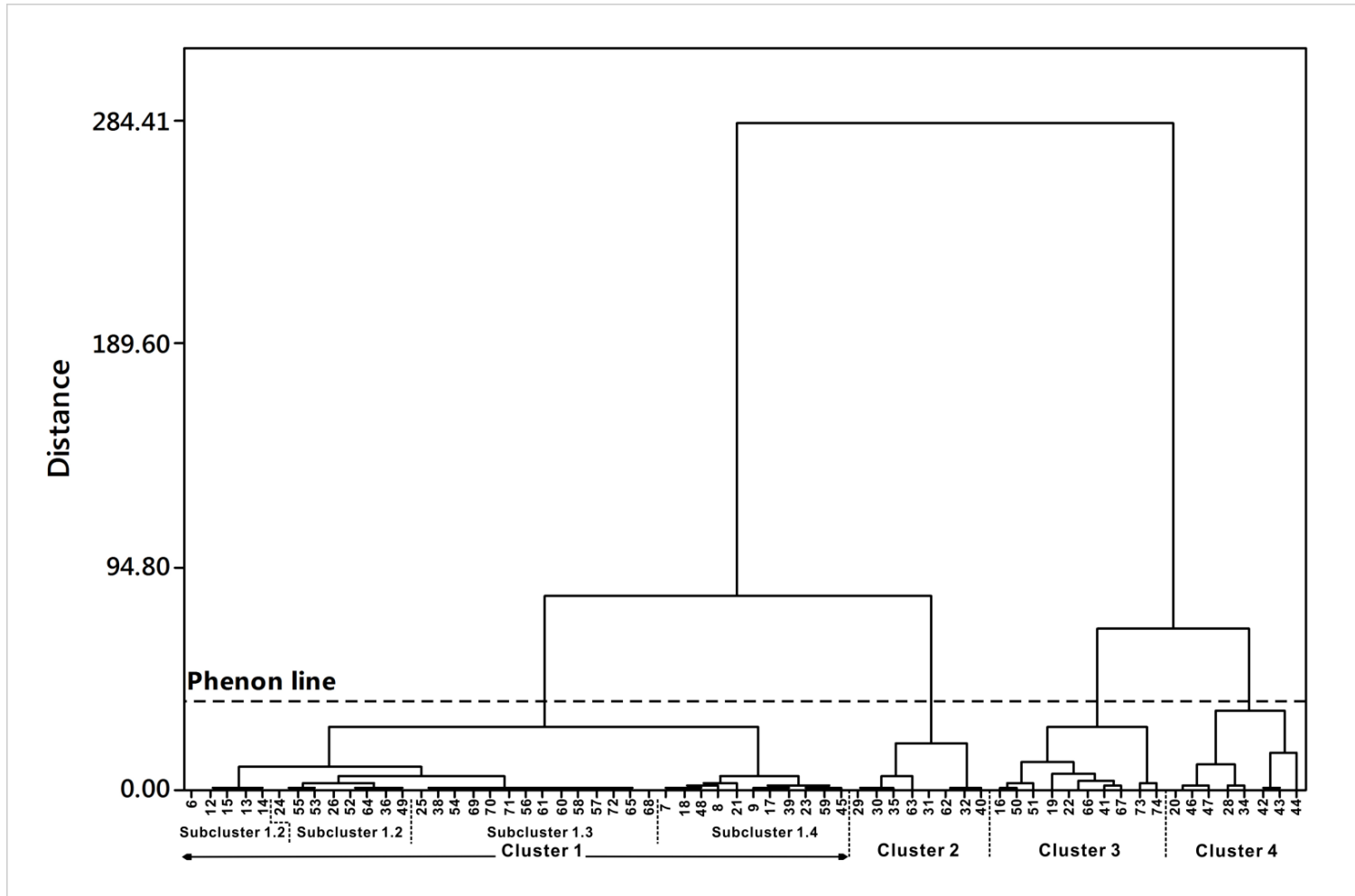


Fig. 4.8 Dendrogram for the groundwater samples from the Quaternary aquifer classified into four clusters. The horizontal broken line (*phenon line*) is an arbitrary line that defines clusters.

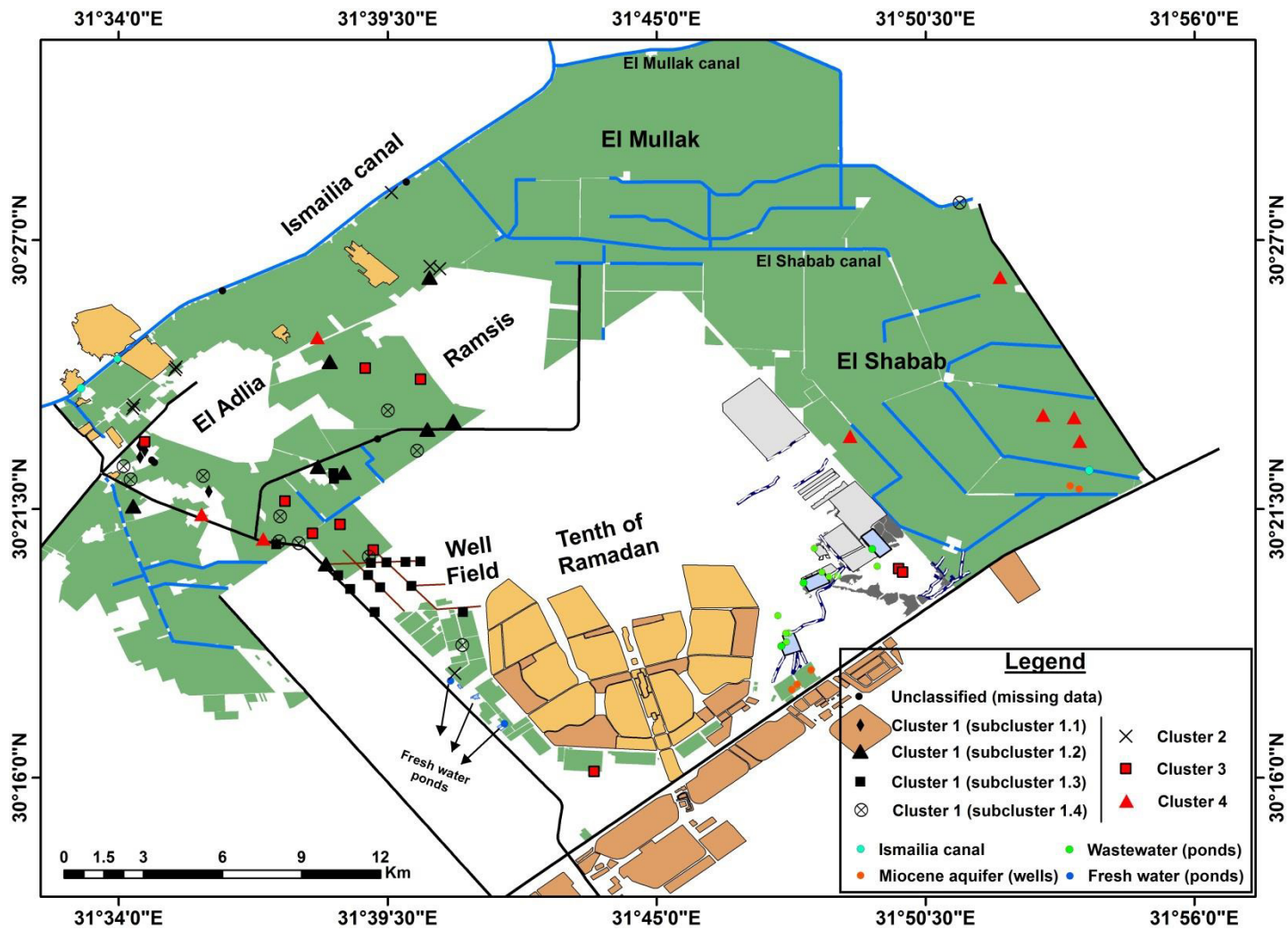


Fig. 4.9 Spatial distribution of four clusters in the groundwater of the Quaternary aquifer.

Table 4.7 The calculated eigenvalues and their contribution to the total variance

	PC1	PC2	PC3	PC4	PC5	PC6	PC7	PC8	PC9
Eigenvalue	5.582	1.703	0.975	0.368	0.184	0.082	0.051	0.034	0.022
Variability (%)	62.019	18.918	10.836	4.086	2.040	0.911	0.571	0.379	0.241
Cumulative %	62.019	80.937	91.773	95.859	97.899	98.810	99.380	99.759	100.000

Table 4.8 Component loadings, eigenvalues, explained variance, and cumulative percentages of variance for the two significant principal components (PC1 and PC2) after varimax normalized rotation

Variables	PC1	PC2
EC	0.921	-0.238
Na⁺	0.890	-0.268
Mg²⁺	0.815	-0.080
Ca²⁺	0.889	-0.146
HCO₃⁻	-0.325	0.583
Cl⁻	0.888	-0.348
SO₄²⁻	0.864	-0.180
δ²H	-0.206	0.952
δ¹⁸O	-0.068	0.973
Eigenvalue	5.514	1.880
Explained variance (%)	53.146	27.790
Cumulative % of variance	53.146	80.937

Bold values are loadings > 0.7

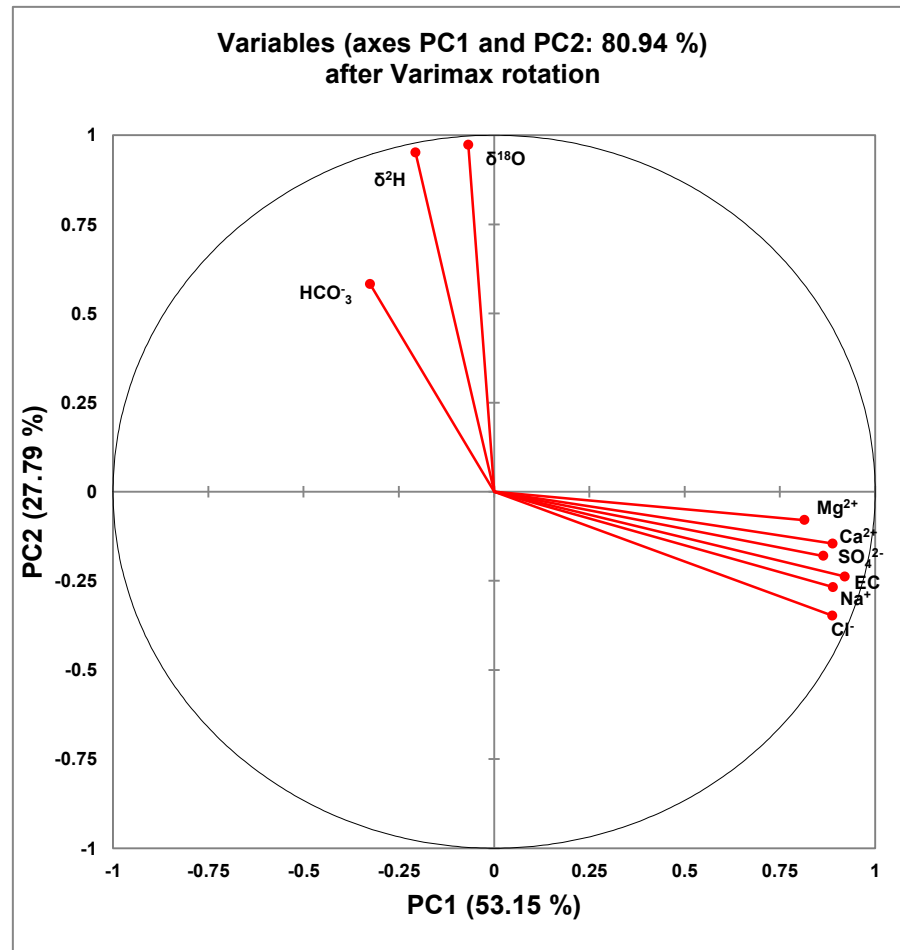


Fig. 4.10 Correlation circle of the nine variables and each of the PCs

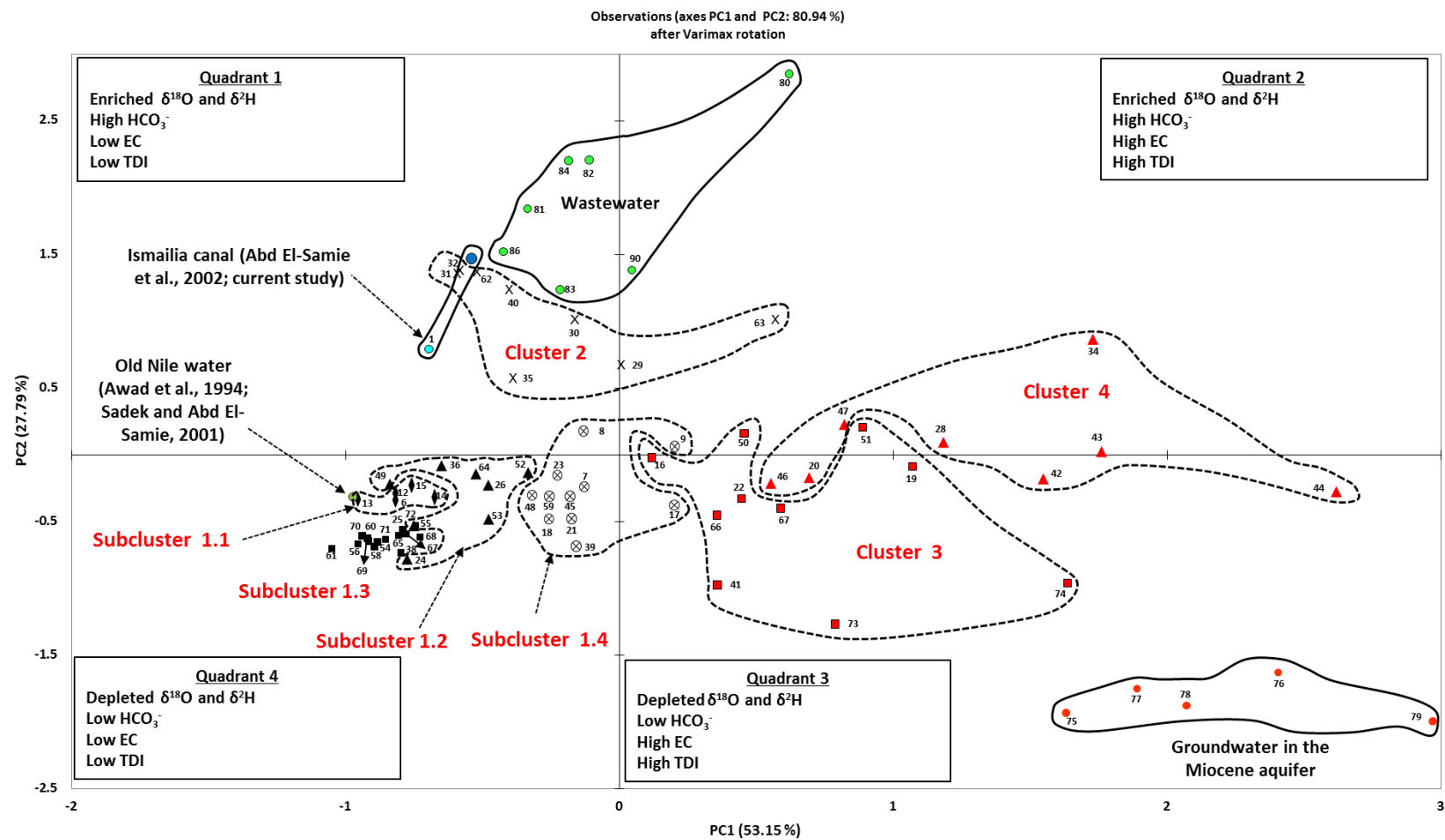


Fig. 4.11 Plot of principal component scores for the first two components for all water groups with groundwater samples from the Quaternary aquifer coded according to the HCA groupings.

Table 4.9 Average, median, and range values of the hydrochemical and stable isotopic composition of the four clusters in the Quaternary aquifer determined from HCA.

Cluster	Subcluster	N	parameter	EC ($\mu\text{S/cm}$)	Cations (mg/l)				Anions (mg/l)			$\delta^2\text{H}$ (‰)	$\delta^{18}\text{O}$ (‰)
					Na ⁺	Mg ²⁺	Ca ²⁺	HCO ₃ ⁻	Cl ⁻	SO ₄ ²⁻	*NO ₃ ⁻		
1	1.1	5	Average	956	118	17	43	145	127	175	5.3	2.8	-0.70
			Median	899	111	16	42	148	99	161	3.1	3.3	-0.70
			Range	507-1564	54-205	14-21	30-57	130-160	68-228	49-307	3.1-9.8	1.0-3.7	-0.87- -0.53
	1.2	8	Average	1764	362	8	39	178	331	286	5.8	0.1	-0.80
			Median	1724	361	6	31	184	316	245	4.5	0.8	-0.70
			Range	1223-2120	255-476	1-16	12-88	131-219	200-481	108-485	3.1-11.3	-6.3- 3.2	-1.44- -0.46
	1.3	14	Average	1335	283	4	34	193	277	141	2	-4.5	-1.60
			Median	1354	290	4	35	191	282	153	1	-4.4	-1.60
			Range	682-2060	228-373	1-8	7-77	166-229	154-396	94-183	0.4-6.6	-6.8- -2.3	-1.74- -1.38
	1.4	11	Average	2950	524	24	88	178	616	485	10.5	-0.9	-1.00
			Median	2890	548	25	98	175	579	520	11.3	-0.9	-0.95
			Range	2270-4300	321-701	2-67	32-135	160-202	432-852	141-816	2-19	-6.5- 6.9	-1.76- -0.04
2	8	Average	1754	300	13	57	241	199	366	23.1	18.0	2.00	
		Median	1483	285	8	37	244	204	321	14.8	19.0	2.00	
		Range	687-4030	97-751	1-36	6-135	190-277	31-466	38-1146	8.6-44.8	10.5-24.4	0.49-2.71	
3	10	Average	3610	718	79	217	132	1120	670	18.5	-5.0	-1.00	
		Median	3655	757	81	191	141	1159	569	24.7	-2.0	-1.00	

		Range	1779-5950	250-1112	28-126	130-396	65-174	321-2035	407-1253	24.7	-18.0 - 3.1	-2.41- -0.47
		Average	6100	1247	41	189	155	1179	1601	36.6	-1.0	0.00
4	8	Median	5600	1270	41	184	169	1079	1491	34.9	-1.0	0.00
		Range	4610-7820	930-1602	18-75	77-383	64-274	843-1626	1041-2881	22.7-50.6	-9.3- 6.4	-1.02- 0.37

*Not considered in HCA , N: Number of observations, EC: Electric Conductivity

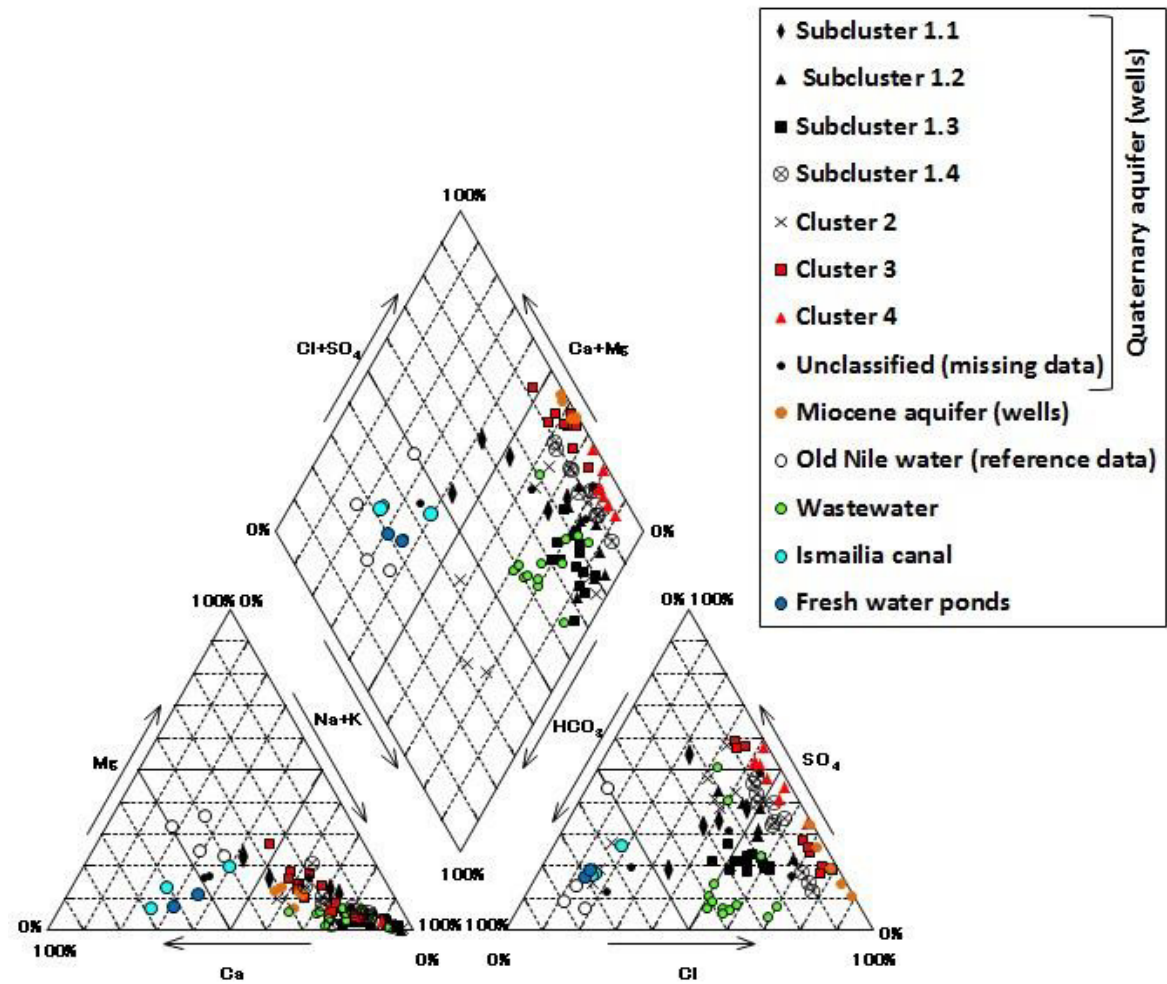


Fig. 4.12 Piper diagram of the analyzed water samples with groundwater samples from the Quaternary aquifer coded according to the HCA groupings.

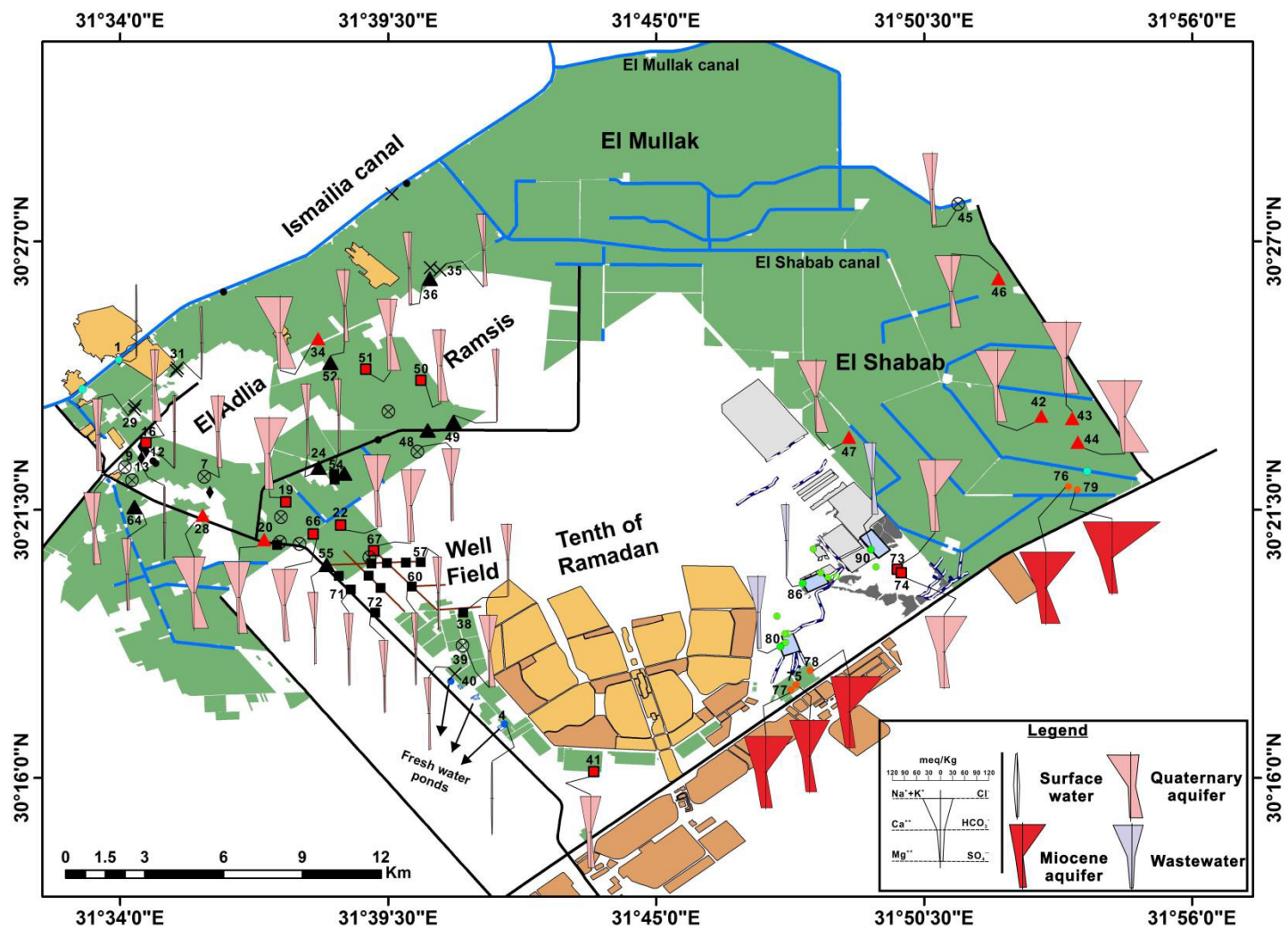


Fig. 4.13 Stiff diagrams of some selected samples in different water groups of the study area (see Fig. 4.9 for the legend sampling points).

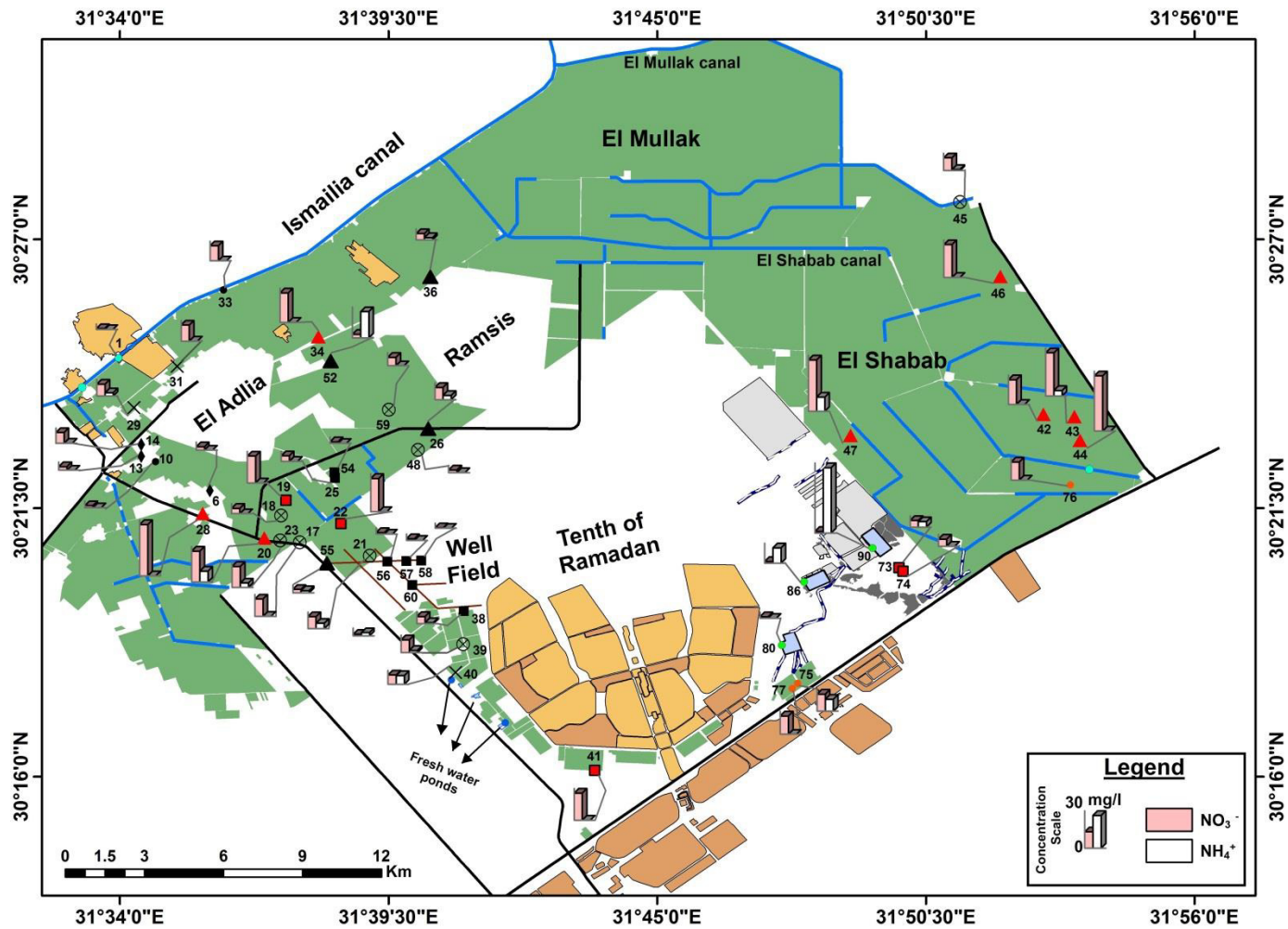


Fig. 4.14 Spatial distribution of nitrogen components (as NO_3^- and NH_4^+) in groundwater from the Quaternary (coded according to HCA groupings) and the Miocene aquifers, surface water and wastewater from the ponds (see Fig. 4.9 for the legend sampling points).

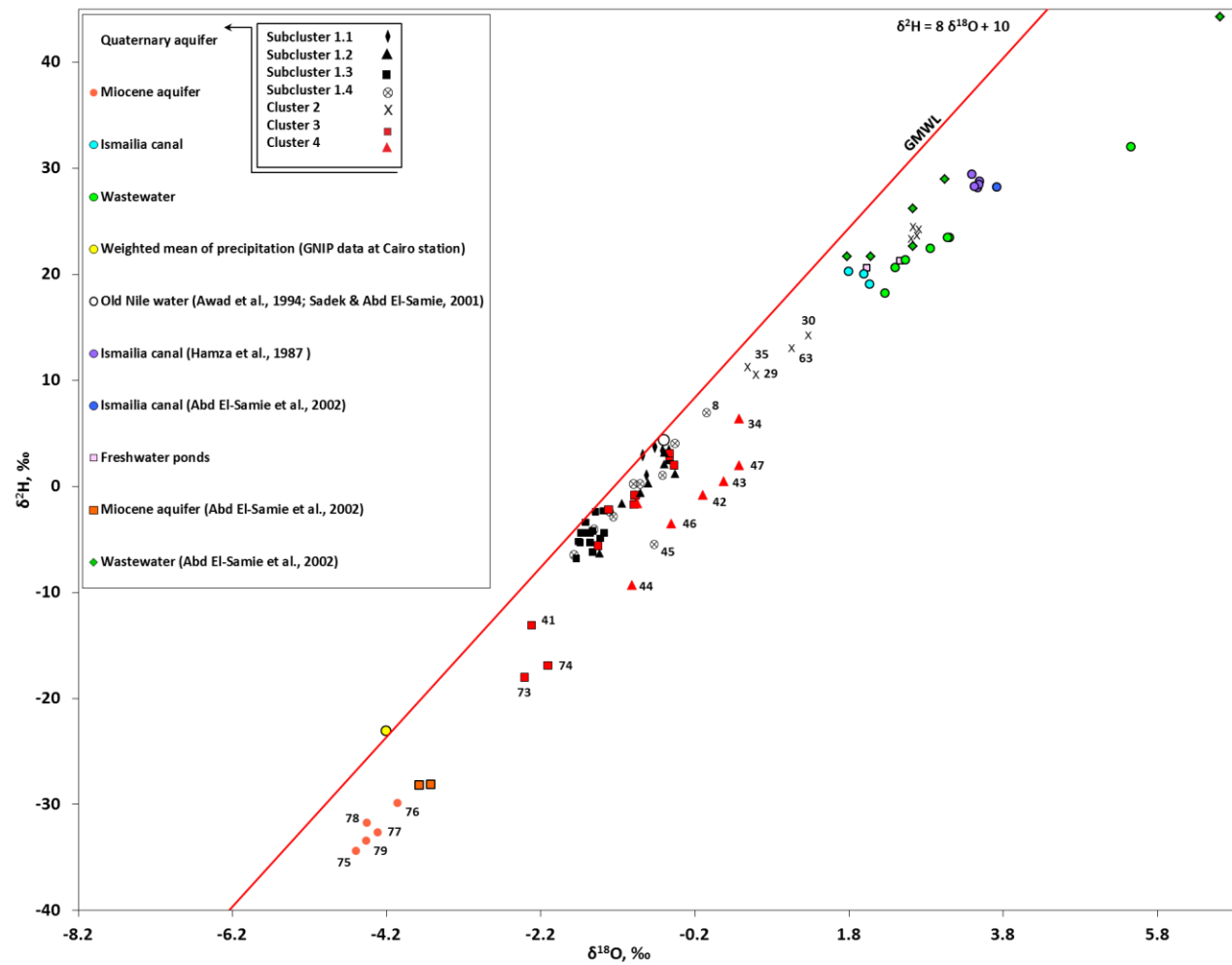


Fig. 4.15 Cross plot of stable isotope data with groundwater samples from the Quaternary aquifer coded according to the HCA groupings.

Table 4.10 Measured $\delta^{13}\text{C}$ (‰) and ^{14}C (pMC) in three groundwater clusters of the Quaternary aquifer

Cluster	Subcluster	Sample No.	$\delta^{13}\text{C}$ (‰)	^{14}C (pMC)
1	1.2	26	-10.9	68.7
		36	-11.2	70.3
		53	-8.8	63.3
	1.3	54	-9.7	44.2
		58	-10.9	54.8
	1.4	17	-11.3	64.3
2		35	-11.8	80.0
3		41	-8.7	52.0
		73	-5.4	42.0
Groundwater in the Miocene aquifer		75	-8.2	35.3

Table 4.11 A summary table for EC (electric conductivity), hydrochemical and isotopic characteristics, and spatial location for different clusters defined in the groundwater of the Quaternary aquifer and water from other groups in the study area, i.e., the old Nile water, water from the Ismailia Canal, groundwater from the Miocene aquifer, and wastewater

Water groups		EC range ($\mu\text{S}/\text{cm}$)	Hydrochemical characteristics (water type)	Stable isotopic characteristics	^{14}C (pMC) and $\delta^{13}\text{C}$ (‰)	Spatial location (Fig. 4.9)
The old Nile water *				Less enriched (4.3 ‰ $\delta^2\text{H}$; -0.6‰ $\delta^{18}\text{O}$)	NA	NA
Surface water from the Ismailia Canal (the recent Nile water) and fresh water ponds		≤ 500	$\text{Ca}^{2+}\text{-HCO}_3^-$	More enriched (from 19.0 to 21.2 ‰ for $\delta^2\text{H}$) (from 1.80 to 2.47‰ for $\delta^{18}\text{O}$)	NA	North and northwest the study area
Groundwater from the Quaternary aquifer	subcluster 1.1	507-1564	$\text{Na}^+\text{-HCO}_3^- (\text{SO}_4^{2-})$	from 1.0 to 3.7 ‰ for $\delta^2\text{H}$ from -0.87 to -0.53 ‰ for $\delta^{18}\text{O}$	NA	El Adlia area
	Subcluster 1.2	1223-2120	$\text{Na}^+\text{-Cl}^- (\text{SO}_4^{2-})$	from -6.3 to 3.2 ‰ for $\delta^2\text{H}$ from -1.44 to -0.46 ‰ for $\delta^{18}\text{O}$	63.3 to 70.3 for ^{14}C -11.2 to -8.8 for $\delta^{13}\text{C}$	Between El Adlia and Ramsis
	Subcluster 1.3	682-2060	$\text{Na}^+\text{-Cl}^- (\text{HCO}_3^-)$	from -6.8 to -2.3 ‰ for $\delta^2\text{H}$ from -1.74 to -1.38 ‰ for $\delta^{18}\text{O}$	44.2 to 54.8 for ^{14}C -10.9 to -9.7 for $\delta^{13}\text{C}$	Well field area
	Subcluster 1.4	2270-4300	$\text{Na}^+\text{-Cl}^- (\text{SO}_4^{2-})$	from -6.5 to 6.9 ‰ for $\delta^2\text{H}$ from -1.76 to -0.04 ‰ for $\delta^{18}\text{O}$	64.3 for ^{14}C -11.3 for $\delta^{13}\text{C}$	Scattered distribution
	Cluster 2	687-4030	$\text{Na}^+\text{-HCO}_3^- (\text{SO}_4^{2-})$	from 10.5 to 24.4 ‰ for $\delta^2\text{H}$	80.0 for ^{14}C	Along and within 3

			from 0.49 to 2.71 ‰ for $\delta^{18}\text{O}$	-11.8 for $\delta^{13}\text{C}$	Km from the Canal
Cluster 3	1779-5950	$\text{Na}^+\text{-Cl}^- (\text{SO}_4^{2-})$	from -18.0 to 3.1 ‰ for $\delta^2\text{H}$ from -2.41 to -0.47 ‰ for $\delta^{18}\text{O}$	42.0 to 52.0 for ^{14}C -8.7 to -5.4 $\delta^{13}\text{C}$	South part of the study area and north the well field area
Cluster 4	4610-7820	$\text{Na}^+\text{-Cl}^- (\text{SO}_4^{2-})$	from -9.3 to 6.4 ‰ for $\delta^2\text{H}$ from -1.02 to 0.37 ‰ for $\delta^{18}\text{O}$	NA	El Shabab agricultural area
Groundwater from the Miocene aquifer	4900-11530	$\text{Na}^+\text{-Cl}^-$	from -34.4 to -29.9 ‰ for $\delta^2\text{H}$ from -4.59 to -4.05 ‰ for $\delta^{18}\text{O}$	35.3 for ^{14}C -8.2 for $\delta^{13}\text{C}$	South part of the study area
Wastewater	774-3440	$\text{Na}^+\text{-HCO}_3^- (\text{SO}_4^{2-}, \text{Cl}^-)$	from 18.2 to 32.0 ‰ for $\delta^2\text{H}$ from 2.27 to 5.46 ‰ for $\delta^{18}\text{O}$	NA	Wastewater ponds

* Available from reference data (Matthess, 1982; Khalil & Hanaa, 1984; Awad et al., 1994; Sadek & Abd El-Samie, 2001)

NA: not available

----- CHAPTER 5: DISCUSSION -----

5.1. DETERMINATION OF END-MEMBERS AND MIXING PROCESSES

According to [Table 4.11](#), the clusters defined for the groundwater in the Quaternary aquifer appear to be derived from different water sources. The possible influence of the old Nile water and water from the Ismailia Canal could be observed for the subcluster 1.1 and cluster 2, respectively ([Table 4.11](#)). Also, clusters 3 and 4 appear to be more affected by the groundwater from the Miocene aquifer ([Table 4.11](#)). It is difficult to estimate the possible mixing processes from [Table 4.11](#) for the other (sub) clusters as they belong mostly to the same $\text{Na}^+\text{-Cl}^- (\text{SO}_4^{2-})$ water type and overlapping in the isotopic characteristics. However, the positions of four groundwater clusters in the Quaternary aquifer relative to other water groups, i.e., water in the Ismailia Canal, the old Nile water, groundwater in the Miocene aquifer, and wastewater, in PCA space ([Fig. 4.11](#)) and $\delta^{18}\text{O}\text{-}\delta^2\text{H}$ diagram ([Fig. 4.15](#)) furnish information concerning the mixing and possible recharge sources of the Quaternary aquifer. Samples assigned to clusters 1 and 2 have lower EC ([Table 4.9](#)) therefore low PC1 Scores (quadrants 1 and 4) in PCA space ([Fig. 4.11](#)) together with water samples from the Ismailia Canal and the old Nile water. With respect to the PC2 axis, subclusters 1.1 and 1.3, and the old Nile water were plotted to quadrant 4, whereas most subcluster 1.2 and cluster 2 in addition to the Ismailia Canal water were plotted to quadrant 1 ([Fig. 4.11](#)). This suggested that the groundwater of the Quaternary aquifer in the northern part of the study area ([Fig. 4.9](#)), i.e., subclusters 1.1 and 1.2, and cluster 2, are in hydraulic connection with the Nile water from the Ismailia canal. In $\delta^{18}\text{O}\text{-}\delta^2\text{H}$ diagram ([Fig. 4.15](#)), these subclusters 1.1, 1.2, and cluster 2 were plotted within the triangle of which apexes were the Ismailia Canal, the old Nile water, and the subcluster 1.3. The water table of the areas surrounding the Ismailia Canal ([Fig. 2.10](#)) shows the recharge of the Canal water to the aquifer, which is also consistent with the PCA results. The previous evidences confirmed that the Nile water from the Ismailia Canal is the end-member for the groundwater from the Quaternary aquifer in the northern part of the study area.

Samples from subcluster 1.3 are more depleted in $\delta^{18}\text{O}$ and $\delta^2\text{H}$ values (Fig. 4.15 and Table 4.9) and show more negative scores on PC2 axis relative to the old Nile water (Fig. 4.11). Thus, a different source other than the Nile water needs to be considered for subcluster 1.3 samples. Subcluster 1.3 samples are plotted at the corner of the data in PCA space (Fig. 4.11), in $\delta^{18}\text{O}$ - $\delta^2\text{H}$ diagram (Fig. 4.15), and in $\delta^{18}\text{O}$ -Cl⁻ diagram (Fig. 5.1). These aspects suggested that the source of recharge of subcluster 1.3 samples is largely different in space and/or in time and might likely represent the “native” groundwater in the Quaternary aquifer.

Samples from clusters 3 and 4 are characterized by high EC (Table 4.9), reflecting by their high positive PC1 scores (quadrants 2 and 3) (Fig. 4.11). Highly depleted $\delta^{18}\text{O}$ and $\delta^2\text{H}$ values (Table 4.9) shifted some cluster 3 samples closer to the space occupied by the groundwater samples from the Miocene aquifer in PCA space (quadrant 3) (Fig. 4.11) and in $\delta^{18}\text{O}$ - $\delta^2\text{H}$ diagram (Fig. 4.15). Given the spatial location (Fig. 4.9) of some cluster 3 samples, i.e., Nos. 41, 73 and 74, adjacent to the southern structural highs (Fig. 3.2), a high degree of hydraulic interaction with the Miocene aquifer could be inferred. Accordingly, the groundwater from the Miocene aquifer is the main end-member for the groundwater of the Quaternary aquifer in the southern part of the study area.

Though cluster 4 samples exhibits a relative similarity in chemical composition (Table 4.9) to cluster 3 samples and also their closer location, i.e., Nos. 42, 43 and 44 (Fig. 4.9), relative to the southern structural highs (Fig. 3.2), cluster 4 samples are plotted to higher positive PC2 scores (quadrant 3) in PCA space (Fig. 4.11) and to the heavier $\delta^{18}\text{O}$ in $\delta^{18}\text{O}$ - $\delta^2\text{H}$ diagram (Fig. 4.15), suggesting additional influence from different component (end-member).

Chemical pattern of subcluster 1.4 samples (Table 4.9) and their position in PCA space (Fig. 4.11) among subclusters 1.2, cluster 2, and cluster 3 might suggest that this subcluster is an intermediate or mixed groundwater among them. Unlike the previous clusters, this subcluster has a sparse spatial distribution in the area of study (Fig. 4.9) that could not be easily related to a specific geologic or

hydrogeologic setting.

5.2. EVIDENCES FROM RADIOCARBON AND DELTA ¹³C

The ¹⁴C activities and δ¹³C data were shown in [Table 4.10](#) and were used to support the previously discussed mixing processes in groundwater of the Quaternary aquifer. Usually, δ¹³C values in the water increases concurrently with the increase in dissolved inorganic carbon (DIC) through the dissolution of carbonate (Clark and Fritz, 1997; Raidla, 2010). However, the δ¹³C values of the groundwater in the Quaternary aquifer is negatively correlated with both DIC (HCO₃⁻ concentration) and ¹⁴C activities ([Fig. 5.2](#)); Quaternary samples with lower δ¹³C values show higher HCO₃⁻ concentration and higher ¹⁴C, while higher δ¹³C values are found in samples with low ¹⁴C and low HCO₃⁻ concentration. This indicates that simple, congruent dissolution of carbonate minerals is not a major source of DIC in the groundwater of the Quaternary aquifer. This is consistent with the geologic composition of the Quaternary aquifer, i.e., primarily siliciclastic deposits with little to no carbonate materials. Within such lithology, DIC doesn't evolve substantially beyond the conditions established in soil (Clark and Fritz, 1997). As a consequence, processes affecting δ¹³C composition in the area of study might be related to atmospheric CO₂ (-8 to -6 ‰ (Cerling et al., 1991)), the decay of plants at the surface (-26 to -9 ‰ according to whether C3 or C4 plants (Mariotti, 1991)), and/or mixing of different δ¹³C water bodies.

The ¹⁴C values progressively increase in the following sequence, subcluster 1.3 (44.2 to 54.8 pMC) to subcluster 1.2 (63.3 to 70.3 pMC) to cluster 2 (80 pMC) ([Table 4.10](#)), i.e., toward the Ismailia Canal ([Fig. 4.9](#)), suggesting the mixing of modern recharge from the Ismailia Canal to the groundwater in the Quaternary aquifer. The δ¹³C composition varies from -10.9 to -9.7 ‰ in subcluster 1.3, from -11.2 to -8.8 ‰ in subcluster 1.2, and -11.8 ‰ in cluster 2 ([Table 4.10](#)). These ranges demonstrate progressive depletion in δ¹³C toward the Ismailia Canal. Relatively depleted δ¹³C likely represents decreased residence time, where the carbon isotopic system is less evolved and there is less hydrochemical evidence of interaction between the aquifer matrix and groundwater (Plummer et al., 1994; Kirby et al., 2014). The

lowest $\delta^{13}\text{C}$, i.e., cluster 2, are located along and near the Ismailia Canal (Fig. 4.9) indicating that a significant fraction of groundwater is the recently infiltrated water from the Canal.

Cluster 3 samples are characterized by low ^{14}C activities (42 to 52 pMC) and enrichment in $\delta^{13}\text{C}$ values (-8.7 to -5.4 ‰) compared to clusters 1 and 2 (Table 4.10). The more enriched $\delta^{13}\text{C}$ corresponds with increased residence time and carbon mass transfer (Clark and Fritz, 1997; Kirby et al., 2014). Carbonate mineral dissolution are processes that can enrich the $\delta^{13}\text{C}$ of DIC incorporated into groundwaters from soil organic-matter and/or atmospheric sources (Cox, 2003). Typical $\delta^{13}\text{C}$ ratios for carbonate minerals range from -7 to 0 ‰ (Mook, 1980) and the extent of enrichment depends on the amount of carbon dissolved (Cox, 2003). Since the carbonate minerals are present throughout the sediment profile of the Miocene aquifer and some cluster 3 samples are located in close proximity to the southern subsurface structural Miocene highs (Fig. 3.1), the relatively high $\delta^{13}\text{C}$ value (-5.4 ‰) of cluster 3 might suggest mixing with groundwater from the Miocene aquifer, which shows very low ^{14}C (35.3 pMC) and relatively enriched $\delta^{13}\text{C}$ (-8.2 ‰) (Table 4.10).

Subcluster 1.3 samples have relatively lower ^{14}C activities (44.2 to 54.8 pMC) (Table 4.10), along with very negative values of $\delta^{18}\text{O}$ and $\delta^2\text{H}$ (Table 4.9) with no to little mixing relations (Figs. 4.11 and 5.1), emphasizing their different origin that might likely represent the “native” groundwater in the Quaternary aquifer. Subcluster 1.3 samples are relatively depleted in $\delta^{13}\text{C}$ values (-10.9 to -9.7 ‰) that might indicate little or no reaction with carbonates and substantial input of groundwater affected by soil gas CO_2 .

5.3. POSSIBLE CONTAMINATION OF THE QUATERNARY AQUIFER

5.3.1. Indication of wastewater infiltration

Because the cluster 4 samples showed the highest concentration in NO_3^- , up to 50 mg/l (Table 4.9 and Fig. 4.14), it appears to be influenced additionally by water from anthropogenic activities, i.e., excess irrigation water and/or wastewater. Nitrate polluted groundwater in cluster 4, i.e., sample Nos. 42,

43, 44, and 47 (Table 4.2 and Fig. 4.14), are located in agricultural area adjoining the unlined wastewater ponds (Fig. 4.9), which are high in ammonia concentration (60 mg/l at pond 3) (Table 4.2 and Fig. 4.14). The possible scenario is that through the process of nitrification the ammonia is converted to nitrate by oxidation. This process normally occurs above the water table, generally in the soil zone where subsurface conditions are aerobic (Aravena et al., 1993; Clark and Fritz, 1997; Kendall, 1998).

The city water balance (Fig. 2.12) suggests that the wastewater discharge significantly exceeds the operational capacity of unlined wastewater ponds, and overflow together with final effluent find its way to the nearby irrigated lands in El Shabab area (Fig. 2.1). The possibility of downward infiltration of the wastewater to the aquifer is further revealed by the discontinuous nature of clay layers in subsurface inferred from geoelectric survey (Fig. 5.3) (Massoud et al., in press). According to Fig. 5.3, four layers were identified in the subsurface medium. The upper three layers are located above the regional water table, whereas the fourth one was interpreted to be fully water saturated. The second layer from the surface is of great importance as it is the low-resistivity clayey layer. This layer is discontinuous along the survey line. Downward infiltration of wastewater from the oxidation ponds is possible especially at the pond No. 2 as the clayey layer was interpreted not to exist at the site (Massoud et al., in press).

Based on the aforementioned aspects, it might be possible to assume that groundwater samples from cluster 4 found nearby the wastewater ponds, i.e., Nos. 42, 43, 44, and 47, are more affected by wastewater recharge that might be infiltrated directly to the subsurface or through illegal application of wastewater for irrigation (sec. 2.7.4.1).

5.3.2. Upconing of deep groundwater from the Miocene aquifer by pumping

The mixing pattern between the groundwater in the Miocene aquifer and the groundwater in the Quaternary aquifer was mainly realized by the similarity in the Stiff diagram and more depleted stable isotopic ratios of some cluster 3 samples located in the southern part of the study area, i.e., Nos. 41, 73, and 74 (Figs. 4.5 and 4.13). However, at the north of the well field, the sample Nos. 19, 22, 66, and 67

were classified in cluster 3 (Figs. 4.5 and 4.13). The existence of cluster 3 samples near the well field area might be attributed to the excessive pumping for irrigation and reclamation activities, which in turn resulted in upconing of the deeper saline groundwater from the Miocene aquifer. It is noteworthy that many irrigation wells in the reclaimed agricultural lands are not under the control of the municipal authority to ensure the safe yield and sustainable groundwater exploitation of the Quaternary aquifer.

5.4. ENVIRONMENTAL CONSIDERATIONS

The groundwater in the Quaternary aquifer is interpreted to be composed of five potential end-members, i.e., native groundwater in the Quaternary aquifer (subcluster 1.3), groundwater in the Miocene aquifer, recent Nile water from the Ismailia Canal, the old Nile water, and wastewater. The average end-members compositions, based on the current and previous studies, are as follows; native groundwater in the Quaternary aquifer ($\text{Cl}^- = 278 \text{ mg/l}$; $\delta^{18}\text{O} = -1.6 \text{ ‰}$; $\delta^2\text{H} = -4.5 \text{ ‰}$) (current study), groundwater in the Miocene aquifer ($\text{Cl}^- = 2863.2 \text{ mg/l}$; $\delta^{18}\text{O} = -4.39 \text{ ‰}$; $\delta^2\text{H} = -32.61 \text{ ‰}$) (Abd El-Samie et al., 2002; current study), the recent Nile water after 1970 ($\text{Cl}^- = 27.4 \text{ mg/l}$; $\delta^{18}\text{O} = 3.1 \text{ ‰}$; $\delta^2\text{H} = 25.6 \text{ ‰}$) (Hamza et al., 1987; Abd El-Samie et al., 2002; current study), the old Nile water before 1970 ($\text{Cl}^- = 11.7 \text{ mg/l}$; $\delta^{18}\text{O} = -0.6 \text{ ‰}$; $\delta^2\text{H} = 4.3 \text{ ‰}$) (Awad et al., 1994; Sadek and Abd El-Samie, 2001), and wastewater ($\text{Cl}^- = 337.5 \text{ mg/l}$; $\delta^{18}\text{O} = 3.1 \text{ ‰}$; $\delta^2\text{H} = 25.1 \text{ ‰}$) (Abd El-Samie et al., 2002; current study). The conceptual groundwater flow model is shown in Fig. 5.4 and the summary of the mixing processes is shown in Table 5.1. Five mixing lines could be drawn in $\delta^{18}\text{O}$ - Cl^- plot among potential end-members. All groundwater samples of the Quaternary aquifer are plotted within two triangle domains (Fig. 5.1).

Groundwater of subcluster 1.1 is plotted in the small triangle of Fig. 5.1 and is represented by the mixing between three end-members; native groundwater in the Quaternary aquifer, the old Nile water, and the recent Nile water from the Ismailia Canal (Table 5.1). This subcluster can only be found in the western part of the El Adlia area, i.e., four kilometers from the Ismailia Canal (Figs. 4.9), suggesting a possible hydrogeologic compartmentalization (Fig. 5.4). The direct infiltration from the Ismailia Canal

seems to be the main mixing process in subcluster 1.1 (Table 5.1). The over-exploitation of the groundwater in the Quaternary aquifer at the north of the well field might be the reason for the contribution of the groundwater from the Miocene aquifer to cluster 3 samples (Fig.5.4; Table 5.1) and foreshadow the possible negative consequences of future expansion in groundwater development at the well field. Salinization problem, especially clusters 3 and 4, are estimated to be from the mixing with the groundwater of the Miocene aquifer and anthropogenic sources, i.e., wastewater (Fig. 5.4). The contribution from the Miocene aquifer is spatially controlled, i.e., gradual southward increase in chloride concentration (Figs. 4.13 and 5.1). Also, the contribution from the Miocene aquifer to almost all clusters of the Quaternary aquifer changed from being structurally controlled in the southern part of the study area to be human controlled, i.e., over-exploitation activities, in the northern part (Fig.5.4; Table 5.1).

Contribution from the recent Nile water seems to be mainly controlled by the distance from the Ismailia canal, i.e., cluster 2 samples are located within four kilometers from the canal course (Fig. 5.4), however, as the irrigated area extends southward (Fig. 2.1), contribution from surface water could be noticed in almost all clusters in different degrees (Fig. 5.1; Table 5.1). Another factor to the groundwater challenges is the pollution caused by infiltration of wastewater (Fig. 5.4; Table 5.1). The effect of wastewater is not only limited to the cluster 4 samples, i.e., No. 42, 43, 44, and 47, but also to include some cluster 3 samples, i.e., Nos. 73 and 74 according to their spatial location (Fig. 4.9) and their plots on the mixing line between groundwater in the Miocene aquifer and wastewater (Fig. 5.1). By the year 2027, the city's wastewater output might reach up to 293.5 MCM/year (GOPP and JICA, 2008) that is three times the 2007 situation (99.2 MCM/year). Considering the failure of the current disposal system to treat the wastewater effectively and handling it in a safe environmental way, the hazard of wastewater infiltration to the subsurface will be worsen in the future.

The infiltrated wastewater from the oxidation ponds was interpreted not to be the cause of the surface seepage emerged at the city centre (Fig. 5.4) because the clayey layer dips toward opposite

direction, i.e., El Shabab agricultural area (Figs. 5.3). The probable sources of the seepage were considered the local surface infiltration from excess irrigation water in the nearby cultivated land and/or leakage from the underground water utilities in the city centre.

5.5. REFERENCES

- Abd El-Samie, S.G., Sadek, M.A., Mahmoud, N.S., 2002. Assessment of groundwater pollution from the oxidation ponds in Tenth of Ramadan city, using isotopic techniques and hydrogeological modeling. Arab J. Nucl. Sci. appl., 35, 35-47.
- Aravena, R., Evans, M. L., Cherry, J. A., 1993. Stable isotopes of oxygen and nitrogen in source identification of nitrate from septic systems. Ground Water, 31, 180-186.
- Awad, M. A., Farid, M. S., Hamza, M. S. 1994. Studies on the recharge of the aquifer systems in the southern portion of the Nile Delta using radioisotopes and hydrochemistry, Isotope Rad. Res., 28(1), 17-25.
- Cerling T.E., Solomon, D.K., Quade, J., Bowman, J.R. 1991. On isotopic composition of carbon in soil carbon dioxide. Geochimica et Cosmochimica Acta 55, 3403–3405.
- Clark, I. D., and Fritz, P. 1997. Environmental Isotopes in Hydrogeology. Lewis Publishers, Boca Raton, FL, 328 p.
- Cox, S.E., 2003. Estimates of residence time and related variations in quality of groundwater beneath submarine Base Bangor and vicinity, Kitsap County, Washington: U.S. Geological Survey Water-Resources investigations report 03-4058, 52p.
- General Organization for Physical Planning (GOPP) and Japan International Cooperation Agency (JICA), 2008. The strategic urban development master plan study of the Greater Cairo region in the Arab Republic of Egypt-Final Report (in Arabic), 2, pp. 182-221.
- Hamza, M. S., Aly, A. I. M., Swailem, F. M., Nada, A., 1987. Environmentally stable isotopes and groundwater recharge in the eastern Nile delta. Int. J. Water Resour. D., 3, 228-232.
- Kendall, C., 1998. Tracing nitrogen sources and cycling in catchments. In "Isotope Tracers in Catchment Hydrology" (C. Kendall and J. J. McDonnell, eds.), Elsevier, Amsterdam, 519-576.

- Kirby, S., Wallace, J., Lowe, M., 2014. Hydrochemistry, Water Quality, Dissolved Gas, and Isotopic Data for Groundwater in the Snake Valley Area and Implications for Groundwater Flow Paths. In Hurlow, H., (Ed.) Hydrogeologic Studies and Groundwater Monitoring in Snake Valley and Adjacent Hydrographic Areas, West-central Utah and East-central Nevada. Bulletin 135, Utah Geological Survey, 129-193.
- Mariotti, A. 1991. Le carbone 13 en abondance naturelle, traceur de la dynamique de la matière organique des sols et de l'évolution des paléoenvironnements continentaux. Cahiers Orstom, s'é. Pédologie **26**(4), 299–313.
- Massoud, U., Khalil, M.M., Tokunaga, T., Santos, F.A.M. *in press*. Preliminary hydrogeophysical investigation at the 10th of Ramadan City, Egypt, by 1-D and 2-D inversion of VES data. Near Surface Geophysics.
- Mazor, E., 2004. Chemical and isotopic groundwater hydrology: the applied approach, 3rd ed. Marcel Dekker, Inc., New York.
- Mook, W.G., 1980. Carbon-14 in hydrogeological studies: in Fritz, P., and Fontes, J.C., eds., Handbook of environmental isotope geochemistry, Volume 1: New York, Elsevier Scientific Publishing Company, p. 49-74.
- Plummer, L.N., Prestemon, E.C., Parkhurst, D.L., 1994. An interactive code (NETPATH) for modeling net geochemical reactions along a flow path, version 2.0: U.S. Geological Survey Water-Resources Investigations Report 94-4169, 130 p.
- Raidla, V., 2010. Chemical and isotope evolution of groundwater in the Cambrian-Vendian aquifer system in Estonia. Dissertationes Geologicae Universitatis Tartuensis , 28 , Tartu Ülikooli Kirjastus , Tartu.
- RIGW/IWACO, 1990. Hydrogeological inventory and groundwater development plan western Nile Delta region, TN 77.01300-91-11, Research Institute of Groundwater, Kanater El-Khariria, Cairo, Egypt.

- Rose, T.P., Davisson, M.L., Hudson, G.B., Varian, A.R., 1997. Environmental isotope investigation of groundwater flow in the Honey Lake Basin, California and Nevada. Lawrence Livermore National Laboratory, UCRL-ID-127978, pp. 42.
- Sadek, M.A., Abd El-Samie, S.G., 2001. Pollution vulnerability of the Quaternary aquifer near Cairo, Egypt, as indicated by isotopes and hydrochemistry. *Hydrogeology J.*, 9, 273–281.

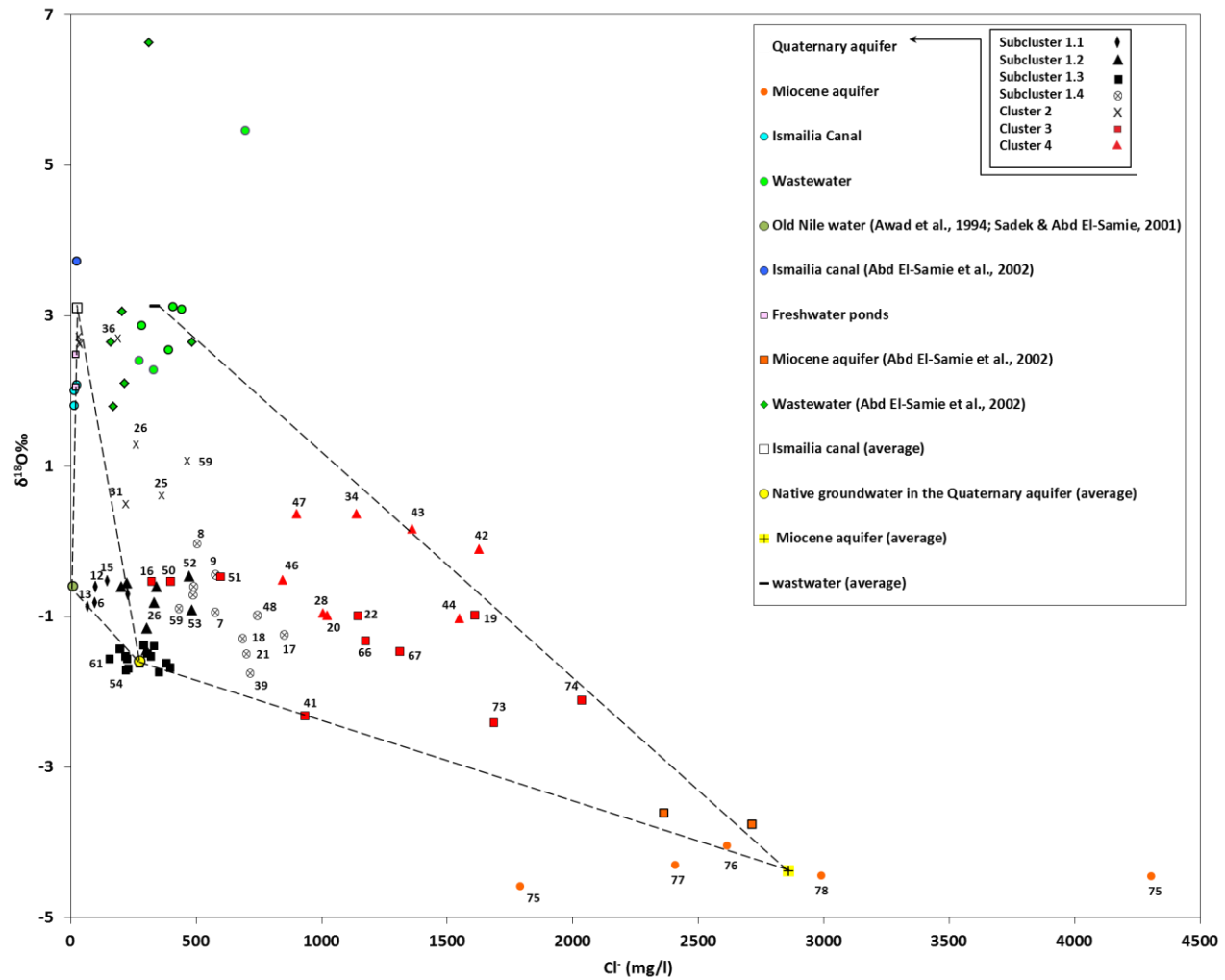


Fig. 5.1 Cross plot of $\delta^{18}O-Cl^-$

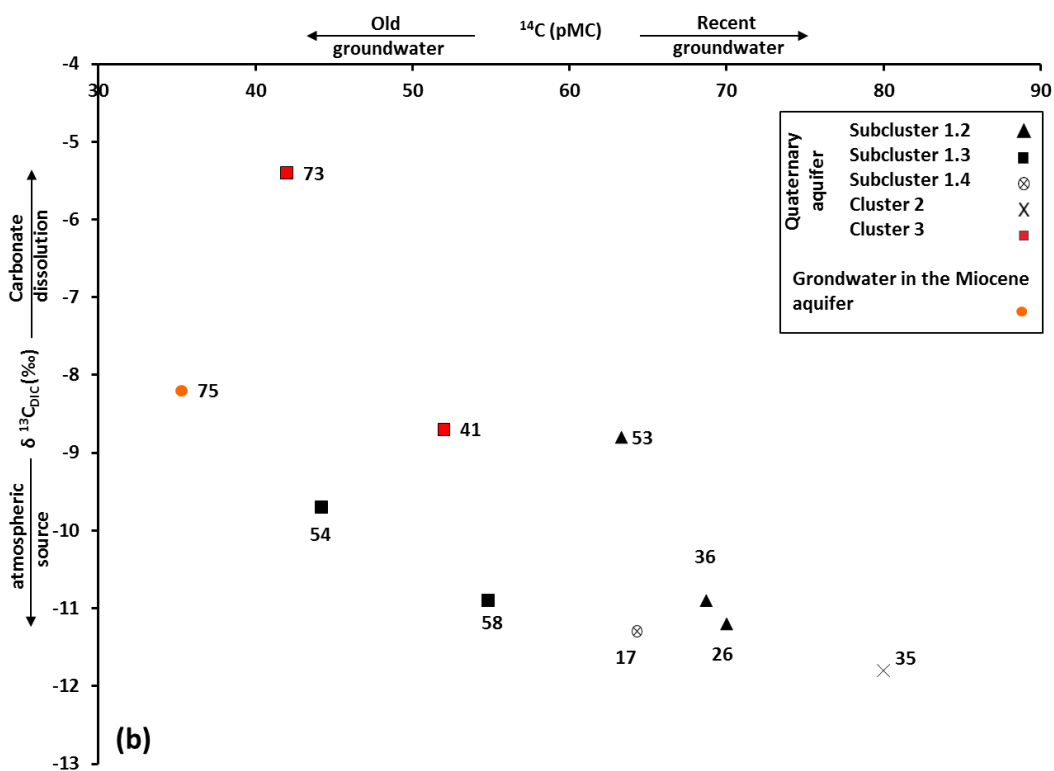
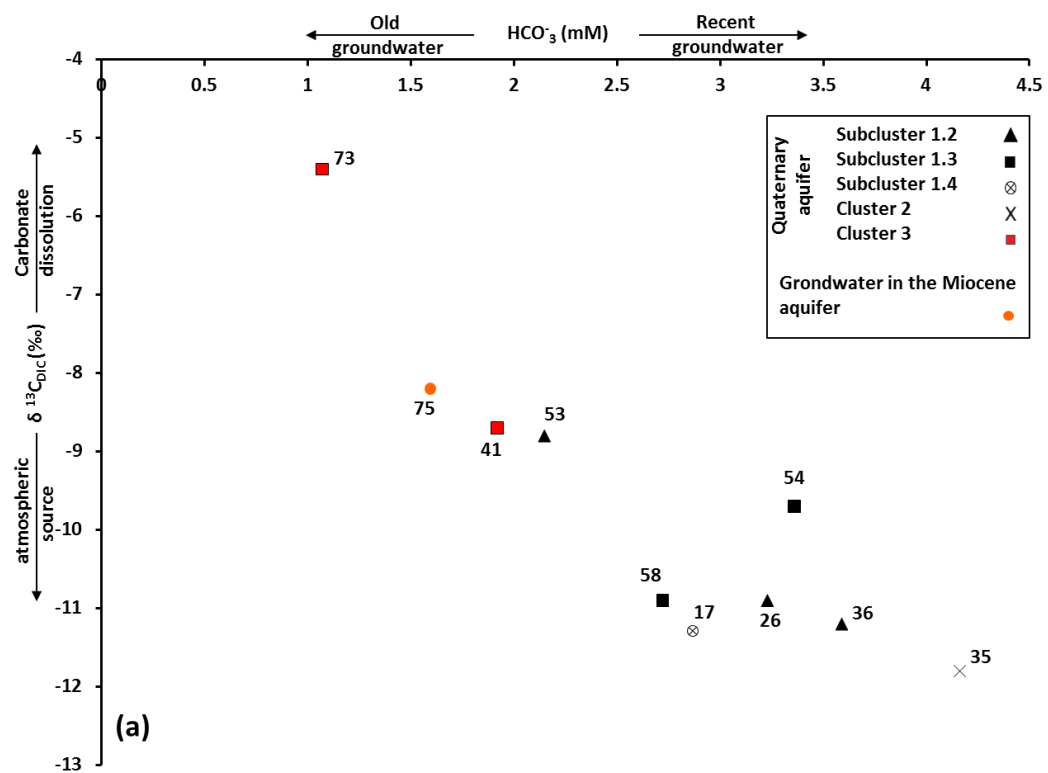
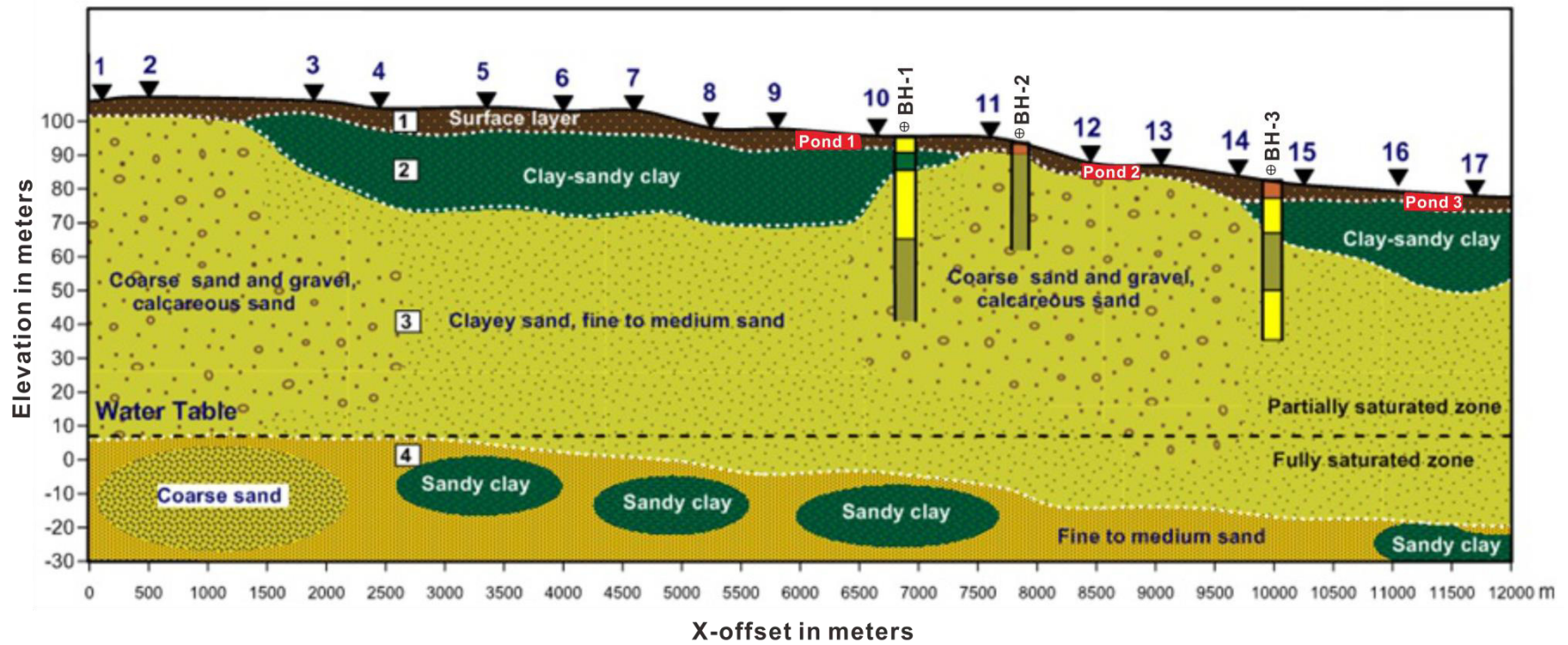


Fig. 5.2 $\delta^{13}\text{C}$ as a function of (a) HCO_3^- concentration and (b) ^{14}C activities



- Wastewater ponds
- 1
Sounding points
- ⊕ Borehole locations

Fig. 5.3 Geoelectric cross section of the area underlying the wastewater ponds, modified after Massoud et al., in press.

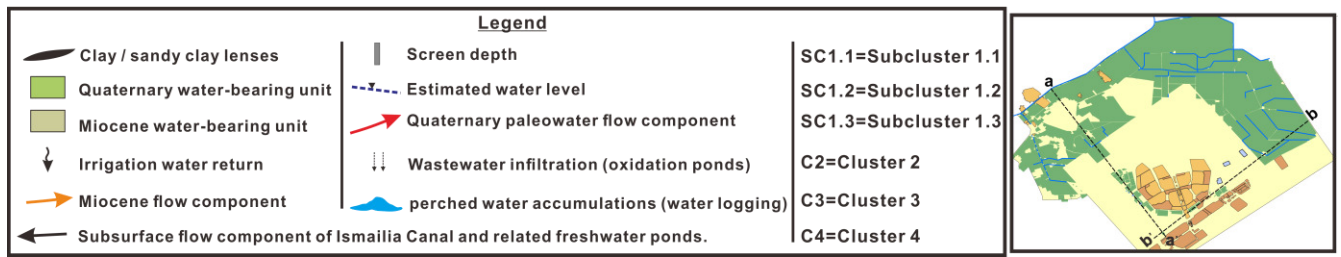
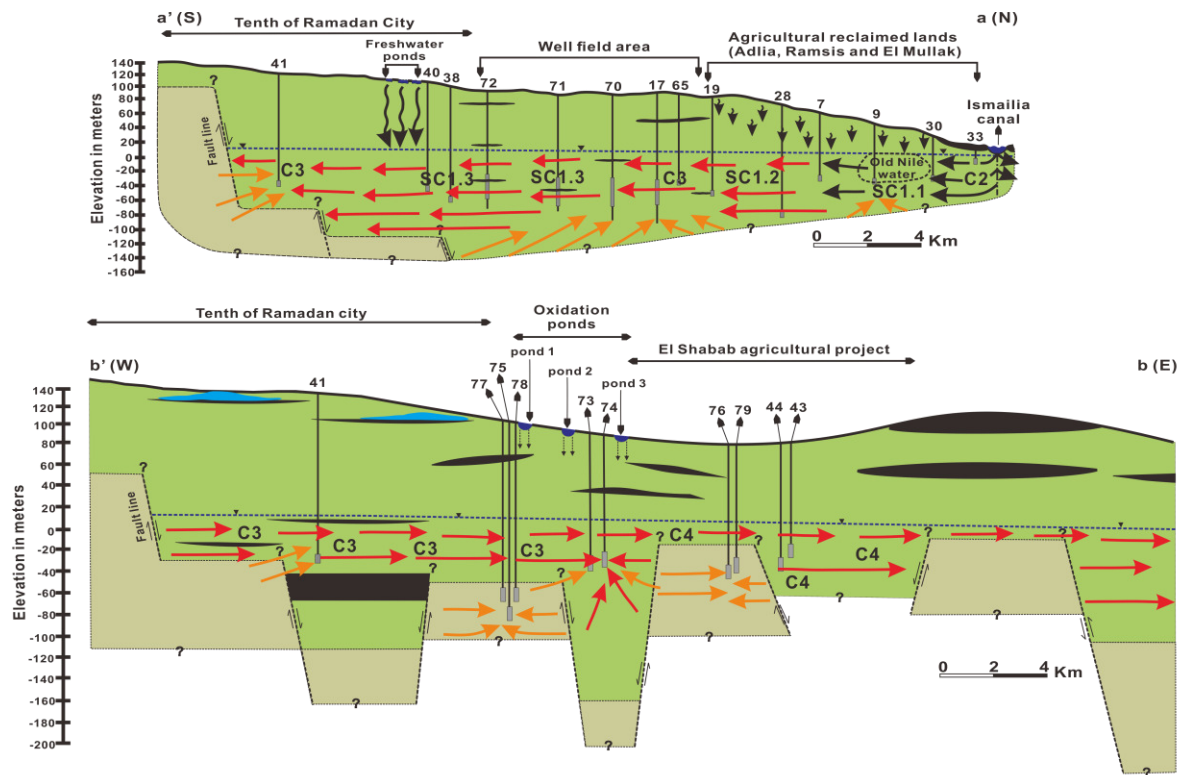


Fig. 5.4 Conceptual groundwater flow model of the study area

Table 5.1 Summary of end-members and possible mixing processes for four clusters defined for the groundwater in the Quaternary aquifer.

Clusters	End-members			Possible mixing processes	Supporting evidences		
	Major	→	Minor				
Cluster 1	subcluster 1.1	ON	Q	RN	Infiltration from the Ismailia Canal	Figs. 4.5, 4.9, 4.11, 4.13, 4.14, 4.15, 5.1, and 5.4	
	Subcluster 1.2	Q	RN	M	Infiltration from the Ismailia Canal and Irrigation - Pumping		
	Subcluster 1.3		Q		Aquifer origin (?)		
	Subcluster 1.4	Q	RN	M	Pumping		
Cluster 2		RN	Q	M	Infiltration from the Ismailia Canal, freshwater ponds, and Irrigation		
Cluster 3		M	Q	W	RN	Hydraulic connection with the Miocene aquifer - Excessive pumping- Infiltration from wastewater ponds and Irrigation	
Cluster 4		M	Q	W	RN	Hydraulic connection with the Miocene aquifer - Infiltration from wastewater ponds and Irrigation	

ON: the old Nile water, Q: Groundwater in the Quaternary aquifer, RN: the recent Nile water, M: groundwater in the Miocene aquifer, W: wastewater from the ponds.

----- CHAPTER 6: CONCLUSIONS -----

6.1. RESEARCH OUTPUTS

Given the complex set of environmental and anthropogenic issues, information required to diagnose the drivers of groundwater quality/quantity degradation and aquifer depletion, and to assess management and/or protection options are usually difficult. This is even more relevant for groundwater aquifers in areas that were historically called “deserts” and represent nowadays some of the most cultivated lands with high economic significance in arid environments. The different methodologies, i.e., environmental tracers, hydrochemistry, multivariate analysis techniques, water balance estimation, and geophysics, in the study of these hydrogeological systems, were applied in a new reclaimed land with complex array of human activities, i.e., agriculture, industry, and unlined wastewater ponds to resolve the impact of surface development on groundwater environment.

A multiple isotopic ($\delta^{18}\text{O}$, $\delta^2\text{H}$, $\delta^{13}\text{C}$ and ^{14}C) and water chemistry approach in combination with multivariate statistics, principal component analysis (PCA) and hierarchical cluster analysis (HCA), were used to gain information on mixing phenomena in groundwater of the Quaternary aquifer stressed by land-use changes and subsequent anthropogenic impacts. The HCA allowed the sorting of the 69 groundwater samples from the Quaternary aquifer into four clusters. Four clusters were largely differentiated by their EC, total dissolved ions (TDI), and stable isotopic composition. PCA revealed two components, PC1 and PC2, which explained a combined 82.2% of the total variance in the data. The PC1 is associated with the change in EC and concentrations of major ions except HCO_3^- , while the PC2 is characterized by increase in loadings of $\delta^{18}\text{O}$, $\delta^2\text{H}$ and HCO_3^- concentration. The PCA plot, PC1 vs. PC2, was used to visualize the clustering of the data as well as to identify possible end-members of the groundwater in the Quaternary aquifer. The information obtained from the analysis of ^{14}C and $\delta^{13}\text{C}$, city water balance, and recent geophysical data supported the PCA results. Accordingly, contributions from different end-members, i.e., native groundwater in the Quaternary aquifer, groundwater in the Miocene

aquifer, recent Nile water from the Ismailia Canal, the old Nile water, and wastewater, were qualitatively discussed.

6.2. RESEARCH APPLICATIONS

Based on the qualitative mixing discussion, the risks of the groundwater development in arid desert areas are mainly found to be salinization, overexploitation and contamination from inappropriate wastewater disposal while the pros might be associated with expansion of irrigation activities, i.e., freshwater ponds. Future exploitation and protection policies of this aquifer will have to account for the salinity factor from the Miocene aquifer, the pumping scheme at the well field area to prevent upconing of high-salinity Miocene aquifer water, the influence of water recharged from the wastewater ponds, along with the future shortage of surface water.

Although conducted on local scale, this study is expected to have broader significance since urbanization and agricultural development of many drylands can be expected to place similar pressures on the development of water resources. The link between major changes in land use and groundwater environment has been well recognized in this study by identifying possible end-members of the groundwater in the Quaternary aquifer. This link has been translated into a simple conceptual groundwater flow model that could be used as a basis for modeling the long-term impact of dryland development on groundwater and assesses the management and protection plans.

6.3. FUTURE WORK

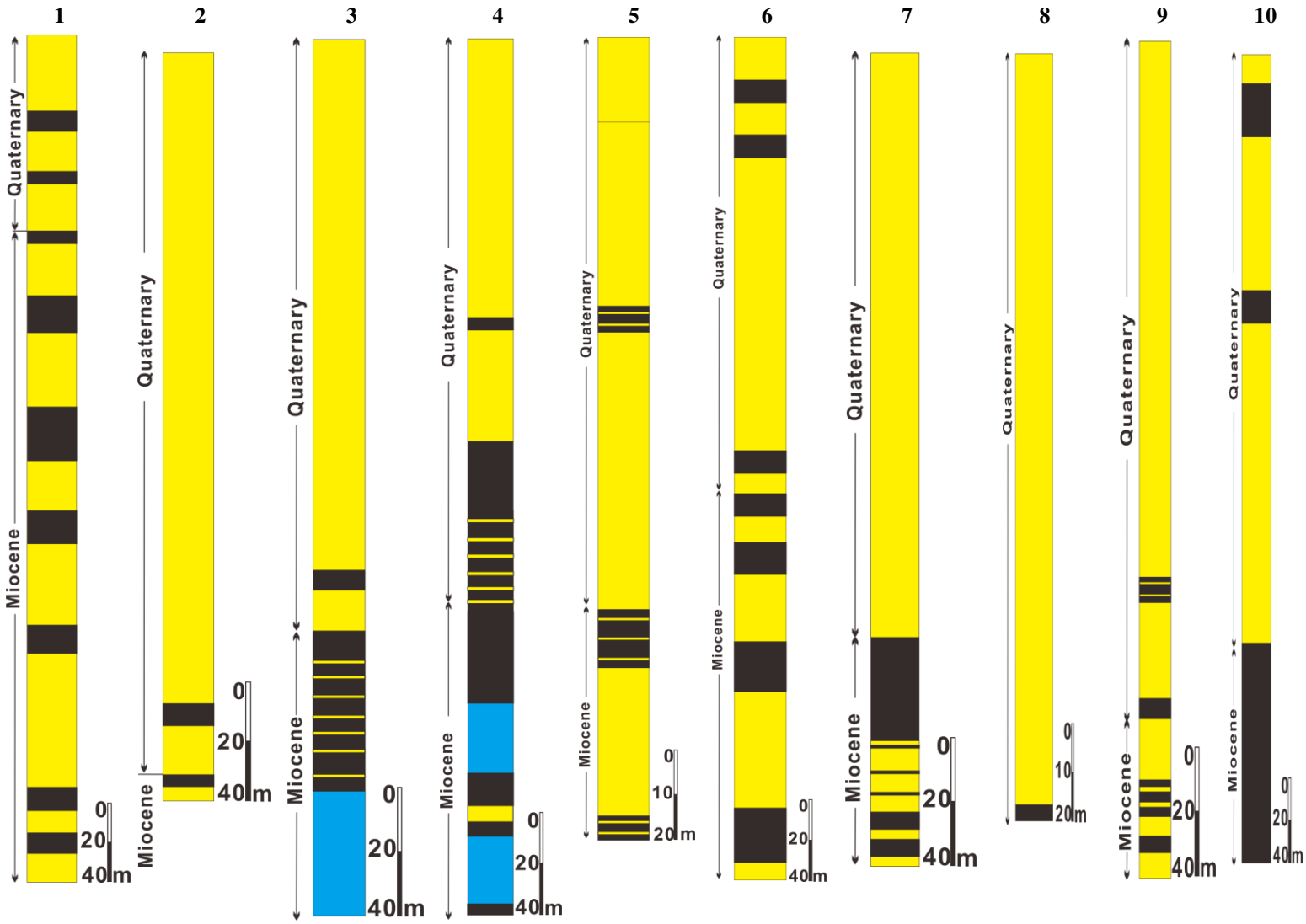
Effective groundwater management plans in such areas of high groundwater use and emerging groundwater problems need a quantitative discussion of the different end-members. However, this is not possible considering the current dataset. The chemical and isotopic composition of the water from the Ismailia Canal, irrigation water, and wastewater from the ponds are almost similar that constrain to introduce a quantitative discussion of the different end-members to the groundwater in the Quaternary aquifer. Further tracers to clarify those end-members should be identified.

Appendix A:

WELL LITHOLOGIC DATA

Well No.

Lithologic logs



Legend : Sand & gravel Clay Sandy limestone

Well No.

Lithologic logs

